

LEVEL III

2

yw

DNA 5066F-1

AD A099052

**RESPONSE OF BASIC STRUCTURAL ELEMENTS
AND B-52 STRUCTURAL COMPONENTS TO
SIMULATED NUCLEAR OVERPRESSURE**

**Volume I - Program Description and Results
(Basic Structural Elements)**

Boeing Wichita Company
3801 South Oliver Street
Wichita, Kansas 67210

**DTIC
ELECTE
MAY 18 1981**

30 September 1979

Final Report for Period 1 June 1977-30 September 1979

CONTRACT No. DNA 001-77-C-0166

APPROVED FOR PUBLIC RELEASE;
DISTRIBUTION UNLIMITED.

THIS WORK SPONSORED BY THE DEFENSE NUCLEAR AGENCY
UNDER RDT&E RMSS CODE B342078464 N99QAXAJ50202 H2590D.

Prepared for
Director
DEFENSE NUCLEAR AGENCY
Washington, D. C. 20305

FILE COPY

81 5 18 081

Destroy this report when it is no longer
needed. Do not return to sender.

PLEASE NOTIFY THE DEFENSE NUCLEAR AGENCY,
ATTN: STTI, WASHINGTON, D.C. 20305, IF
YOUR ADDRESS IS INCORRECT, IF YOU WISH TO
BE DELETED FROM THE DISTRIBUTION LIST, OR
IF THE ADDRESSEE IS NO LONGER EMPLOYED BY
YOUR ORGANIZATION.



UNCLASSIFIED

SECURITY CLASSIFICATION OF THIS PAGE (When Data Entered)

19 REPORT DOCUMENTATION PAGE		READ INSTRUCTIONS BEFORE COMPLETING FORM
1. REPORT NUMBER 18) DNA 5066F-1	2. GOVT ACCESSION NO. AD-A099 052	3. RECIPIENT'S CATALOG NUMBER
4. TITLE (and Subtitle) 6) RESPONSE OF BASIC STRUCTURAL ELEMENTS AND B-52 STRUCTURAL COMPONENTS TO SIMULATED NUCLEAR OVERPRESSURE. Volume I—Program Description and Results (Basic Structural Elements)		5. TYPE OF REPORT & PERIOD COVERED 9) Final Report, for Period 1 Jun 77—30 Sep 79
7. AUTHOR(s) 10) Roger P./Syring Richard L./Grubb PEL:7041		6. PERFORMING ORG. REPORT NUMBER D3-11108-8, Vol I
9. PERFORMING ORGANIZATION NAME AND ADDRESS Boeing Wichita Company 3801 South Oliver Street Wichita, Kansas 67210 17) J502		8. CONTRACT OR GRANT NUMBER(s) 15) DNA 001-77-C-0166
11. CONTROLLING OFFICE NAME AND ADDRESS Director Defense Nuclear Agency Washington, D.C. 20305 12) 122		10. PROGRAM ELEMENT, PROJECT, TASK AREA & WORK UNIT NUMBERS 16) Subtask N99QAXAJ502-02
14. MONITORING AGENCY NAME & ADDRESS (if different from Controlling Office) 14) D3-11108-8-VOL-1		12. REPORT DATE 11) 30 September 1979
		13. NUMBER OF PAGES 122
		15. SECURITY CLASS (of this report) UNCLASSIFIED
		15a. DECLASSIFICATION/DOWNGRADING SCHEDULE
16. DISTRIBUTION STATEMENT (of this Report) Approved for public release; distribution unlimited.		
17. DISTRIBUTION STATEMENT (of the abstract entered in Block 20, if different from Report)		
18. SUPPLEMENTARY NOTES This work sponsored by the Defense Nuclear Agency under RDT&E RMSS Code B342078464 N99QAXAJ50202 H2590D.		
19. KEY WORDS (Continue on reverse side if necessary and identify by block number) Static Test NOVA-2 Shock Load Test Aircraft Vulnerability Shock Tube Nuclear Hardness Nuclear Overpressure B-52 Components Structural Response Analysis		
20. ABSTRACT (Continue on reverse side if necessary and identify by block number) This document reports on the following: (1) experimental determination of the response of 16 basic structural elements and 7 B-52 components to simulated nuclear overpressure environments (utilizing Sandia Corporation's Thunderpipe Shock Tube), (2) analysis of these test specimens utilizing the NOVA-2 computer program, and (3) correlation of test and analysis results. ↑		

xlk

Accession For	
NTIS GRA&I	<input checked="" type="checkbox"/>
DTIC TAB	<input type="checkbox"/>
Unannounced	<input type="checkbox"/>
Justification	
By _____	
Distribution/	
Availability Codes	
Dist	Avail and/or Special
A	

Conversion factors for U.S. customary to metric (SI) units of measurement.

To Convert From	To	Multiply By
degree (angle)	radian (rad)	1.745 329 X E -2
foot	meter (m)	3.048 000 X E -1
foot-pound-force	joule (J)	1.355 818
inch	meter (m)	2.540 000 X E -2
kip (1000 lbf)	newton (N)	4.448 222 X E +3
kip/inch ² (ksi)	kilo pascal (kPa)	6.894 757 X E +3
mil	meter (m)	2.540 000 X E -5
pound-force (lbf avoirdupois)	newton (N)	4.448 222
pound-force inch	newton-meter (N*m)	1.129 848 X E -1
pound-force/inch	newton/meter (N/m)	1.751 268 X E +2
pound-force/foot ²	kilo pascal (kPa)	4.788 026 X E -2
pound-force/inch ²	kilo pascal (kPa)	6.894 757
pound-mass (lbm avoirdupois)	kilogram (kg)	4.535 924 X E -1
pound-mass-foot ² (moment of inertia)	kilogram-meter ² (kg*m ²)	4.214 011 X E -2
pound-mass/foot ³	kilogram/meter ³ (kg/m ³)	1.601 846 X E +1

PREFACE

This report was prepared by the Boeing Wichita Company, a division of The Boeing Company, under Contract No. DNA 001-77-C-0166, P00002, and documents the overall program description, test specimens and procedures, test results, analysis results, observations, and conclusions. The work was funded by the Defense Nuclear Agency and the Aeronautical Systems Division and was performed under the following:

<u>Program Element</u>	<u>Project</u>	<u>Task Area</u>	<u>Work Unit</u>
NWED 62704H	N99QAXA	E502	08
NWED 62704H	N99QAXA	J502	02
NWED 62704H	Q56QAXA	J502	02

Inclusive dates of research and development as documented herein were June 1977 through September 1979.

Volumes I and II are associated with 16 basic structural elements. Volume I summarizes the program description, test specimens and procedures, test results, analysis results, and conclusions. Volume II contains photographs, listings of NOVA-2 analysis models, and measured test data.

Volumes III and IV are associated with seven B-52 structural components. Volume III summarizes the program description, test specimens and procedures, test results, analysis results, and conclusions. Volume III is classified SECRET. Volume IV contains photographs, listings of NOVA-2 analysis models, and measured test data.

Mr. Kenneth L. Roger was the Program Manager for this task. Principal investigator was Roger P. Syring.

Appreciation is expressed to Capt. Mike Rafferty (DNA/SPAS), Mr. Dudley Ward (ASD/ENFTV), and Mr. Gerald Campbell (AFWL/DYV) for their interest and support of this program.

TABLE OF CONTENTS (VOLUME I)

		<u>PAGE</u>
	LIST OF FIGURES -----	5
	LIST OF TABLES -----	8
	NOMENCLATURE -----	9
1.0	INTRODUCTION -----	11
2.0	TEST FACILITIES -----	12
3.0	TEST SPECIMENS -----	14
3.1	General Discussion -----	14
3.2	Test Specimens 18-21 -----	14
3.3	Test Specimens 22-23 -----	14
3.4	Test Specimens 24-25 -----	14
3.5	Test Specimens 26-27 -----	19
3.6	Test Specimens 28-29 -----	19
3.7	Test Specimen 30 -----	19
3.8	Test Specimen 31 -----	19
3.9	Test Specimen 32 -----	19
3.10	Test Specimen 33 -----	19
4.0	TEST FIXTURES -----	20
5.0	INSTRUMENTATION -----	22
6.0	TEST PROCEDURES -----	30
6.1	Static Test -----	30
6.2	Shock Load Test -----	30
7.0	ANALYSIS PROCEDURES -----	33
7.1	General Discussion -----	33
7.2	Classical Techniques -----	33
7.3	Finite Element Techniques -----	33
7.4	NOVA-2LT -----	34
8.0	RESULTS -----	35
8.1	General Discussion -----	35
8.2	Static Load Test/Analysis -----	35
8.2.1	Test Specimens 18-21 -----	35
8.2.2	Test Specimens 22-23 -----	39

		<u>PAGE</u>
8.0	(Continued)	
8.2.3	Test Specimens 24-25 -----	43
8.2.4	Test Specimens 26-27 -----	43
8.2.5	Test Specimens 28-29 -----	43
8.2.6	Test Specimen 30 -----	43
8.2.7	Test Specimen 31 -----	54
8.2.8	Test Specimen 32 -----	54
8.2.9	Test Specimen 33 -----	64
8.3	Shock Load Test/Analysis -----	70
8.3.1	Test Specimens 18-21 -----	70
8.3.2	Test Specimens 22-23 -----	74
8.3.3	Test Specimens 24-25 -----	74
8.3.4	Test Specimens 26-27 -----	80
8.3.5	Test Specimens 28-29 -----	80
8.3.6	Test Specimen 30 -----	80
8.3.7	Test Specimen 31 -----	86
8.3.8	Test Specimen 32 -----	95
8.3.9	Test Specimen 33 -----	102
8.4	Summary of Static Load Test/Analysis Results -----	102
8.5	Summary of Shock Load Test/Analysis Results -----	110
8.6	Static Test Results Vs. Shock Test Results -----	114
9.0	OBSERVATIONS AND CONCLUSIONS -----	115
	REFERENCES -----	117

LIST OF FIGURES

<u>Figure No.</u>	<u>Title</u>	<u>Page</u>
1	Thunderpipe Shock Tube -----	13
2	Test Hardware -----	21
3	Instrumentation Locations - Specimens 18-29 -----	23
4	Instrumentation Locations - Specimens 30-31 -----	24
5	Instrumentation Locations - Specimen 32 -----	25
6	Instrumentation Locations - Specimen 33 -----	26
7	Instrumentation Locations - Fixtures -----	27
8	Stress Vs. Static Pressure - Gauge S18-1 - Specimen No. 18 -	36
9	Lateral Displacement Vs. Pressure - Specimen No. 18 -----	37
10	Stress Vs. Lateral Displacement - Specimen No. 18 -----	38
11	Stress Vs. Static Pressure - Gauge S22-1 (Specimen 22) and Gauge S23-2 (Specimen 23) -----	40
12	Lateral Displacement Vs. Static Pressure - Specimens 22-23 -	41
13	Stress Vs. Lateral Displacement - Specimens 22-23 -----	42
14	Stress Vs. Static Pressure - Gauge S24-1 (Specimen 24) and Gauge S25-2 (Specimen 25) -----	44
15	Lateral Displacement Vs. Static Pressure - Specimens 24-25 -	45
16	Stress Vs. Lateral Displacement - Specimens 24-25 -----	46
17	Stress Vs. Static Pressure - Gauge S27-1 (Specimen 27) -----	47
18	Lateral Displacement Vs. Static Pressure - Specimen 27 -----	48
19	Stress Vs. Lateral Displacement - Specimen 27 -----	49
20	Stress Vs. Static Pressure - Gauge S28-2 (Specimen 28) and Gauge S29-2 (Specimen 29) -----	50
21	Lateral Displacement Vs. Static Pressure - Specimens 28-29 -	51
22	Stress Vs. Lateral Displacement - Specimens 28-29 -----	52
23	Stress Vs. Static Pressure - Gauges S30-3 and S30-5 - Specimen 30 -----	53
24	Deflection Vs. Static Pressure - Gauge D30-9 - Specimen 30 -	55
25	Stress Vs. Static Pressure - Gauge S30-2 - Specimen 30 -----	56
26	Stress Vs. Static Pressure - Gauges S31-3 and S31-5 - Specimen 31 -----	57
27	Deflection Vs. Static Pressure - Gauge D31-9 - Specimen 31 -	58

LIST OF FIGURES (Cont'd)

<u>Figure No.</u>	<u>Title</u>	<u>Page</u>
28	Stress Vs. Static Pressure - Gauge S31-2 - Specimen 31 -----	59
29	Stress Vs. Static Pressure - Gauges S32-14 and S32-23 - Specimen 32 -----	60
30	Stress Vs. Static Pressure - Gauges S32-2 and S32-18 - Specimen 32 -----	61
31	Stress Vs. Angular Location - Specimen 32 (Inner Flange) ---	62
32	Stress Vs. Angular Location - Specimen 32 (Outer Flange) ---	63
33	Stress Vs. Static Pressure - Gauge S33-14 - Specimen 33 ----	65
34	Stress Vs. Static Pressure - Gauges S33-9 and S33-17 - Specimen 33 -----	66
35	Stress Vs. Static Pressure - Gauges S33-2 and S33-18 - Specimen 33 -----	67
36	Stress Vs. Angular Location - Specimen 33 (Inner Flange) ---	68
37	Stress Vs. Angular Location - Specimen 33 (Outer Flange) ---	69
38	Box Holding Fixture -----	71
39	Pin-Ended Column Loading Device -----	72
40	Clamp-Ended Column Loading Device -----	73
41	Maximum Stress Vs. Incident Overpressure - Specimens 18-21 -	75
42	Strain Time History - Specimen 21 -----	76
43	Maximum Stress Vs. Incident Overpressure - Specimens 22-23 -	77
44	Strain Time History - Specimen 23 -----	78
45	Maximum Stress Vs. Incident Overpressure - Specimens 24-25 -	79
46	Strain Time History - Specimen 25 -----	81
47	Maximum Stress Vs. Incident Overpressure - Specimens 26-27 -	82
48	Strain Time History - Specimen 26 -----	83
49	Maximum Stress Vs. Incident Overpressure - Specimens 28-29 -	84
50	Strain Time History - Specimen 28 -----	85
51	Maximum Stress Vs. Incident Overpressure - Specimen 30 - Gauges S30-3 and S30-5 -----	87
52	Maximum Stress Vs. Incident Overpressure - Specimen 30 - Gauge S30-2 -----	88
53	Maximum Deflection Vs. Incident Overpressure - Specimen 30 - Gauge D30-9 -----	89
54	Deflection Time History - Specimen 30 -----	90

LIST OF FIGURES (Cont'd)

<u>Figure No.</u>	<u>Title</u>	<u>Page</u>
55	Maximum Stress Vs. Incident Overpressure - Specimen 31 - Gauges S31-3 and S31-5 -----	91
56	Maximum Stress Vs. Incident Overpressure - Specimen 31 - Gauge S31-2 -----	92
57	Maximum Deflection Vs. Incident Overpressure - Specimen 31 - Gauge D31-9 -----	93
58	Deflection Time History - Specimen 31 -----	94
59	Maximum Stress Vs. Incident Overpressure - Specimen 32 - Gauge S32-14 -----	96
60	Maximum Stress Vs. Incident Overpressure - Specimen 32 - Gauges S32-10 and S32-21 -----	97
61	Maximum Stress Vs. Incident Overpressure - Specimen 32 - Gauges S32-7 and S32-20 -----	98
62	Maximum Stress Vs. Incident Overpressure - Specimen 32 - Gauges S32-3 and S32-22 -----	99
63	Strain Time History - Specimen 32 -----	100
64	Maximum Stress Vs. Incident Overpressure - Specimen 33 - Gauge S33-14 -----	103
65	Maximum Stress Vs. Incident Overpressure - Specimen 33 - Gauge S33-9 -----	104
66	Maximum Stress Vs. Incident Overpressure - Specimen 33 - Gauge S33-7 -----	105
67	Maximum Stress Vs. Incident Overpressure - Specimen 33 - Gauge S33-18 -----	106
68	Strain Time History - Test Data - Specimen 33 -----	107
69	Strain Time History - Analysis Data - Specimen 33 -----	108
70	Effect of Panel Geometry on Accuracy of Static Load Stress Predictions at Center of Clamped Edge -----	110
71	Effect of Panel Geometry on Accuracy of Shock Load Stress Predictions at Center of Clamped Edge -----	112

LIST OF TABLES

<u>Table No.</u>	<u>Title</u>	<u>Page</u>
1	Specimen Description -----	15
2	Mechanical Properties -----	16
3	Frame Geometry -----	17
4	Specimen Part Numbers -----	18
5	Fixture Part Numbers -----	20
6	Fixture/Specimen Relationships -----	20
7	Instrumentation -----	22
8	Test Shot Summary -----	32
9	Effects of Column Initial Eccentricities - Specimens 18-21 --	39
10	Comparison of Specimen 12 and 32 Stress Data in Frame Inner Flange -----	101
11	Static Load Test/Analysis Results - Specimens 30-33 -----	109
12	Shock Load Test/Analysis Results - Specimens 18-33 -----	111
13	Test and Analysis Results in the Plastic Region -----	113
14	Test and Analysis Structural Response Frequencies -----	113
15	Comparison of Static Test Data and Shock Load Test Data - Specimens 30-33 -----	114

NOMENCLATURE

AFWL	Air Force Weapons Laboratory
ASD	Aeronautical Systems Division
DNA	Defense Nuclear Agency
E	Modulus of elasticity
F_{c_y}	Compressive yield stress
F_{t_y}	Tensile yield stress
Hz	Hertz
IMP	Imperfection
IN	Inches
KSI	Thousand pounds per square inch
KT	Kiloton
l	Length
NO	Number
PSI	Pounds per square inch
R.H.	Right Hand
δ	Displacement or initial imperfection
ΔP	Pressure
ϵ	Strain
μ	Poisson's Ratio
ρ	Radius of gyration
σ	Stress
θ	Angular Location

1.0 INTRODUCTION

The ability of an airframe to resist nuclear blast effects (gust and overpressure) and thermal radiation is a primary concern in a nuclear hardness assessment. Because of the nature of blast loading, gust effects are generally considered when determining the dynamic response of low-frequency, primary structural components, such as an aircraft wing, fuselage or empennage. Conversely, overpressure loading is the significant blast effect when determining the response of high-frequency structural components, such as aircraft skin panels, stringers, frames and radomes.

As a result of the moratorium on nuclear weapons effects tests in the atmosphere, response of systems to nuclear environments is usually determined analytically, supported by laboratory experiments. Techniques such as NOVA-2 (Reference 1) are frequently used for determining structural response to nuclear overpressure and are supplemented with experimental data obtained from tests conducted in nuclear overpressure simulation facilities similar to those described in Reference 2. However, experimental data describing the response of basic structural elements (e.g., skin panels, stringers, frames, columns) to nuclear overpressure has been found to be extremely limited. To help alleviate this deficiency in this critical area of technology, a program was accomplished during 1975-76 for the Defense Nuclear Agency by the Boeing Wichita Company (Reference 3) to determine the response of 17 basic structural elements to simulated nuclear overpressure loading.

To expand the experimental data base that was developed in the Reference 3 program and to advance technology to a level that is required to adequately assess the nuclear vulnerability of complex weapon systems to nuclear overpressure effects, additional testing and analysis was accomplished in a follow-on program and is described in detail in this report.

This follow-on program involved 16 additional basic structural elements (columns, skin panels, and skin/frame cylinders) as well as complex structural assemblies from seven B-52 components. The B-52 components consisted of the nose radome, doppler radome, wing leading edge, inboard flap, rudder, center bomb bay doors, and a section of the aft fuselage.

Documentation of this follow-on test program is contained in four volumes. Volumes I and II are associated with the basic structural elements. Volume I summarizes the program description, test specimens and procedures, test results, analysis results, and conclusions. Volume II contains photographs, listings of NOVA-2 analysis models, and measured test data. Volumes III and IV are associated with the complex structural assemblies from B-52 aircraft components. Volume III summarizes the program description, test specimens and procedures, test results, analysis results, and conclusions. Volume IV contains photographs, listings of NOVA-2 analysis models, and measured test data.

2.0 TEST FACILITIES

The simulated nuclear overpressure testing was conducted at Sandia Corporation's THUNDERPIPE shock tube in Albuquerque, New Mexico during August-September 1978. As illustrated in Figure 1, this shock tube consists of 229.4 feet of 2-foot diameter driver chamber, 296.8 feet of 6-foot diameter pipe, and 65 feet of 19-foot diameter test section. Conical sections shown in Figure 1 provide transition between the three major sections of the shock tube. A portion of the shock tube wall is constructed of three-inch thick, mild steel, and the remainder of the shock tube wall is constructed of one-inch thick, mild steel. In addition, the 19-foot diameter test section is reinforced with circumferential stiffeners at approximately 10-foot intervals.

Blast waves, simulating a nuclear overpressure pulse, were generated by igniting PETN primacord and composition 4 explosive charges. The explosive was positioned in the centerline of the driver chamber by a rack constructed of steel reinforcing rods. Use of the long explosive charges resulted in the desired positive phase duration of the pressure pulse (approximately 80 milliseconds). Peak intensity of the incident pressure pulse was controlled by the longitudinal position of the test specimen within the test section as well as the density of the explosive charge.

The inside wall of the test section was instrumented with five pressure transducers to measure incident overpressure and three transducers to measure reflected overpressure. These transducers were positioned in the wall of the test section in such a manner that an accurate definition of the incident overpressure time histories at the test specimen location was available.

Sandia Laboratories provided all signal conditioning and recording equipment as well as personnel (e.g., ordinance personnel, mechanics, equipment operators, and technicians) to conduct the test shots under the guidelines established by Boeing-Wichita. Sandia Laboratories was also responsible for recording test data on analog tapes, digitizing the test data, and furnishing plots of all test data.

In addition to the simulated nuclear overpressure testing, static testing was accomplished to determine structural response associated with spacially uniform, statically - applied, external pressure and to check out selected instrumentation. The static testing was accomplished in the Structural Test Laboratories of the Boeing Wichita Company in Wichita, Kansas.

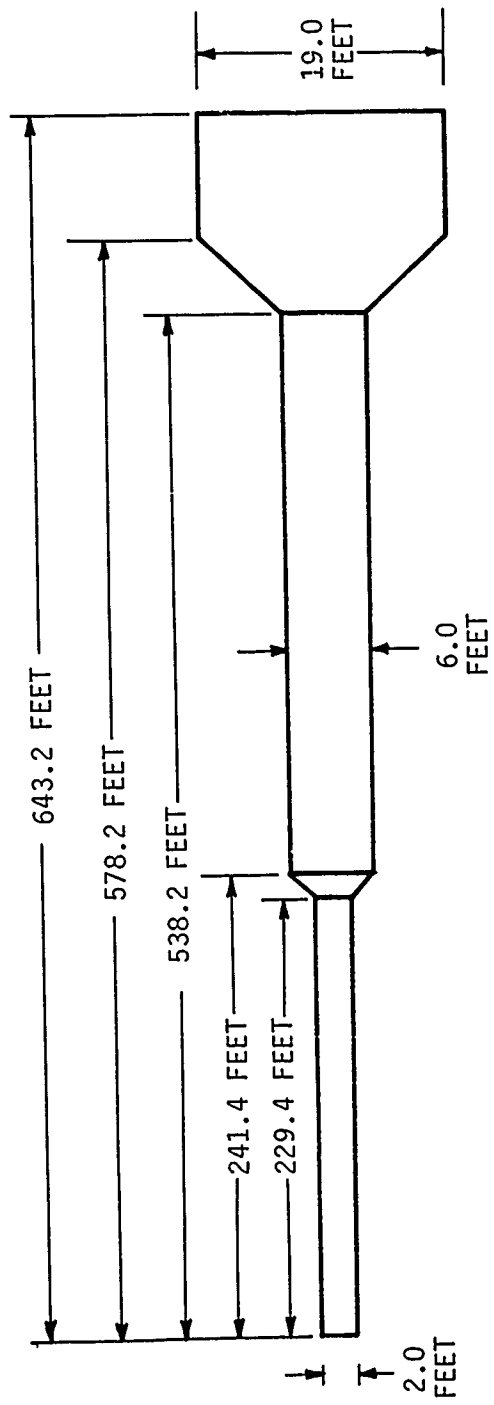


Figure 1. THUNDERPIPE Shock Tube

3.0 TEST SPECIMENS

3.1 General Discussion

Sixteen aluminum test specimens were designed and manufactured specifically for this study. These test specimens were designed to simulate basic structural elements representative of structure primarily found in aircraft. The guidelines that were utilized in selecting this group of test specimens were: (1) inclusion of a wide variety of parameters that influence structural response characteristics such as boundary conditions, geometry, failure mechanism, and construction type, (2) inclusion of test specimens that the NOVA-2LT computer program was potentially capable of properly analyzing, and (3) inclusion of test specimens that would complement those in the Reference 3 program.

As shown in Table 1, the set of test specimens included buckling sensitive columns, flat unstiffened panels, and skin/frame cylinders. Table 2 describes the material properties of the test specimens. These properties were established by tensile coupon tests of material taken from the same stock from which the specimen was made. In addition, Table 3 illustrates the frame spacing and frame cross section geometry for the skin/frame cylinder specimens. All test specimens are defined by Boeing drawings and part numbers as shown in Table 4.

3.2 Test Specimens 18-21

Both pinned and clamped columns were included in this program to supplement the results obtained from the clamped columns of the Reference 3 program. As shown in Table 1, test specimens 18-21 were pin-ended columns which were ten inches long, five inches wide, and 0.033 inches thick. Table 2 shows that these columns were constructed of 6061-T6 material. The initial lateral eccentricities at the column centers were measured prior to the shock load testing. These eccentricities were determined to be 0.015, 0.02, 0.025, and 0.01 inches for specimens 18, 19, 20, and 21, respectively.

3.3 Test Specimens 22-23

Test specimens 22-23 were pin-ended columns ten inches long, five inches wide, and 0.028 inches thick. These columns were also constructed of 6061-T6. Initial lateral eccentricities were determined to be 0.075 and 0.025 inches for specimens 22 and 23, respectively.

3.4 Test Specimens 24-25

Test specimens 24-25 were clamp-ended columns ten inches long, five inches wide, and 0.028 inches thick. These columns were constructed of 6061-T6. Initial lateral eccentricities were determined to be 0.57 and 0.05 inches for specimens 24 and 25, respectively. The large eccentricity for specimen 24 resulted from inadvertent yielding of the column during the static test.

TABLE 1
SPECIMEN DESCRIPTION

SPECIMEN NUMBER	DESCRIPTION	LENGTH (INCH)	WIDTH (INCH)	THICKNESS (INCH)	BOUNDARY CONDITIONS
18-21	COLUMNS	10.0	5.0	0.033	PINNED
22-23	COLUMNS	10.0	5.0	0.028	PINNED
24-25	COLUMNS	10.0	5.0	0.028	CLAMPED
26-27	COLUMNS	10.0	5.0	0.025	PINNED
28-29	COLUMNS	10.0	5.0	0.025	CLAMPED
30	FLAT PANEL	22.0	22.0	0.039	4 SIDES CLAMPED
31	FLAT PANEL	22.0	22.0	0.062	4 SIDES CLAMPED
32	SKIN/FRAME CYLINDER	36.0	24 INCH RADIUS	0.020 SKIN 	FRAMES CLAMPED AT $\theta = 0^\circ$ AND 180°
33	SKIN/FRAME CYLINDER	36.0	24 INCH RADIUS	0.020 SKIN 	FRAMES CLAMPED AT $\theta = 0^\circ$ AND 180°

 For frame geometry see Table 3

TABLE 2
MECHANICAL PROPERTIES

SPECIMEN NUMBER	ALUMINUM MATERIAL	YIELD STRESS (PSI)	ULTIMATE STRESS (PSI)	% ELONGATION	MODULUS OF ELASTICITY (PSI x 10 ⁻⁶)
18-21	6061-T6	42,200	47,360	11.875	10.10
22-23	6061-T6	41,180	46,060	11.500	10.70
24-25	6061-T6	41,180	46,060	11.500	10.70
26-27	6061-T42	25,310	38,760	20.000	10.85
28-29	6061-T42	24,940	38,685	19.500	10.25
30	6061-T6	38,360	46,790	15.000	11.70
31	6061-T6	42,330	47,840	12.000	10.60
32	6061-T42	19,990	38,470	20.000	11.40
33	6061-T42	20,480	38,250	20.500	10.40

TABLE 3
FRAME GEOMETRY

SPECIMEN NUMBER	STIFFENER SPACING (INCH)	CROSS SECTION	DIMENSIONS (INCH)					
			A	B	C	D	E	F
32	9.0		0.106	0.460	0.106	1.893	2.003	0.705
33	9.0		0.154	0.704	0.597	0.705	----	----

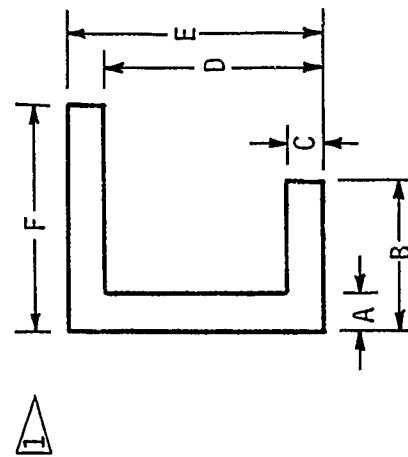
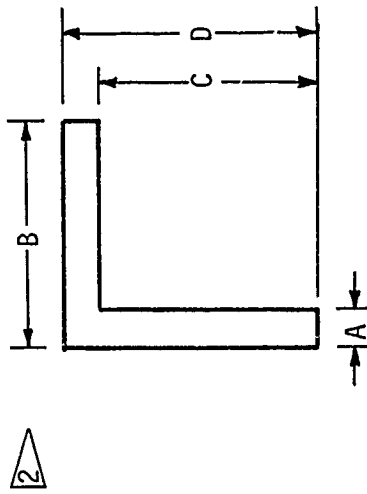


TABLE 4
SPECIMEN PART NUMBERS

SPECIMEN	PART NUMBER
18	EX3031-501
19	EX3031-502
20	EX3031-503
21	EX3031-504
22	EX3031-505
23	EX3031-506
24	EX3031-507
25	EX3031-508
26	EX3031-509
27	EX3031-510
28	EX3031-511
29	EX3031-512
30	EX3027-501
31	EX3027-502
32	EX3030-501
33	EX3030-502

3.5 Test Specimens 26-27

Test specimens 26-27 were pin-ended columns ten inches long, five inches wide, and 0.025 inches thick. These columns were constructed of 6061-T42 material. Specimen 26 exhibited an initial lateral eccentricity of 0.13 inches, whereas specimen 27 was essentially free of eccentricity.

3.6 Test Specimens 28-29

Test specimens 28-29 were clamp-ended columns ten inches long, five inches wide, and 0.025 inches thick. These columns were constructed of 6061-T42 material. Specimen 28 exhibited an initial lateral eccentricity of 0.01 inches, whereas similar data for specimen 29 was less than 0.005 inches.

3.7 Test Specimen 30

To supplement data from the Reference 3 study associated with flat homogeneous skin panels, this program included two panels that were 22 inches square. Specimen 30 was 0.039 inches thick and was constructed of 6061-T6 material. All sides of this panel were clamped.

3.8 Test Specimen 31

Specimen 31 was similar to 30 except that it was 0.062 inches thick. In addition, the 6061-T6 material properties were found to be slightly different than those for specimen 30.

3.9 Test Specimen 32

The Reference 3 study also included two skin/frame circular cylinders with a 48 inch diameter and a 36 inch length. Since the NOVA-2LT computer program models the actual frame cross section as a symmetric cross section regardless of the actual geometry, the frames were designed to be symmetric (I and T cross sections).

To provide data on the response of frames with non-symmetric cross sections, this program included specimens 32 and 33. Specimen 32 consisted of a skin/frame cylinder with channel cross section frames as described in Tables 1-4. These frames were sized to provide essentially the same cross sectional area and bending stiffness about an axis parallel to the longitudinal axis of the cylinder as that for specimen 12 of the Reference 3 study.

3.10 Test Specimen 33

Specimen 33 was identical to specimen 32 except for frame cross section as shown in Table 3. In addition, material properties for specimen 32 and 33 frames were slightly different from each other. Specimen 33 was designed to be similar to specimen 13 of the Reference 3 study. Measurements of frame geometry indicated that cross sectional areas of the specimen 13 and 33 frames was essentially identical. However, bending stiffness of the specimen 33 frames about an axis parallel to the longitudinal axis of the cylinder was 60 percent greater than comparable data for specimen 13.

4.0 TEST FIXTURES

The test holding fixtures, which were obtained from the Reference 3 program, consisted of: (1) a master frame which bolted to two longitudinal rails that were welded to the shock tube floor, (2) a rectangular box holding fixture which attached to the master frame and to which was mounted all flat test specimens, and (3) a pair of circular end plates that served as the interface between the master frame and the skin/frame cylinders. Figure 2 illustrates the installation of the master frame and fixtures in the shock tube.

The fixtures are defined by Boeing drawings. A list of the fixtures and their respective part numbers is shown in Table 5.

TABLE 5
FIXTURE PART NUMBERS

FIXTURE	BOEING PART NO.
Box Holding Fixture	EX3032-21
Small Panel Adapter Plate	EX3032-26
End Plates (2)	EX3032-30
Partial Cylinder Adapter	EX3032-33
Frame Assemblies	EX3032-35, 36

In addition, Table 6 illustrates the various test specimens that were mounted to the test fixtures.

TABLE 6
FIXTURE/SPECIMEN RELATIONSHIPS

FIXTURE	SPECIMEN NUMBER															
	18	19	20	21	22	23	24	25	26	27	28	29	30	31	32	33
Box Holding Fixture	X	X	X	X	X	X	X	X	X	X	X	X	X	X	X	
Small Panel Adapter Plate													X	X		
End Plates															X	X
Frame Assemblies															X	X

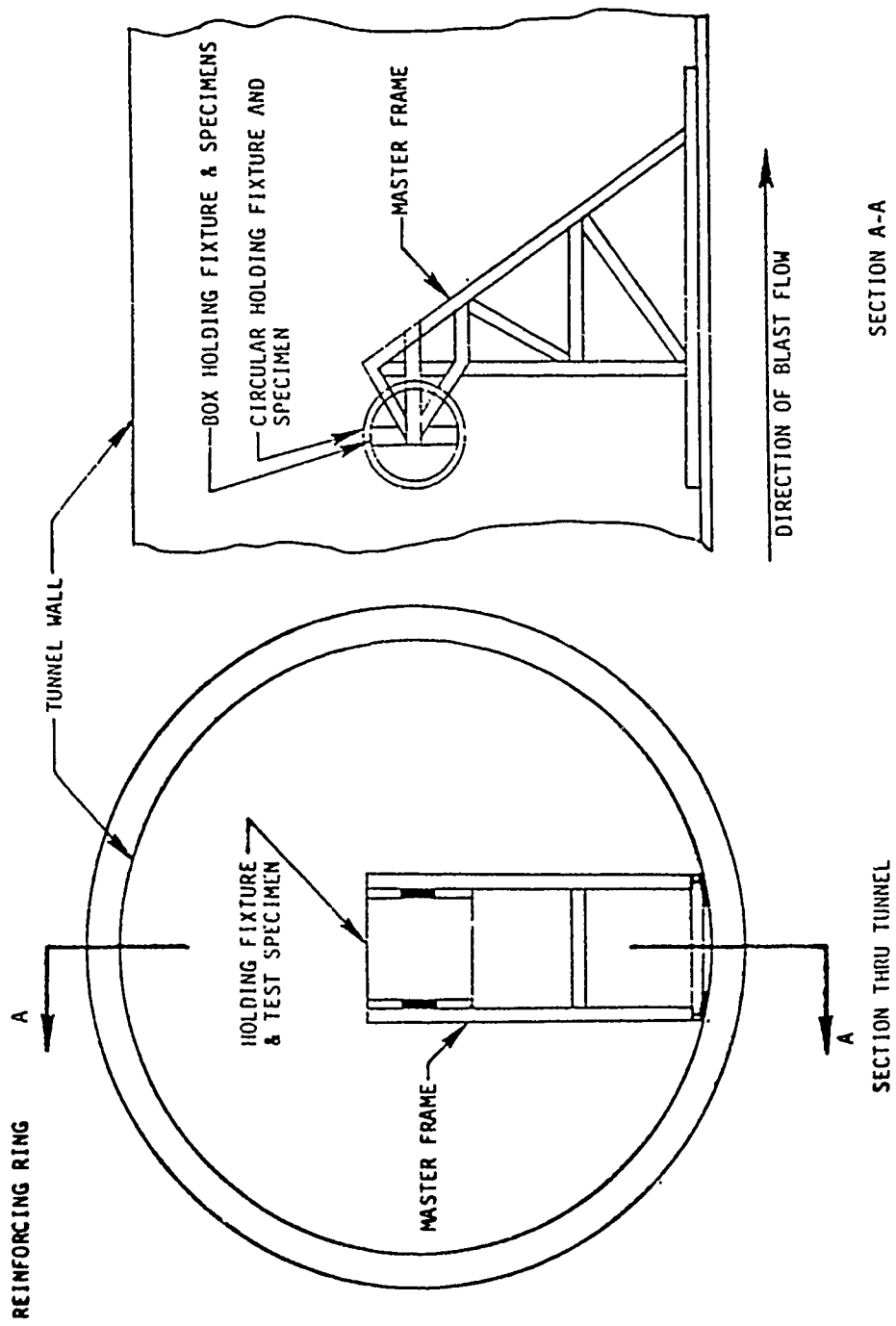


Figure 2. Test Hardware

5.0 INSTRUMENTATION

In addition to the pressure transducers that were mounted in the wall of the shock tube test section, various instrumentation was mounted on the test specimens and holding fixtures as well as inside the test fixture/specimen cavities. During the shock load testing, several different test set-ups were required, utilizing equipment that is illustrated in Table 7.

TABLE 7

INSTRUMENTATION

PARAMETER	SENSOR DESCRIPTION	
Pressure	ENDEVCO 8510-15M2	
Strain	MICRO-MEASUREMENTS	
	EA-09-125RD-350	CEA-13-125UR-350
	EA-13-125BT-350	CEA-13-125UW-350
	EA-13-125-BZ-350W	CEA-13-125UT-350
	EA-13-125AC-350	
Deflection	KD-2300-10CU Proximity Gauge	

The Sandia Laboratories instrumentation equipment consisted of bridge conditioning, ENDEVCO signal conditioning, RED COR differential amplification, EMR voltage controlled oscillators, and CEC VR 3300 analog tape recorders.

Strain gauge locations were selected to be in the areas of maximum strain as determined by analysis. Axial gauges were utilized in both uniaxial and bi-axial stress fields. Single gauges were utilized in uniaxial stress fields. Two gauges per location (rotated 90° with respect to each other) were utilized in bi-axial stress fields where the principal stress direction was known. In addition, 45° rosettes were utilized in bi-axial stress fields where principal stress directions were not known. A detailed illustration of all instrumentation locations is shown in Figures 3-7. The letters P,S,&D represent pressure, strain, and deflection, respectively. The digit adjacent to the letter is the specimen number and the dash number is simply the serial number of the transducer associated with that specimen.

The strain channel circuits consisted of a three leadwire system from the strain gauge to a bridge completion unit. The bridge completion units consisted of a precision certified compensating gauge plus half bridge. By connecting a shunt calibration resistor across the compensating gauge, system check-out and system calibration was performed one time per channel per specimen. When using this type of system calibration, knowing the bridge voltage, leadwire resistance, and cable resistance was not necessary for obtaining accurate system calibration. Since the instrumentation system was not of the null balance variety, an unknown bridge voltage change between calibration and testing was a potential source of significant error. Therefore, the bridge voltages were checked prior to

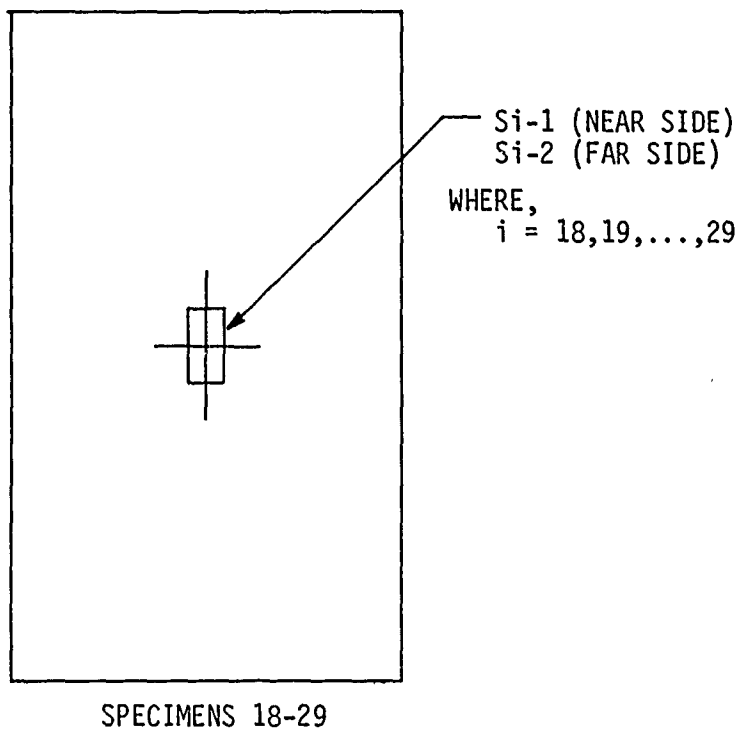
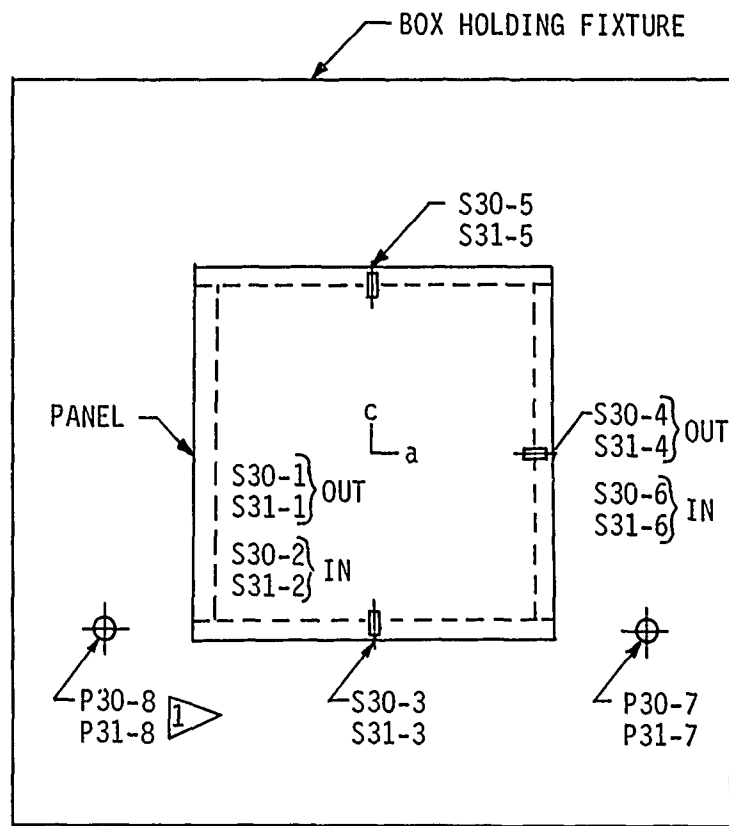


Figure 3. Instrumentation Locations - Specimens 18-29



SPECIMEN NO. 30 & 31

1 BACK SIDE OF BOX HOLDING FIXTURE ONLY

Figure 4. Instrumentation Locations - Specimens 30 and 31

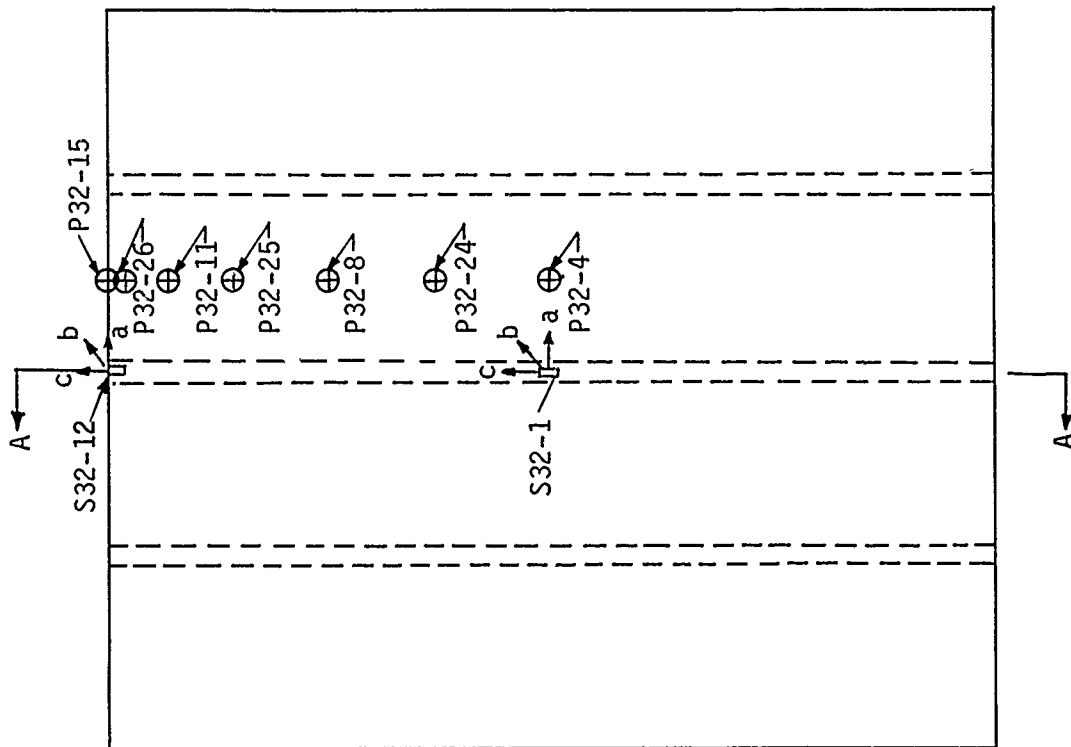
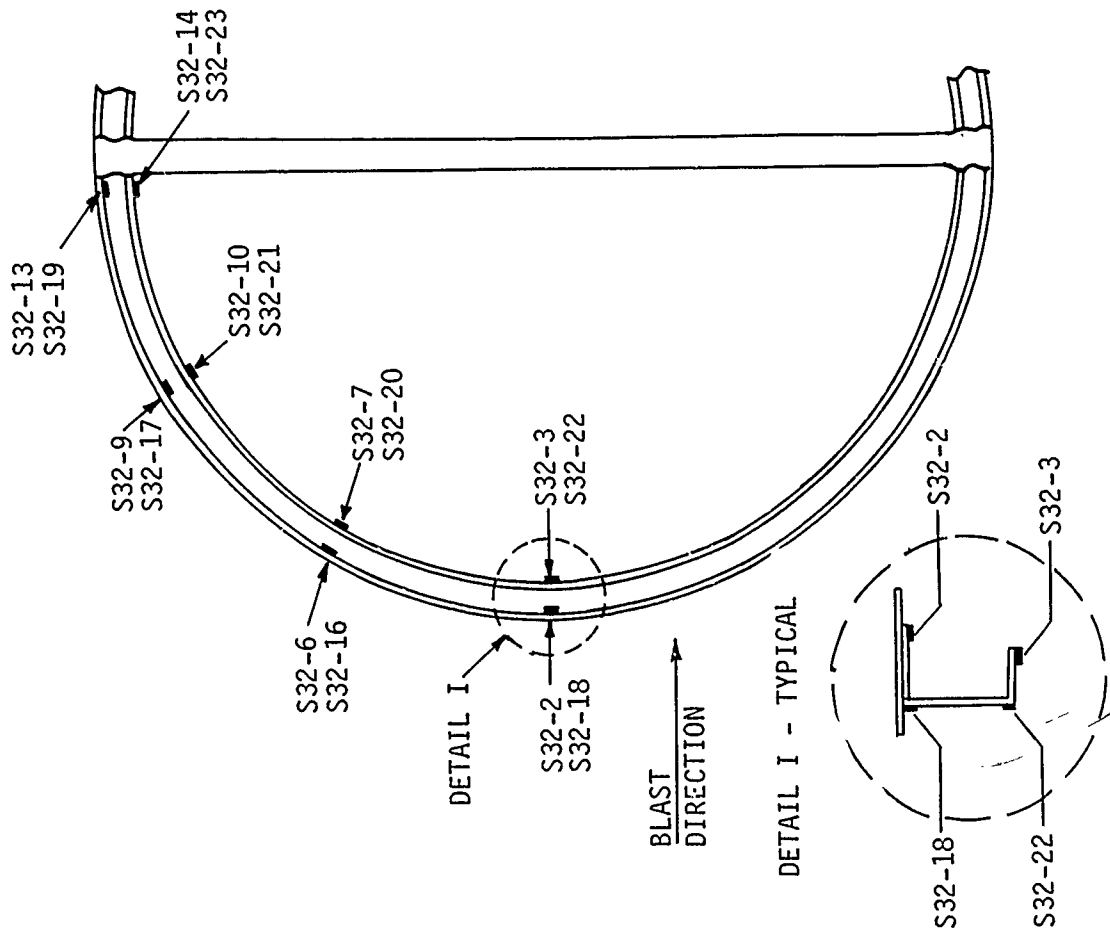


Figure 5. Instrumentation Locations - Specimen 32

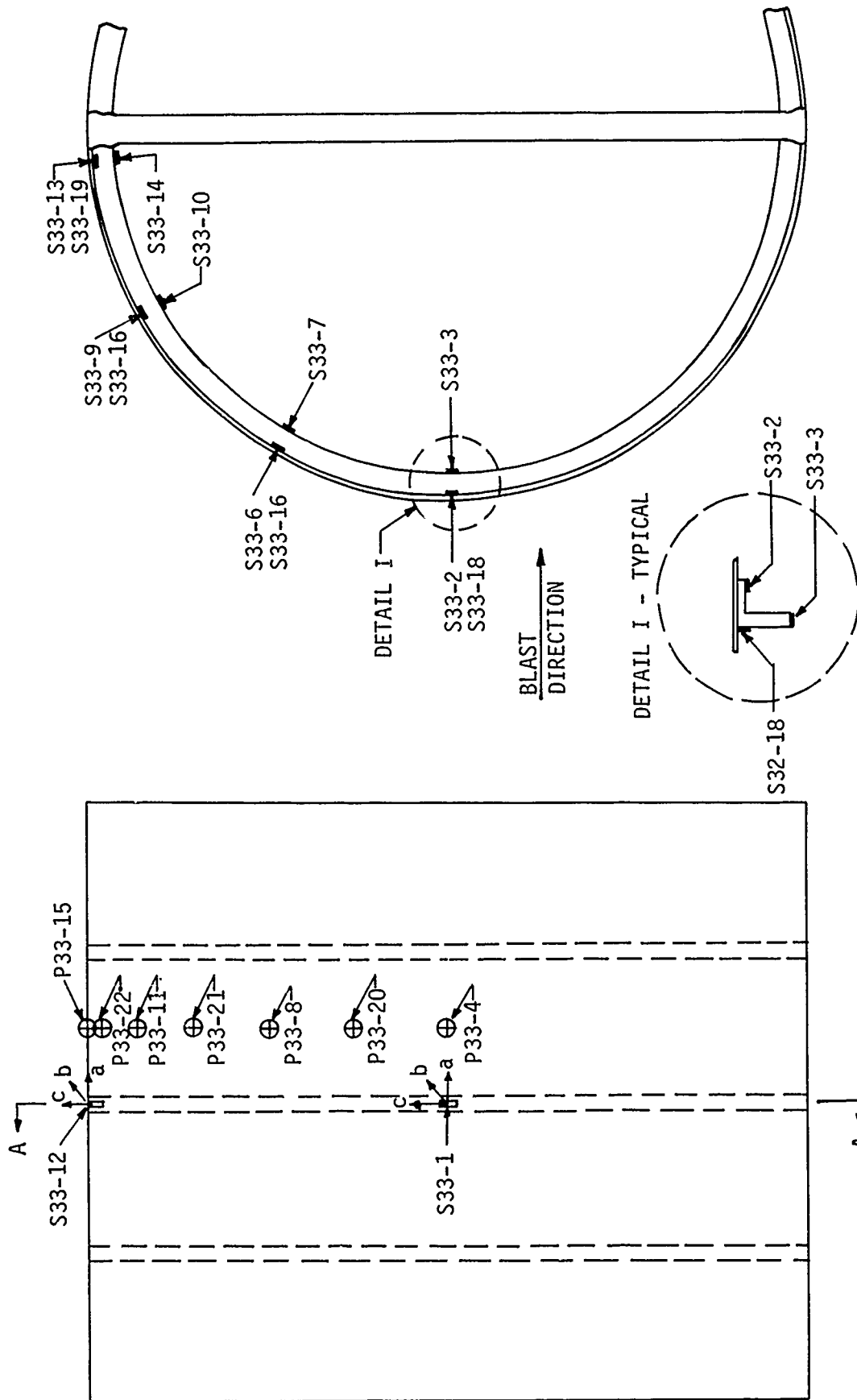
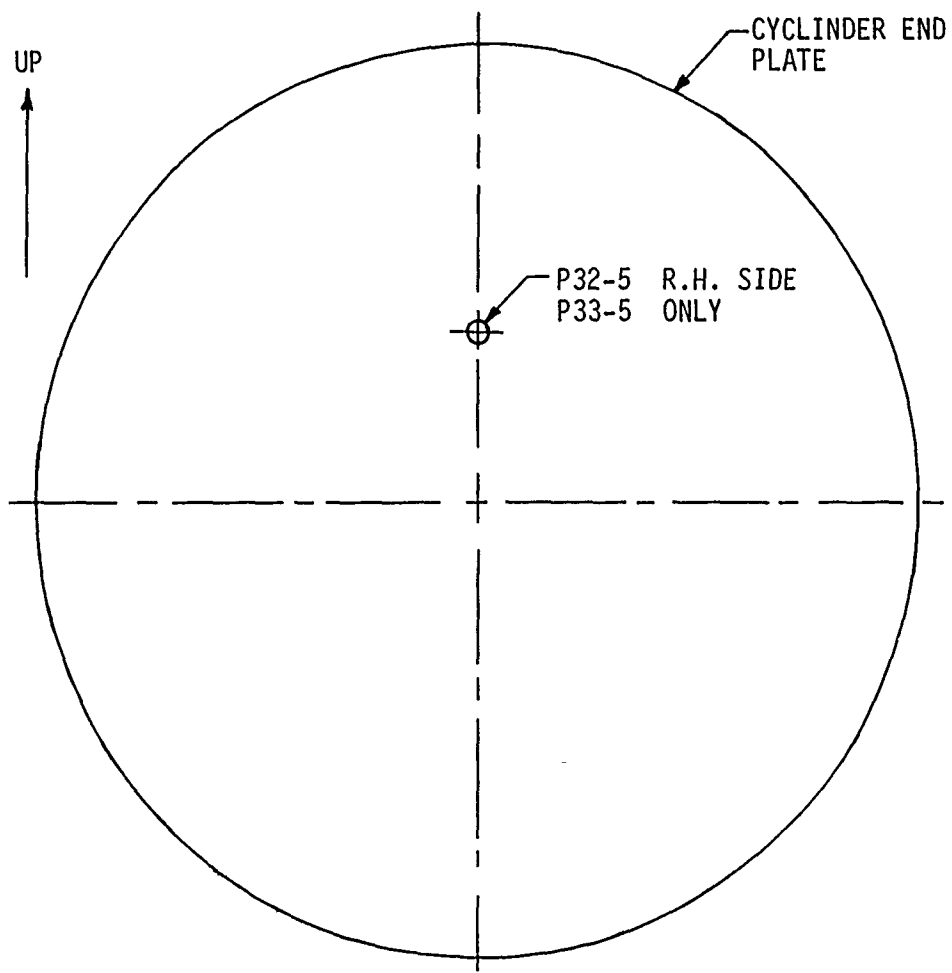
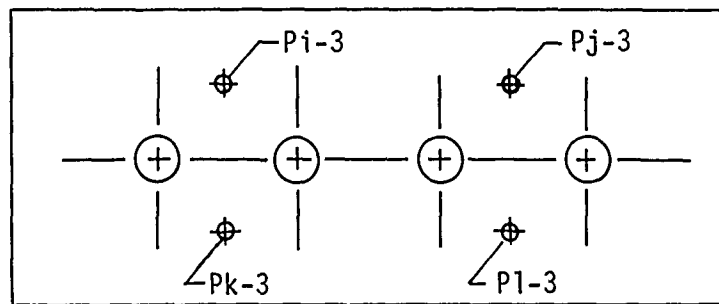


Figure 6. Instrumentation Locations - Specimen 33



R.H. SIDE VIEW - DRUM



WHERE: $i = 18, 22, 24$
 $j = 19, 23, 25$
 $k = 20, 26, 28$
 $l = 21, 27, 29$

Figure 7. Instrumentation Locations - Fixtures

each test shot and, if required, were adjusted to the bridge voltage value present during system calibration. Balancing, setting calibration output, and adjusting the voltage controlled oscillators were also performed at this time.

The pressure channel circuits consisted of full bridge transducers. These transducers were certified prior to shock load testing, and output voltage per test parameter per input voltage was known. The instrumentation was set up utilizing this information.

The deflection system's specification stated a frequency response that was essentially flat from 0 to 2000 Hz. However, a frequency response evaluation was conducted prior to usage which verified its operational characteristics in the frequency range of interest (0-200Hz). Prior to selected test shots, the deflection system was calibrated statically by displacing the sensor and monitoring voltage output versus displacement.

Static load testing also required the use of the test setups which utilized the strain gauges and deflection gauge illustrated in Table 7. In addition, the following certified equipment was utilized: two BLH Model 225 switch and balance units, one BLH Model 120 strain indicator, one Wallace and Tiernam pressure indicator, and two deflection measuring, dial indicators.

Strain data from the strain gauges were reduced to stresses in accordance with the following formulas:

Uni-directional stress - no constraints

$$\sigma = E \epsilon$$

Uni-directional stress - restrained transverse strain

$$\sigma = \frac{E \epsilon}{1-\mu^2}$$

Bi-axial stress - direction known

$$\sigma_a = \frac{E (\epsilon_a + \mu \epsilon_c)}{1-\mu^2}$$

$$\sigma_c = \frac{E (\epsilon_c + \mu \epsilon_a)}{1-\mu^2}$$

Bi-axial stress - direction unknown

$$\sigma_{MAX} = E \left(\frac{\epsilon_a + \epsilon_c}{2(1-\mu)} + \sqrt{\frac{2[(\epsilon_a - \epsilon_b)^2 + (\epsilon_b - \epsilon_c)^2]}{2(1+\mu)}} \right)$$

$$\sigma_{MIN} = E \left(\frac{\epsilon_a + \epsilon_c}{2(1-\mu)} - \sqrt{\frac{2[(\epsilon_a - \epsilon_b)^2 + (\epsilon_b - \epsilon_c)^2]}{2(1+\mu)}} \right)$$

Where:

σ = Stress

E = Modulus of Elasticity (Young's Modulus)

ϵ = Strain

μ = Poisson's Ratio

a) = Subscripts referencing
b) each leg of bi-axial or
c) 45 degree shear rosette strain gauges

6.0 TEST PROCEDURES

6.1 Static Test

Prior to the shock load testing, static overpressure load testing was accomplished for all test specimens. The objectives of the static testing were: (1) to provide experimental data on the structural response of the test specimens to spatially uniform, statically applied overpressure for comparison with static analysis results and subsequent shock test results and (2) to provide a checkout of the strain gauges and deflection measuring system. Since these test specimens were to be shock tested subsequent to the static tests, the static test of each specimen was stopped prior to initiation of yielding. However, minor yielding of two columns inadvertently occurred during static testing. The procedures that were followed during static testing were as delineated below:

- (1) The instrumented specimen was loaded into the appropriate test fixture and instrumentation wiring was connected.
- (2) Photographs were taken.
- (3) Zero load readings were recorded.
- (4) The test fixture was sealed against significant air leaks.
- (5) Except for the column specimens, air was evacuated from within the test fixture/specimen cavity causing an externally applied, uniformly distributed, differential pressure on the specimen. The column specimens were loaded by gradually applying dead weight to a driver piston which was connected to the column.
- (6) Instrumentation readings were recorded at each load increment and evaluated to determine whether the specimen was capable of withstanding the next load increment without yielding.
- (7) After reaching the maximum load established by the test engineer, the load was released and zero load readings were recorded.

6.2 Shock Load Test

The objective of the shock load testing was to expose the test specimens individually (however, the column specimens were tested in sets of four) to a series of simulated nuclear overpressure pulses to determine: (1) the response characteristics of the specimens in the elastic range, (2) the level of free field overpressure defining the threshold of damage (yielding), which will be referred to as the critical free field overpressure, and (3) the degree of permanent deformation resulting from one test shot per specimen at a pressure intensity significantly greater than the respective critical overpressures.

To accomplish the objectives stated above, the flat test specimens were oriented in the shock tube such that the shock propagation vector was perpendicular to the plane of the specimen, whereas the skin/frame cylinders were oriented such that shock propagation vector was perpendicular to the longitudinal axis of the cylinder and also perpendicular to the tangent plane at the midspan of the frame. The columns were oriented such that the shock propagation vector was parallel to the longitudinal axis of the columns.

The procedures that were followed during shock load testing were detailed in advance by Reference 4 and were as delineated below:

- (1) The instrumented test specimen was mounted to the appropriate test fixture.
- (2) The test fixture, complete with specimen, was mounted to the master frame.
- (3) The master frame/fixture/specimen was installed in the shock tube at the pre-selected test station.
- (4) Instrumentation wiring was connected to appropriate cables, and calibration was completed.
- (5) Photographs were taken.
- (6) Based on the requested free field shock intensity, an appropriate amount of explosive was loaded into the driver chamber.
- (7) Immediately after firing, visicorder copies of twelve channels of data were available for examination. In addition, visual inspection of the test setup was conducted after most test shots.
- (8) Based on examination of the structural response data, the next pressure intensity was chosen.
- (9) Steps 5-8 were repeated until yielding occurred (usually four shots per specimen were required).
- (10) A final pressure intensity was chosen such that significant permanent deformation occurred.
- (11) Photographs were taken.
- (12) All instrumentation wiring was disconnected and the specimen/fixture disassembled after each test series.
- (13) The specimen was examined for failure and the nature of the failure recorded.

Thirty-two test shots were conducted for this phase of the program as shown in Table 8.

TABLE 8
TEST SHOT SUMMARY

SANDIA EVENT NO.	TEST SPECIMEN NO.	TEST SPECIMEN TYPE	INCIDENT OVERPRESSURE (PSI)
78-295	18-21	Pinned Columns	1.03
78-296	18-21	Pinned Columns	2.20
78-297	18-21	Pinned Columns	3.50
78-298	18-21	Pinned Columns	4.30
78-327	33	Cylinder	0.5
78-328	33	Cylinder	1.0
78-329	33	Cylinder	1.5
78-330	33	Cylinder	2.0
78-331	33	Cylinder	3.0
78-334	30	Panel	0.58
78-335	30	Panel	0.95
78-336	30	Panel	1.40
78-337	30	Panel	2.60
78-338	30	Panel	4.80
78-339	31	Panel	0.57
78-342	31	Panel	0.85
78-343	31	Panel	1.40
78-344	31	Panel	4.80
78-345	32	Cylinder	0.98
78-346	32	Cylinder	2.0
78-347	32	Cylinder	2.74
78-348	32	Cylinder	5.05
78-349	22,23,26,27	Pinned Columns	1.48
78-350	22,23,26,27	Pinned Columns	3.30
78-351	22,23,26,27	Pinned Columns	7.0
78-352	18-21	Pinned Columns	7.7
78-353	18-21	Pinned Columns	9.5
78-354	24,25,28,29	Clamped Columns	3.2
78-355	24,25,28,29	Clamped Columns	6.2
78-356	24,25,28,29	Clamped Columns	7.0
78-357	24,25,28,29	Clamped Columns	9.5
78-358	24,25,28,29	Clamped Columns	17.0

▷ Due to equipment malfunction the incident overpressure time histories for these test shots were not recorded on magnetic tape. These peak values were read from visicorder data.

7.0 ANALYSIS PROCEDURES

7.1 General Discussion

A variety of analysis techniques were employed in accomplishing this program. For the static load analysis, these techniques included classical strength analysis techniques such as those described in Reference 5 and 6, finite element techniques such as NASTRAN (References 7 - 10), and the NOVA-2LT computer code. For the simulated nuclear overpressure dynamic analysis, NOVA-2LT was utilized exclusively.

7.2 Classical Techniques

Classical stress analysis techniques were utilized where possible to size the test specimens. This sizing was accomplished to provide specimen strengths in the desired overpressure range. Classical techniques are defined as those techniques commonly found in recognized texts or handbooks on the subject of stress analysis which are written by such well-known authors as Roark and Sechler & Dunn (References 5 and 6).

7.3 Finite Element Techniques

The NASTRAN computer code was utilized in the static stress analysis of test specimens 32 and 33, the skin/frame cylinders. In addition to the static stress analysis, a buckling analysis of specimen 33 and vibration analyses of specimen 32 and 33 were accomplished.

NASTRAN is documented extensively in References 7 through 10, and no attempt will be made here to reproduce these documents. Instead, what follows is a brief description of the NASTRAN computer code, highlighting some of its many capabilities.

NASTRAN (NAsa STRuctural Analyzer) is a general purpose digital computer code designed to analyze the behavior of elastic structures under a range of loading conditions using a finite element displacement method approach.

The code is applicable to almost any type of linear and some nonlinear structures that can be represented by combinations of elements contained in the NASTRAN library, such as beams, rods, shear and twist panels, triangular and quadrilateral plates, conical and toroidal shells, solids of revolution, scalar elements, general elements, and constraint elements.

A wide range of analysis capability has been built into NASTRAN including static response to concentrated and distributed loads, to thermal expansion, and to enforced deformation; dynamic response to transient loads, to steady state sinusoidal loads, and to random excitation; determination of real and complex eigenvalues for use in vibration analysis, dynamic stability analysis, and elastic stability analysis. In addition, there is a limited capability for solving nonlinear problems including piecewise linear analysis of nonlinear static response and transient analysis of nonlinear dynamic response.

7.4 NOVA-2LT

NOVA-2LT (Reference 1) is a digital computer program that performs a complex analysis of structural elements subjected to nuclear overpressure effects. This code was developed by Kaman AvIDyne, a division of Kaman Sciences Corporation, for the Analysis Branch of the Air Force Weapons Laboratory. This computer code is documented in detail in Reference 1, and no attempt will be made to reproduce that document in this report. Rather, the analysis techniques contained in the computer code and the capabilities of the computer code that are applicable to this study have been extracted directly from Reference 1 and summarized in this report.

The NOVA-2LT code provides a technique for predicting the elastic and inelastic response of structural elements to the transient pressure loads associated with the blast wave from a nuclear explosion as well as uniform static preblast pressure loads. The high intensity blast pressure loads are associated with the initial reflected pressure which occurs during diffraction of the blast wave around the structure. Because the pressures exist for such a short time, they excite high frequency, secondary structure such as skin panels, stringers, longerons, frames, ribs, canopies, and radomes.

A single element dynamic analysis technique, which considers both linear elastic and inelastic deformations and assumes that the element does not interact with adjacent elements, reduces the complexity of the modeling and analysis, and thus provides a solution more rapidly than a finite element analysis. A 1 KT nuclear standard, based on data obtained from the AFWL SPUTTER and SAP fluid dynamics programs, provides the time dependent free-air blast characteristics for the BLAST routines. However, the user may supply the overpressure loading data which can be static, dynamic, or static plus dynamic in nature. The program consists of three distinct routines, NOVA, DEPROB (Dynamic Elastic Plastic Response of Beams), and DEPROP (Dynamic Elastic Plastic Response of Panels), written in Fortran IV. The NOVA routine is the master routine which controls the logic of the overall program. It contains the subroutines for predicting the blast pressure environment.

8.0 RESULTS

8.1 General Discussion

Results from this study fall into four general categories: static test, static analysis, shock load test, and shock load analysis. Test results are compared to analysis results in Sections 8.2 - 8.5. Results from the static test and shock load test are compared in Section 8.6. Only those data from the critical locations are shown in the figures in this section. The majority of the test data is shown in Volume II.

8.2 Static Load Test/Analysis

In reviewing the following results, the reader should bear in mind that all static loads were applied as a uniform pressure differential acting from outward to inward on the test fixture except, of course, the column specimens. As mentioned in paragraph 6.1, the column specimens were loaded by lead shot. All loads were applied gradually in increments, and data were recorded at each increment. All specimens were analyzed for stress and deflection under load using the NOVA-2LT computer code and either a classical method of analysis or a finite element method of analysis. NOVA-2LT is not designed to analyze columns for stress or deflection under static load. Comparisons of significant test and analysis results are shown in the accompanying figures for each specimen. Static test photographs and static test recorded data are shown in Volume II.

All analyses were conducted utilizing the modulus of elasticity and yield strength established by coupon tests of the material from which the specimen was made. The analyses also utilized actual specimen measured geometry (thickness, area, etc.) to establish the correct section properties.

8.2.1 Test Specimens 18-21

These four specimens are all like columns and are, therefore, discussed here together. These columns are simple flat plates 0.033 inches thick and five inches wide with a clear span of ten inches. The columns were pinned at their ends. The columns contained the following initial eccentricities at their respective mid-spans: specimen 18 (0.015 inches), specimen 19 (0.02 inches), specimen 20 (0.025 inches), and specimen 21 (0.01 inches).

The configuration of the columns was designed to result in relatively high l/p ratios so that the Euler long-column theory would be applicable. Traditionally, columns are considered to have failed at the point at which they buckle. However, since it was known that these columns would undergo dynamic (shock) testing where load duration is a critical factor, it was desired to examine their residual strength after buckling under static load, up to the point of yielding. Figures 8 through 10 illustrate that this residual strength does exist and exceeds the buckling strength.

TEST SPECIMEN NO. 18
STRESS AT CENTER OF COLUMN
(GAUGE S18-1)

○ TEST DATA

$F_{cy} = -42,200 \text{ PSI}$

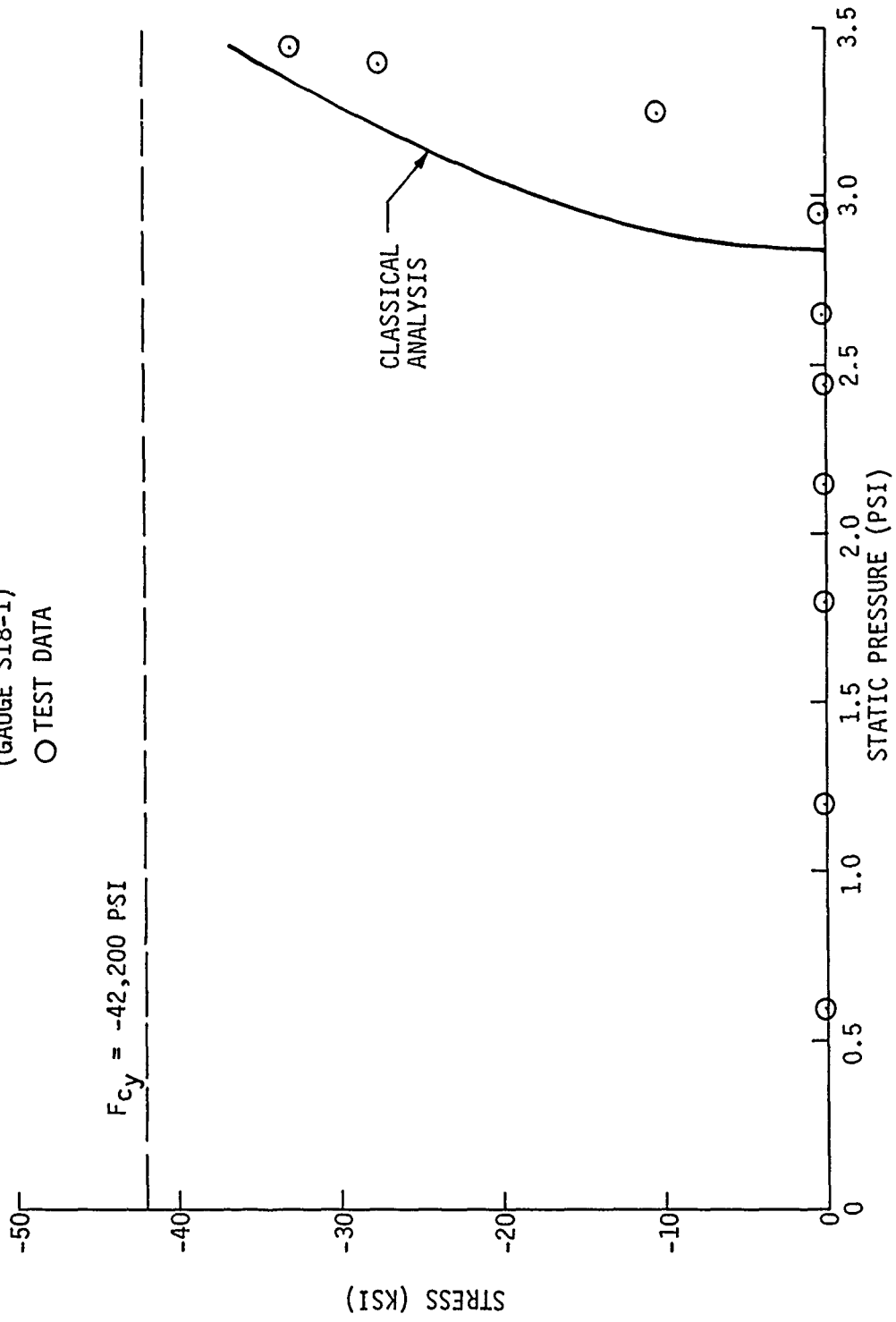


Figure 8. Stress Vs. Static Pressure - Gauge S18-1 - Specimen No. 18

TEST SPECIMEN NO. 18
LATERAL DISPLACEMENT AT
CENTER OF COLUMN

○ TEST DATA

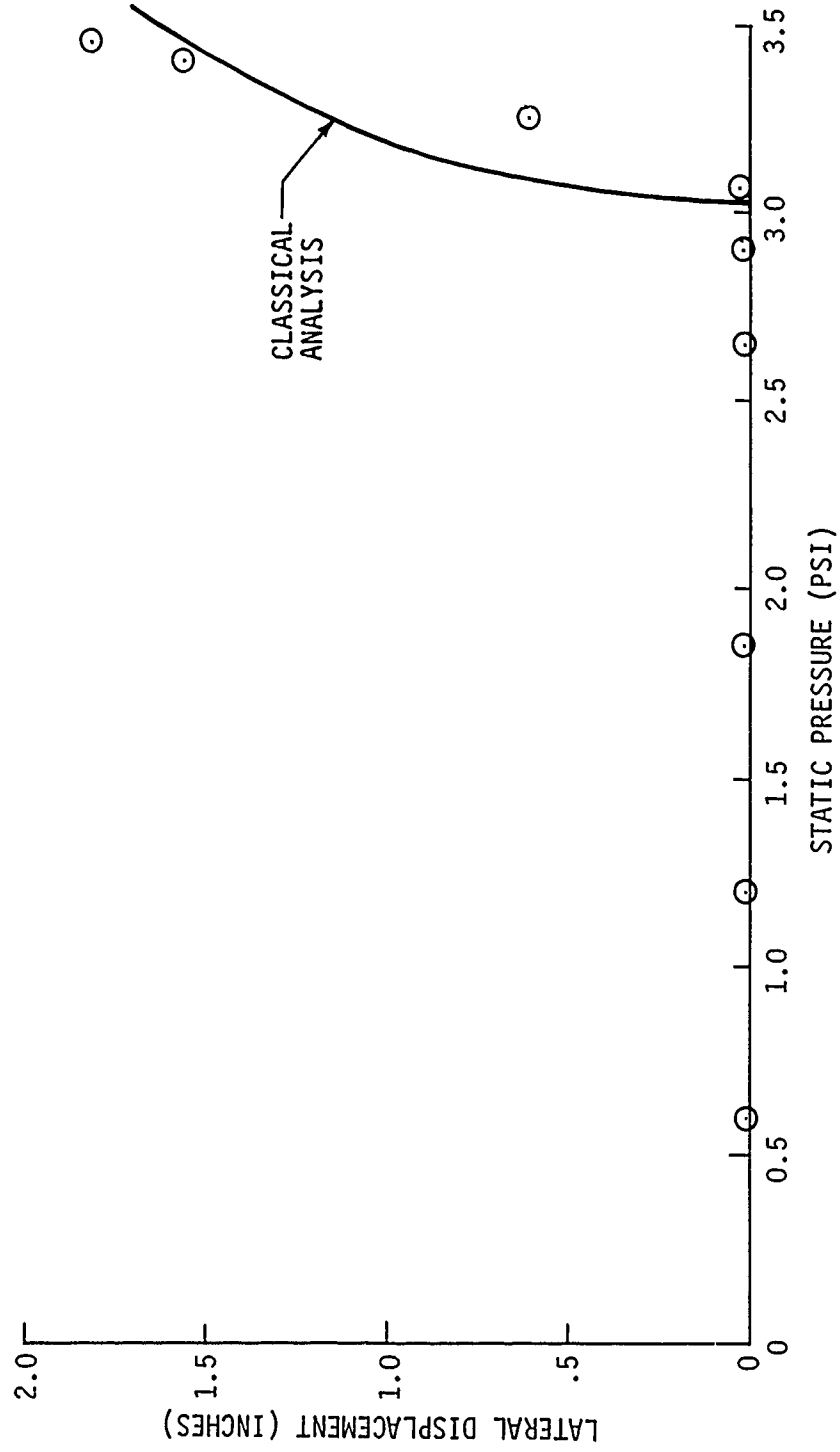


Figure 9. Lateral Displacement Vs. Static Pressure - Specimen No. 18

TEST SPECIMEN NO. 18
STRESS VS. LATERAL DISPLACEMENT
AT CENTER OF COLUMN

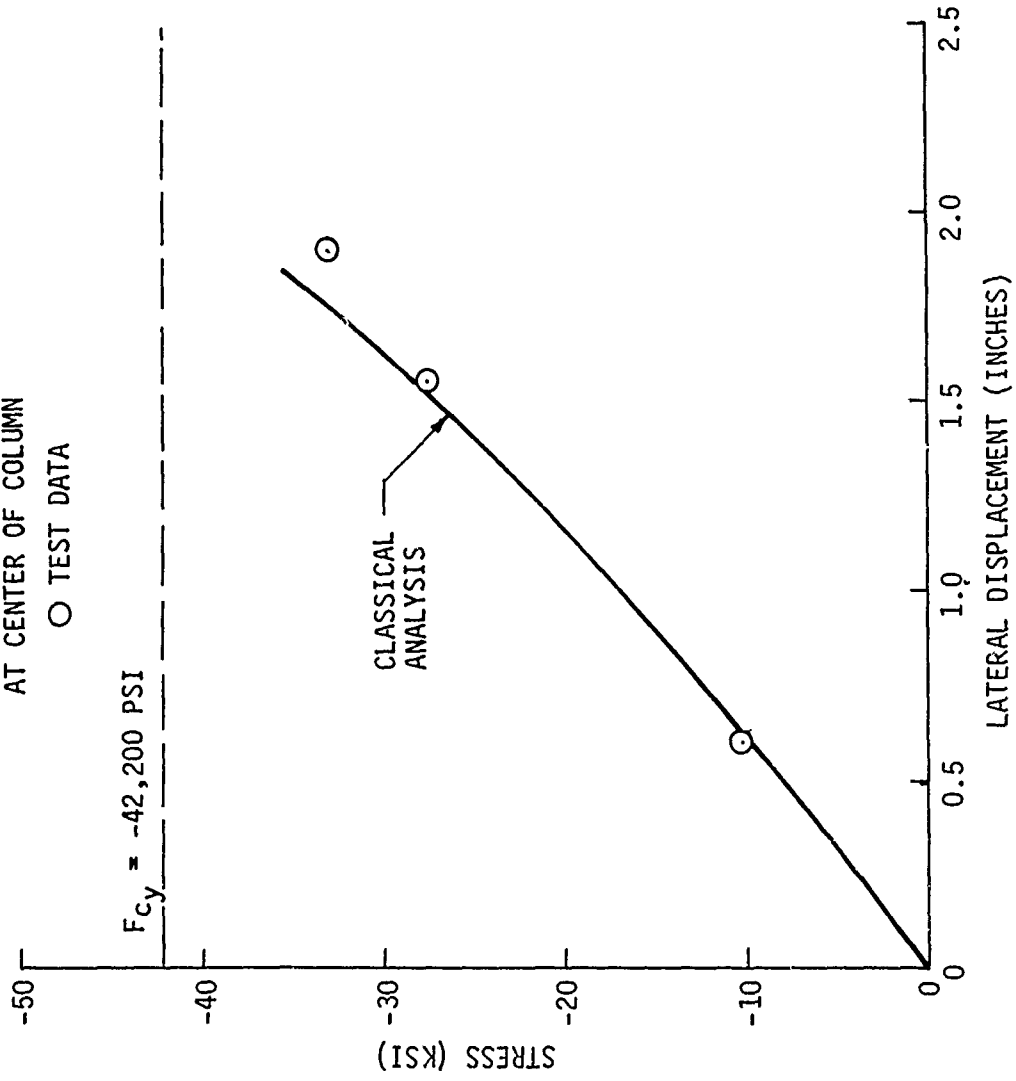


Figure 10. Stress Vs. Lateral Displacement - Specimen No. 18

Analyses of long columns beyond the buckling mode are rare; so an analysis method was derived based on the assumption that the columns displace in a partial sine-wave shape. This assumption was verified by the test as shown in the excellent correlation between test and analysis with regard to deflection as shown in Figures 9 and 10. This analysis method is discussed in detail in Reference 3. NOVA-2LT does not predict the behavior of columns under static load and, therefore, could not be used here.

The effect of initial eccentricity on the response of the columns is illustrated in Table 9. With the exception of several data points, the static test results indicated that as the initial eccentricity increased, response for a given load level also increased. As shown, the amount of initial eccentricity influenced the load level at which the column buckled as well as the response prior to buckling. However, it appeared that all four columns would have yielded at approximately the same load level.

TABLE 9
EFFECTS OF COLUMN INITIAL ECCENTRICITIES
SPECIMENS 18-21

STATIC PRESSURE (PSI)	STRESS AT CENTER OF COLUMNS (PSI)			
	SPEC. 18	SPEC. 19	SPEC. 20	SPEC. 21
	$\delta = 0.015$	$\delta = 0.020$	$\delta = 0.025$	$\delta = 0.010$
2.65	-141	-1183	-2376	-1012
3.26	-10252	-11047	-11903	-9890
3.41	-27543	-28254	-29147	-25788
3.45	-32865	-32885	-32915	-32872

8.2.2 Test Specimens 22-23

These two columns are simple flat plates 0.028 inches thick and five inches wide with a clear span of ten inches. The columns were pinned at their ends and contained the following initial eccentricities at their respective mid-spans: specimen 22 (0.075 inches) and specimen 23 (0.025 inches).

Figures 11 through 13 illustrate stress and lateral displacement at the center of the two columns versus applied load and the relationship between stress and lateral displacement. Also shown are analysis results from the classical Euler theory. Figures 11 and 12 also indicate the effect of initial imperfection on the response characteristics of the columns.

TEST SPECIMENS 22-23
STRESS AT CENTER OF COLUMNS

- GAUGE S22-1
- △ GAUGE S23-2

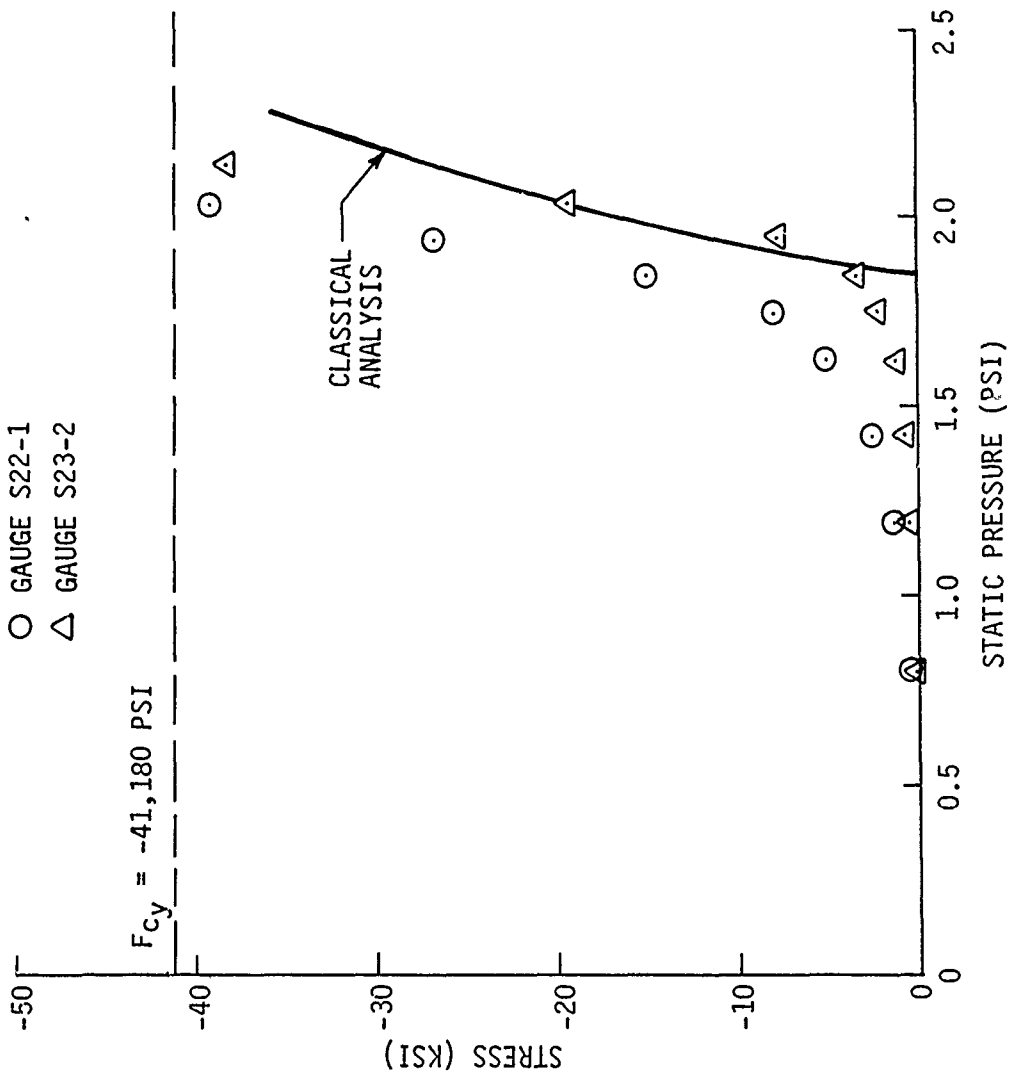


Figure 11. Stress Vs. Static Pressure - Gauge S22-1 (Specimen No. 22) and Gauge S23-2 (Specimen No. 23)

TEST SPECIMENS 22-23
 LATERAL DISPLACEMENT AT
 CENTER OF COLUMNS

- SPECIMEN NO. 22
- △ SPECIMEN NO. 23

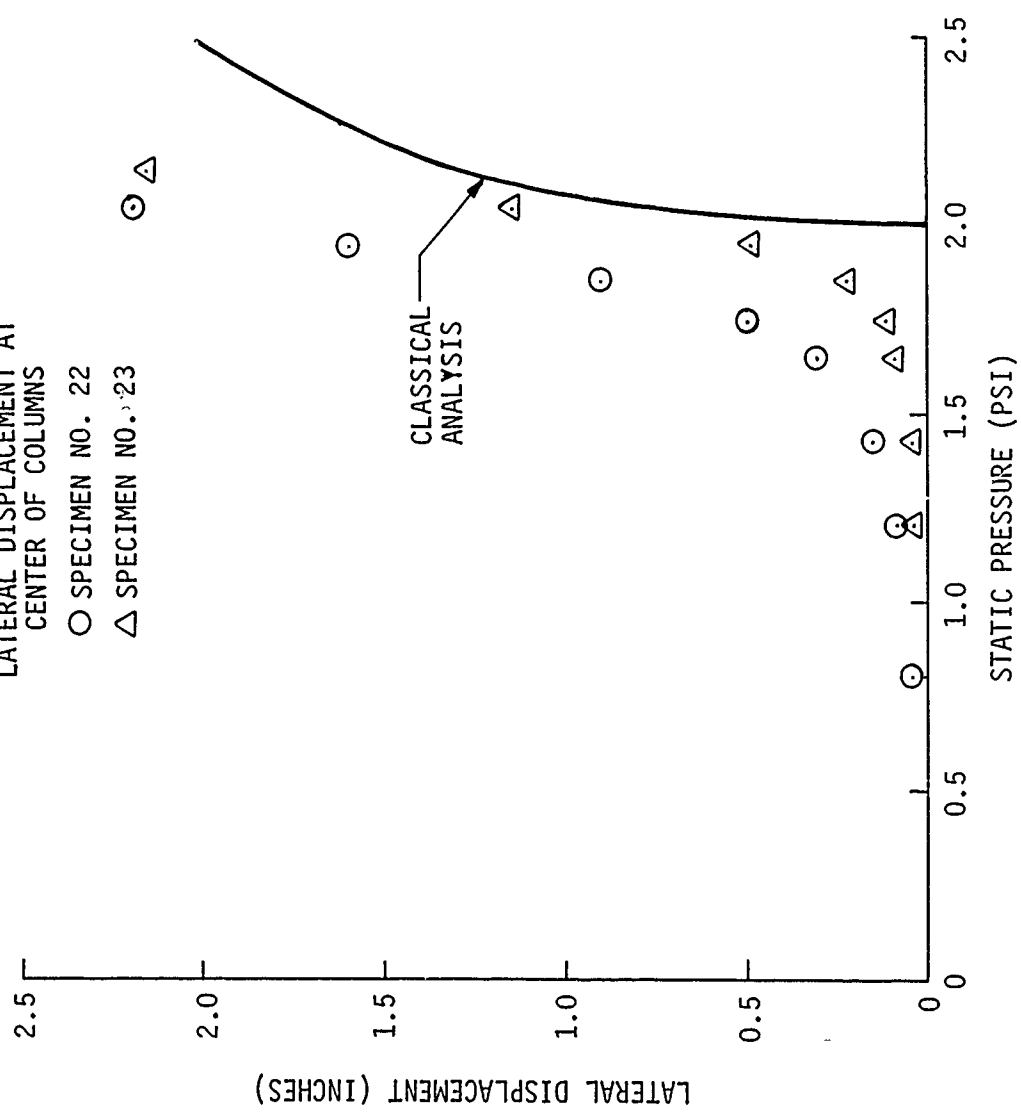


Figure 12. Lateral Displacement Vs. Static Pressure - Specimens 22-23

TEST SPECIMENS 22-23
STRESS VS. LATERAL DISPLACEMENT
AT CENTER OF COLUMNS

○ SPECIMEN NO. 22
△ SPECIMEN NO. 23

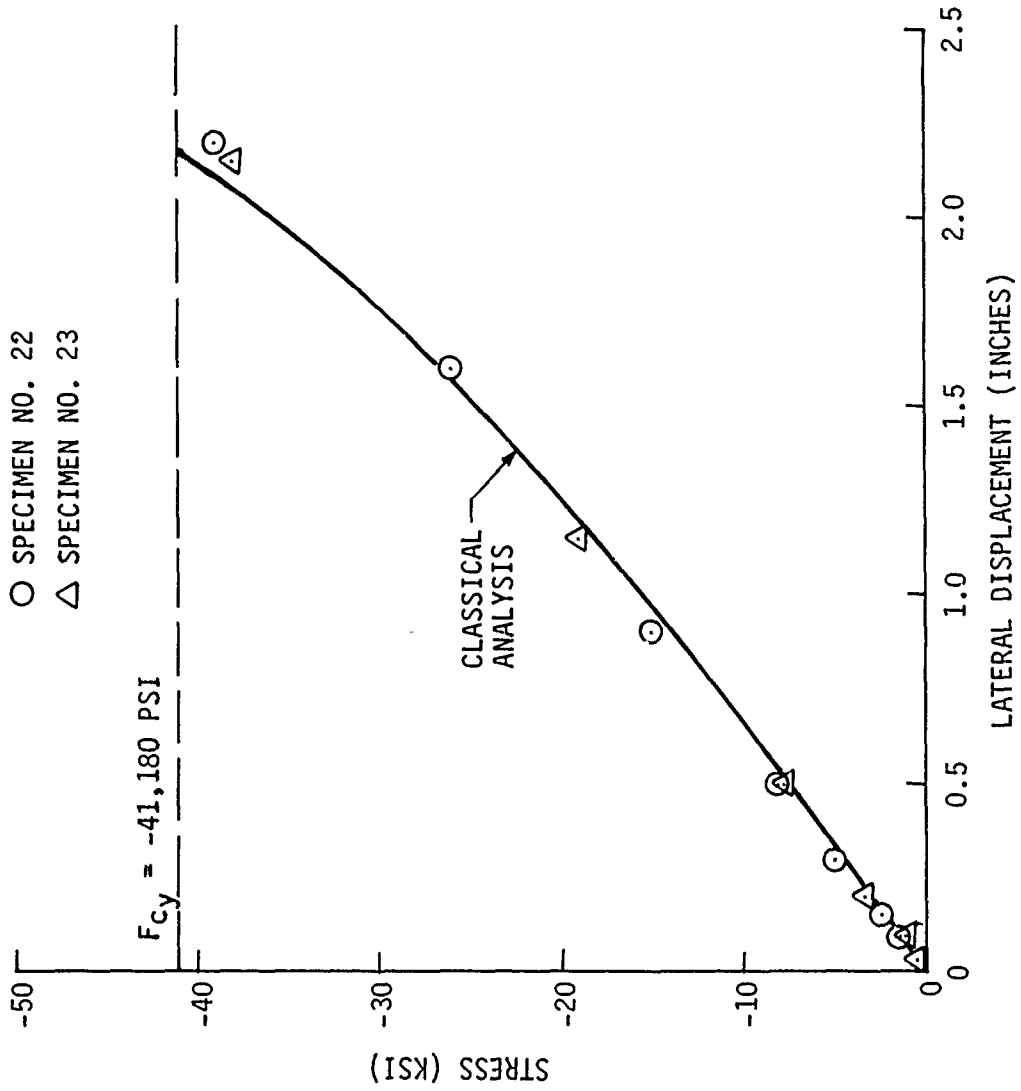


Figure 13. Stress Vs. Lateral Displacement - Specimens 22-23

8.2.3 Test Specimens 24-25

These two columns are simple flat plates 0.028 inches thick and five inches wide with a clear span of ten inches. These columns were clamped at their ends and contained the following initial eccentricities at their respective mid-spans: specimen 24 (0.57 inches) and specimen 25 (0.05 inches). As indicated earlier in this report, the large eccentricity for specimen 24 resulted from the fact that it was inadvertently yielded during the static test.

Figures 14 and 15 illustrate stress and lateral displacement at the center of the two columns versus applied load. Figure 16 shows the relationship between stress and lateral displacement. Also shown are analysis results from the classical Euler theory. The effect of initial eccentricity on the response characteristics of the two columns is very significant as shown in Figures 14 and 15.

8.2.4 Test Specimens 26-27

Specimens 26 and 27 are simple flat plates 0.025 inches thick and five inches wide with a clear span of ten inches. These columns were pinned at their ends and contained the following initial eccentricities at their respective mid-spans: specimen 26 (0.13 inches) and specimen 27 (less than 0.005 inches). Similar to specimen 24, specimen 26 was inadvertently yielded during the static test.

Figures 17 and 18 illustrate stress and lateral displacement at the center of specimen 26 versus applied load. Figure 19 shows the relationship between stress and lateral displacement. Also shown are analysis results from the classical Euler theory.

8.2.5 Test Specimens 28-29

Specimens 28 and 29 are simple flat plates 0.025 inches thick and five inches wide with a clear span of ten inches. These columns were clamped at their ends and contained the following initial eccentricities at their respective mid-spans: specimen 28 (0.01 inches) and specimen 29 (less than 0.005 inches).

Figures 20 and 21 illustrate stress and lateral displacement at the center of the two columns versus applied load. Figure 22 shows the relationship between stress and lateral displacement. Also shown are analysis results from the classical Euler theory.

8.2.6 Test Specimen 30

Specimen 30 is a flat, homogeneous, 6061-T6 panel. The panel is 22 inches square, 0.039 inches thick, and clamped along all four sides. Based on the geometry of this panel (span/thickness = 564), it is categorized as a membrane.

Similar to the data shown in Reference 3 for membrane panels, test stresses at the center of the fixed edges were considerably higher than predicted as shown in Figure 23. This phenomenon is commonplace in membrane structures

TEST SPECIMENS 24-25
STRESS AT CENTER OF COLUMNS

- GAUGE S24-1
- △ GAUGE S25-1

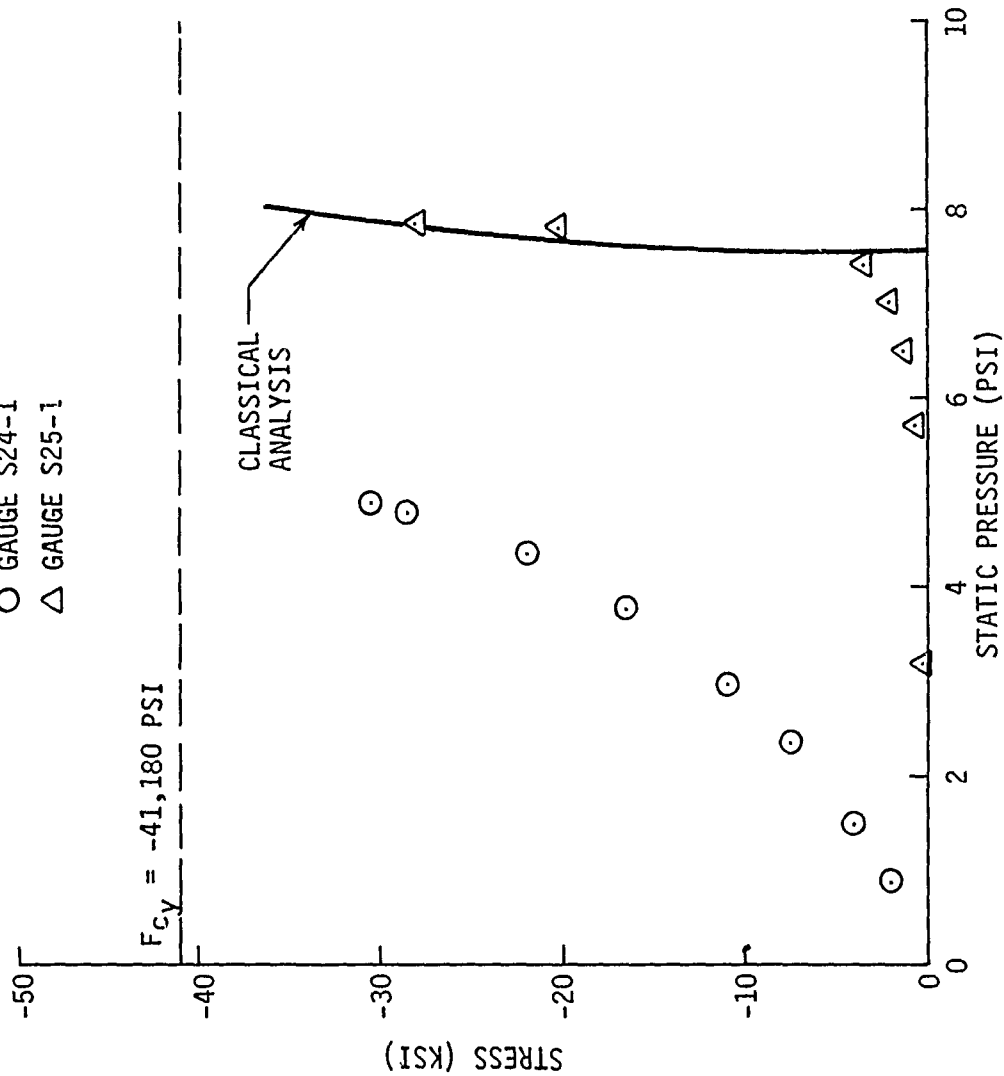


Figure 14. Stress Vs. Static Pressure - Gauge S24-1 (Specimen No. 24) and Gauge S25-2 (Specimen No. 25)

TEST SPECIMENS 24-25
LATERAL DISPLACEMENT AT
CENTER OF COLUMNS

- SPECIMEN NO. 24
- △ SPECIMEN NO. 25

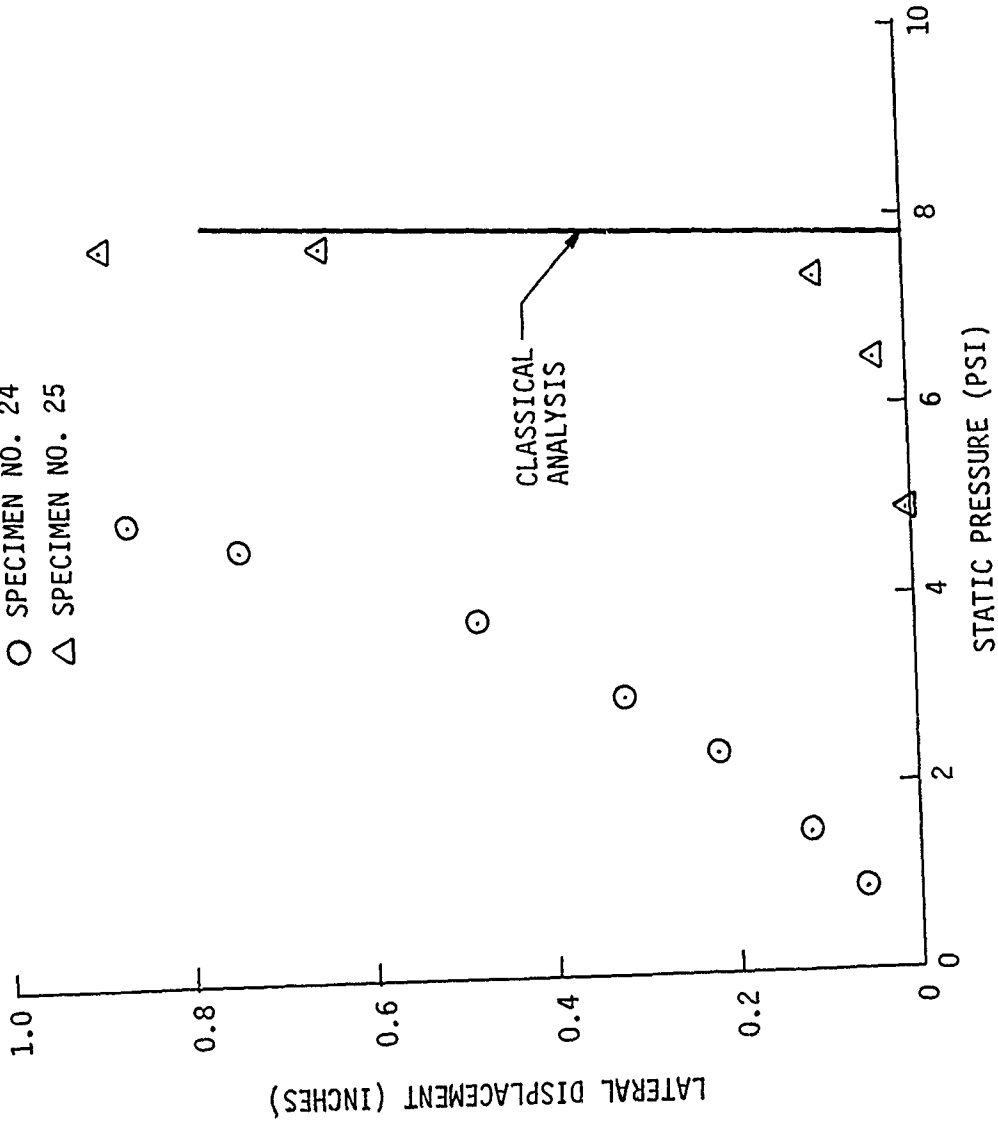


Figure 15. Lateral Displacement Vs. Static Pressure - Specimens 24-25

TEST SPECIMENS 24-25
STRESS VS. LATERAL DISPLACEMENT
AT CENTER OF COLUMNS

○ SPECIMEN NO. 24

△ SPECIMEN NO. 25

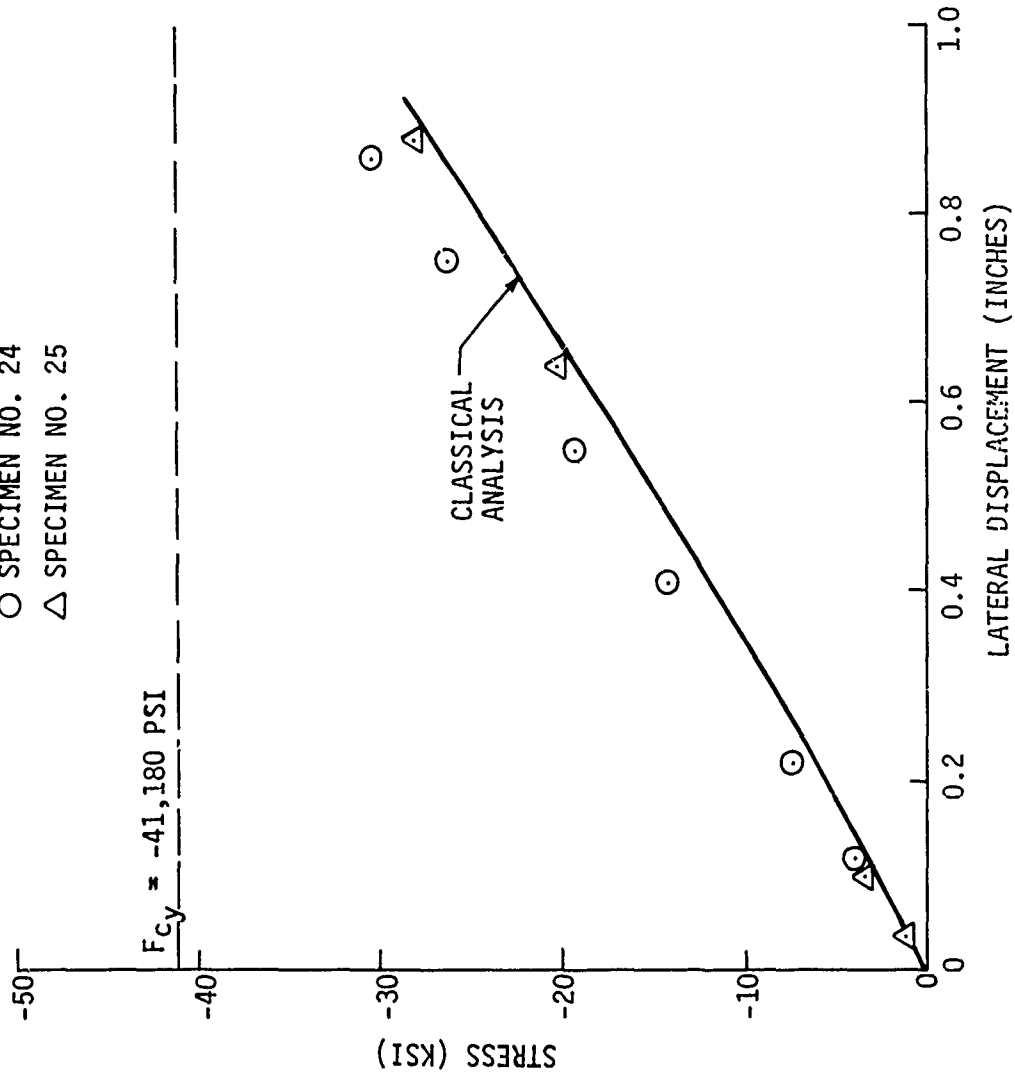


Figure 16. Stress Vs. Lateral Displacement - Specimens 24-25

TEST SPECIMEN NO. 27
STRESS AT CENTER OF COLUMN

○ GAUGE S27-1

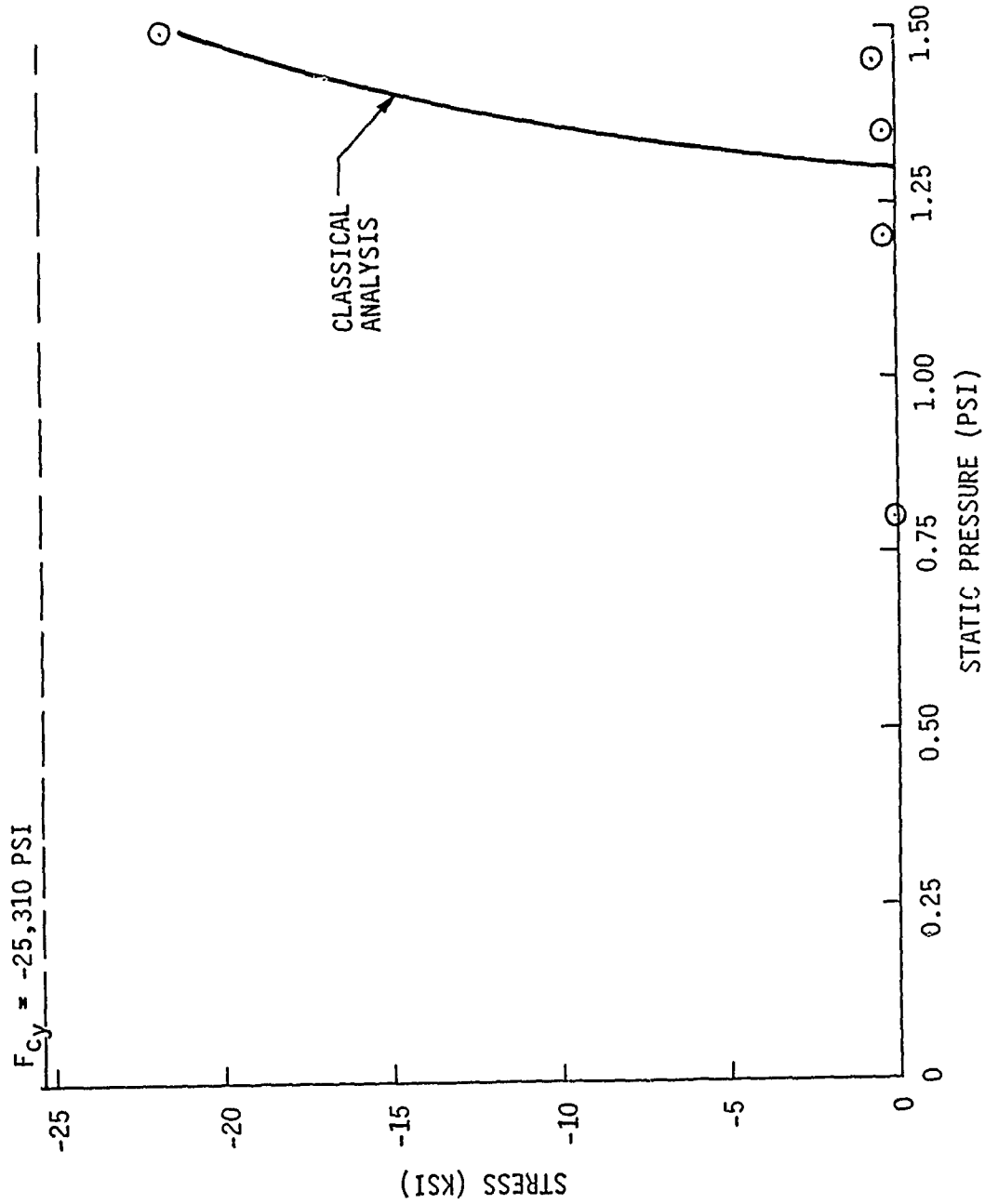


Figure 17. Stress Vs. Static Pressure - Gauge S27-1 (Specimen No. 27)

TEST SPECIMEN NO. 27
LATERAL DISPLACEMENT AT
CENTER OF COLUMN

○ TEST DATA

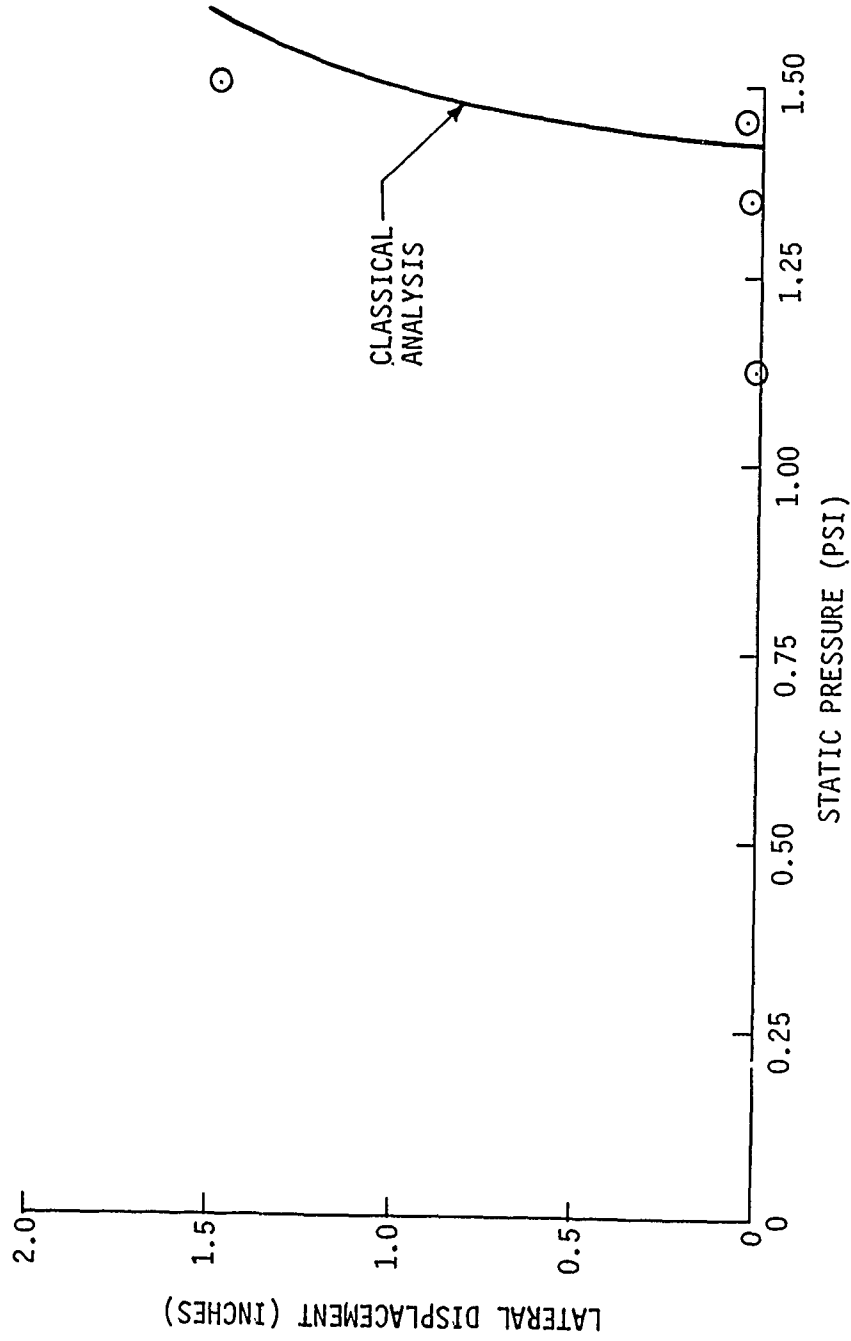


Figure 18. Lateral Displacement Vs. Static Pressure - Specimen No. 27

TEST SPECIMEN NO. 27
STRESS VS. LATERAL DISPLACEMENT
AT CENTER OF COLUMN

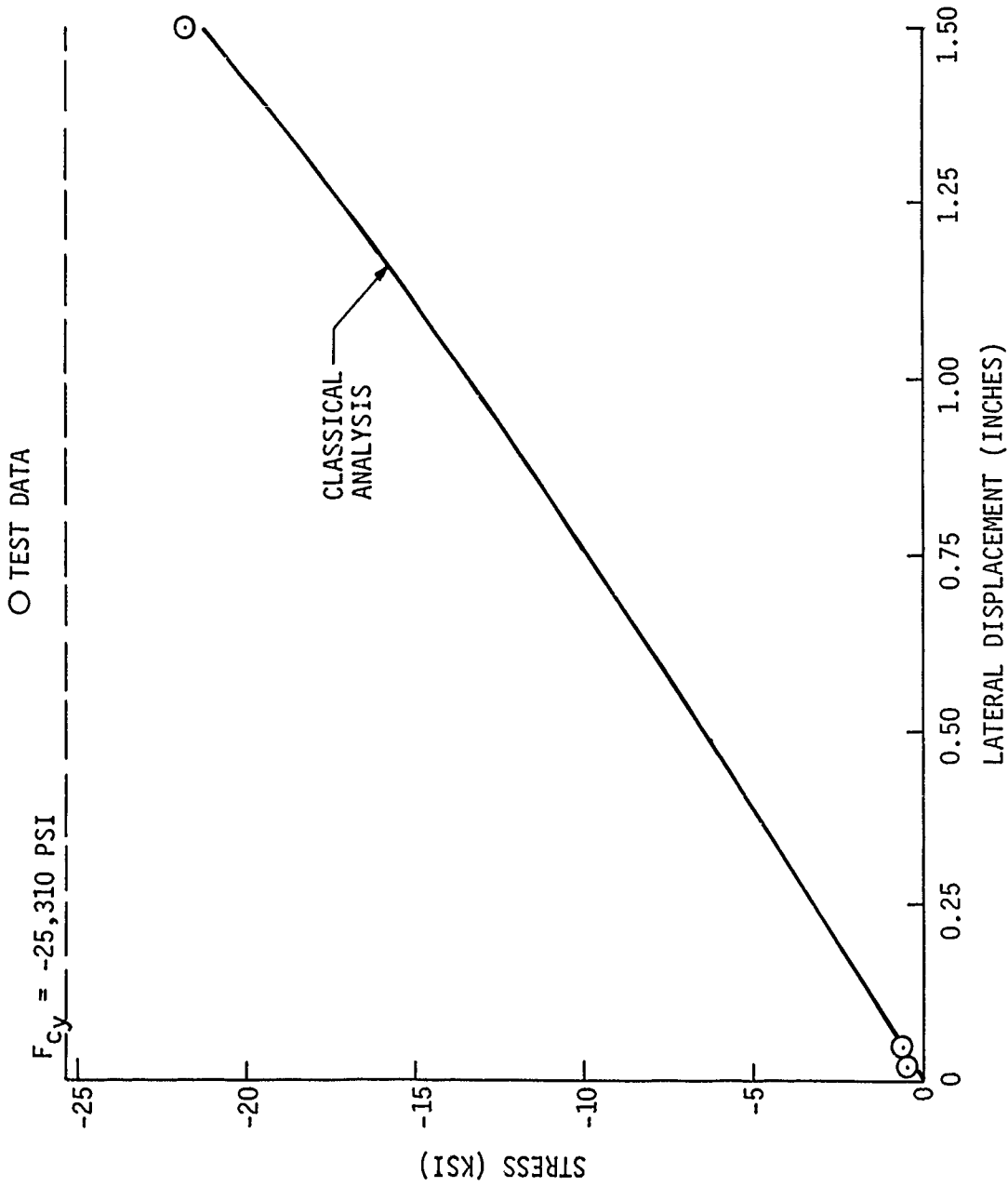


Figure 19. Stress Vs. Lateral Displacement - Specimen No. 27

TEST SPECIMENS 28-29
STRESS AT CENTER OF COLUMNS

- GAUGE S28-2
- △ GAUGE S29-2

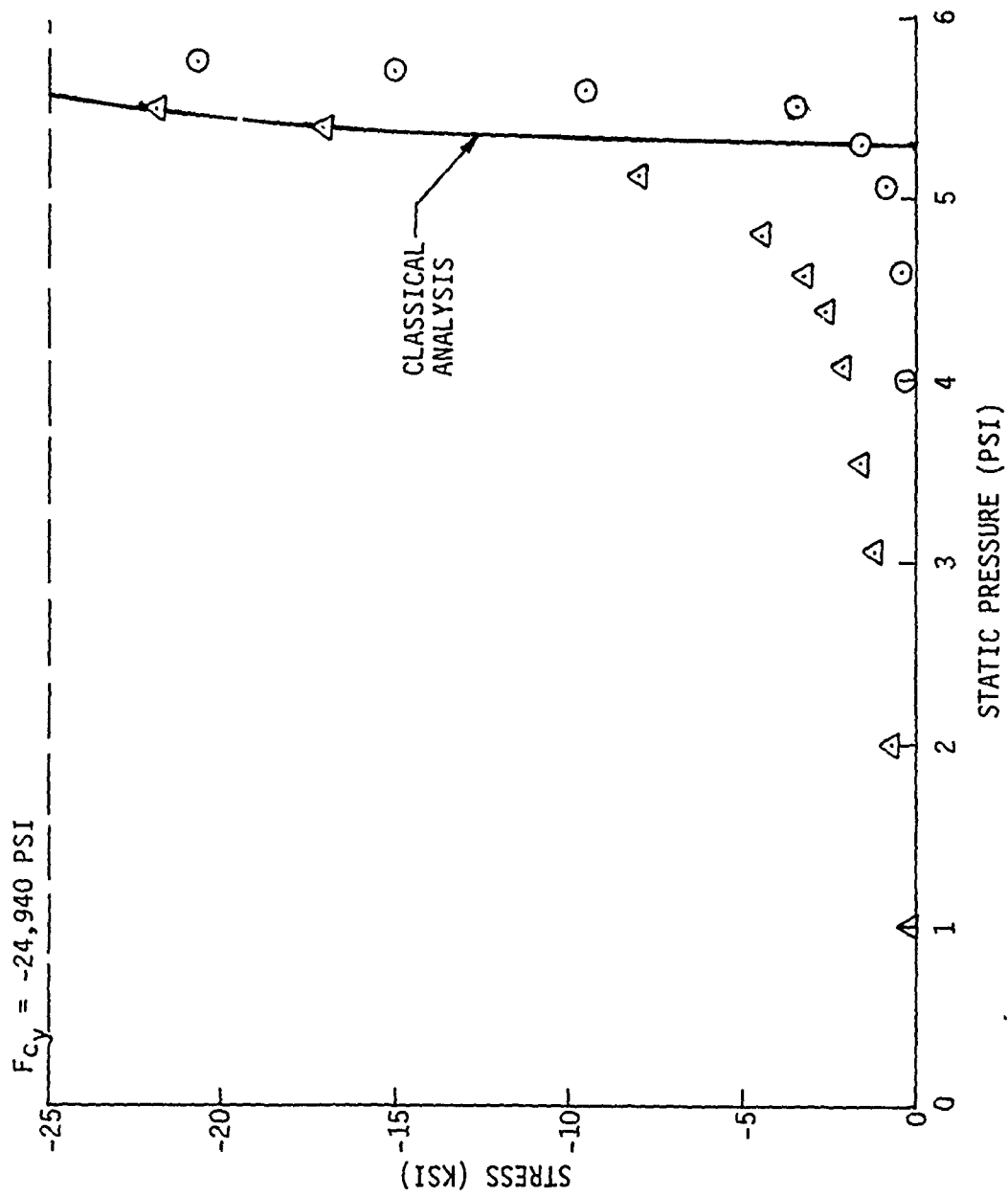


Figure 20. Stress Vs. Static Pressure - Gauge S28-2 (Specimen No. 28) and Gauge S29-2 (Specimen No. 29)

TEST SPECIMENS 28-29
LATERAL DISPLACEMENT AT
CENTER OF COLUMNS

- SPECIMEN NO. 28
- △ SPECIMEN NO. 29

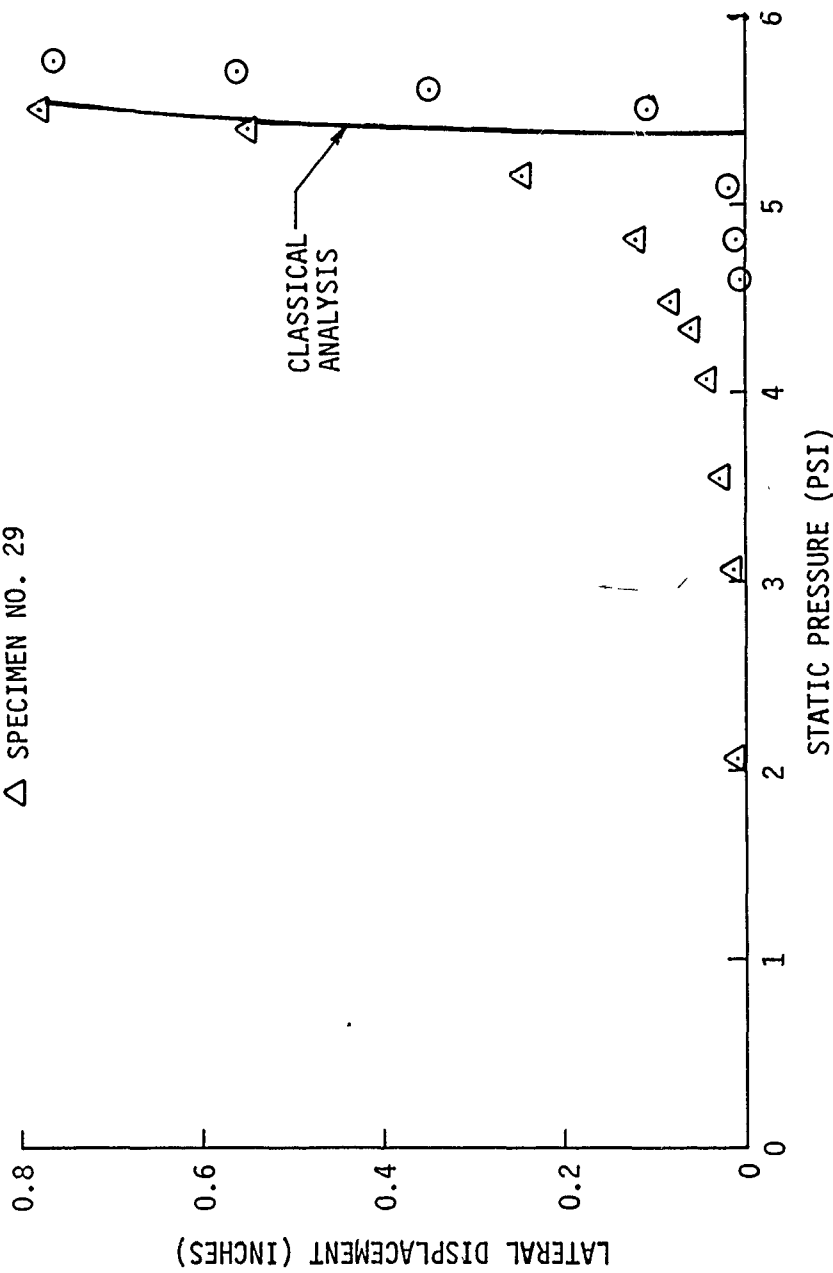


Figure 21. Lateral Displacement Vs. Static Pressure - Specimens 28-29

TEST SPECIMENS 28-29
 STRESS VS. LATERAL DISPLACEMENT
 AT CENTER OF COLUMNS

○ SPECIMEN NO. 28
 △ SPECIMEN NO. 29

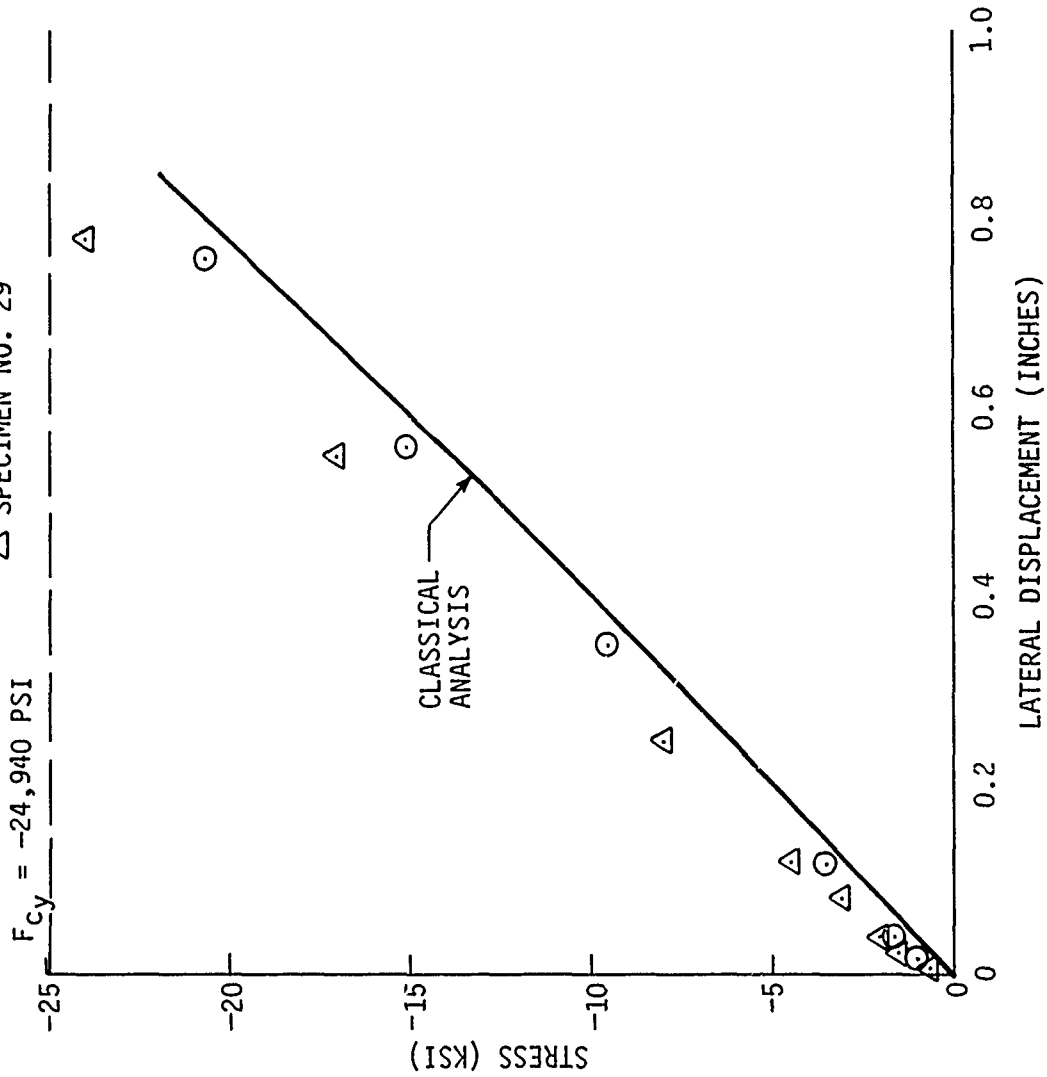


Figure 22. Stress Vs. Lateral Displacement - Specimens 28-29

TEST SPECIMEN NO. 30
STRESS AT EDGE OF PANEL

○ AVERAGE OF S30-3 AND S30-5

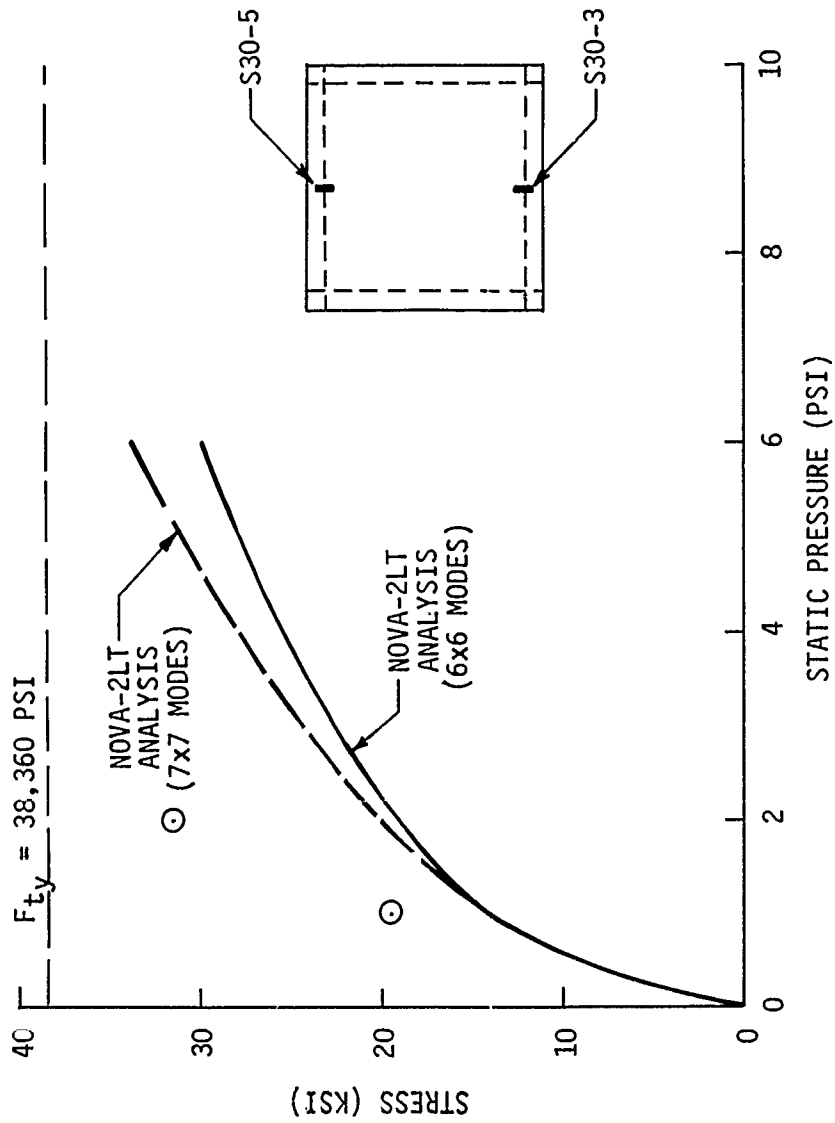


Figure 23. Stress Vs. Static Pressure - Gauges S30-3 and S30-5 - Specimen No. 30

because of the substantial bending of the material that takes place over the supports. This phenomenon has little effect on the panel overall strength since, once the yielding has occurred, the panel behaves as a membrane. As shown in Figure 23, one NOVA-2LT analysis model retained 21 of 36 modal combinations and a 13 by 13 analysis mesh of integration points (see Reference 1). The other NOVA-2LT model retained 25 of 49 modal combinations and a 15 x 15 analysis mesh of integration points. For both models, the test strains diverge from the analysis strains at the higher overpressure intensities. These results are essentially the same as those obtained for the membrane panel which was tested in the Reference 3 study. The correlation between test and analysis regarding stress and displacement at the center of the panel is quite good as shown in Figures 24-25.

8.2.7 Test Specimen 31

Specimen 31 is a flat, homogeneous, 6061-T6 panel. The panel is 22 inches square, 0.062 inches thick, and clamped along all four sides. Based on the geometry of this panel (span/thickness = 355), it is categorized as a thin plate. However, it is more nearly a membrane panel than a thick plate.

Figures 26-28 illustrate test and analysis stress data at the center of the edge and stress as well as deflection data at the center of the panel. Figure 26 shows data similar to that in Figure 23. That is, test stresses at the center of the panel edge were considerably higher than predicted. However, the correlation between test and analysis was considerably better than that for specimen 30. This is due to the fact that the effect of bending at the clamped support is more pronounced for the thinner panel. As the panel thickness is increased, the stress gradient due to bending at the panel edge is easier to predict analytically. The stress and deflection at the panel center were predicted very accurately as shown in Figures 27 and 28.

8.2.8 Test Specimen 32

As mentioned in Section 3.9, this specimen is a stiffened, full cylinder with channel cross-section frames. The frames, in addition to being full cylindrical rings, incorporate a relatively stiff, integral bar that bisects the cylinder at the diameter and spans from side to side. This configuration simulates the ring frame of a circular fuselage fixed to the floor beam. In addition, incorporation of this bar permits utilization of NOVA-2LT as an analysis tool, since it does not analyze a full 360 degree multi-layered structure such as this frame. The frames in specimen 32 were designed to be essentially identical to specimen 12 of Reference 3 regarding cross-sectional area and bending stiffness about an axis parallel to the longitudinal axis of the cylinder. The significant difference between the two specimens discussed above is that the cross-section of specimen 32 is unsymmetric, whereas the cross-section of specimen 12 is symmetric. This design feature of specimen 32 introduced twisting of the frame as well as bending of the frame under applied load.

Static test/analysis results for specimen 32 are shown in Figures 29-32. Figure 29 illustrates stress in the inner flange at a location approximately

TEST SPECIMEN NO. 30
DEFLECTION AT CENTER OF PANEL

○ GAUGE D30-9

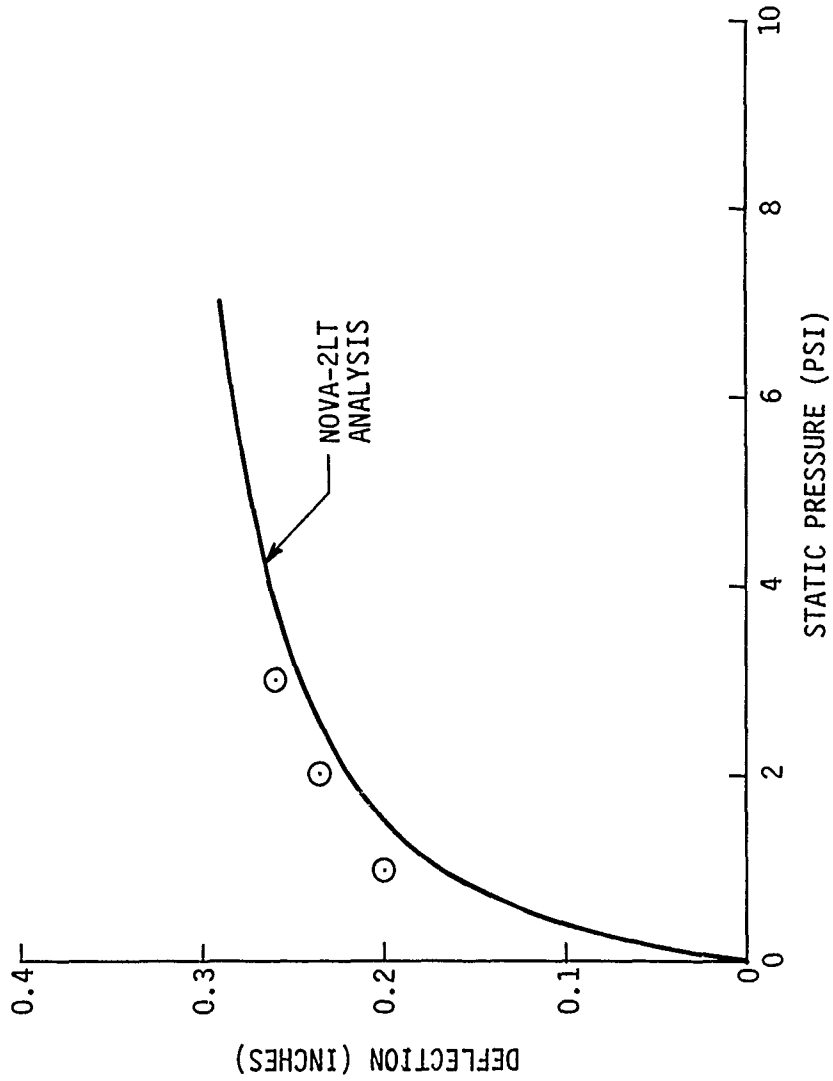


Figure 24. Deflection Vs. Static Pressure - Gauge D30-9 - Specimen No. 30

TEST SPECIMEN NO. 30
STRESS AT CENTER OF PANEL

○ GAUGE S30-2

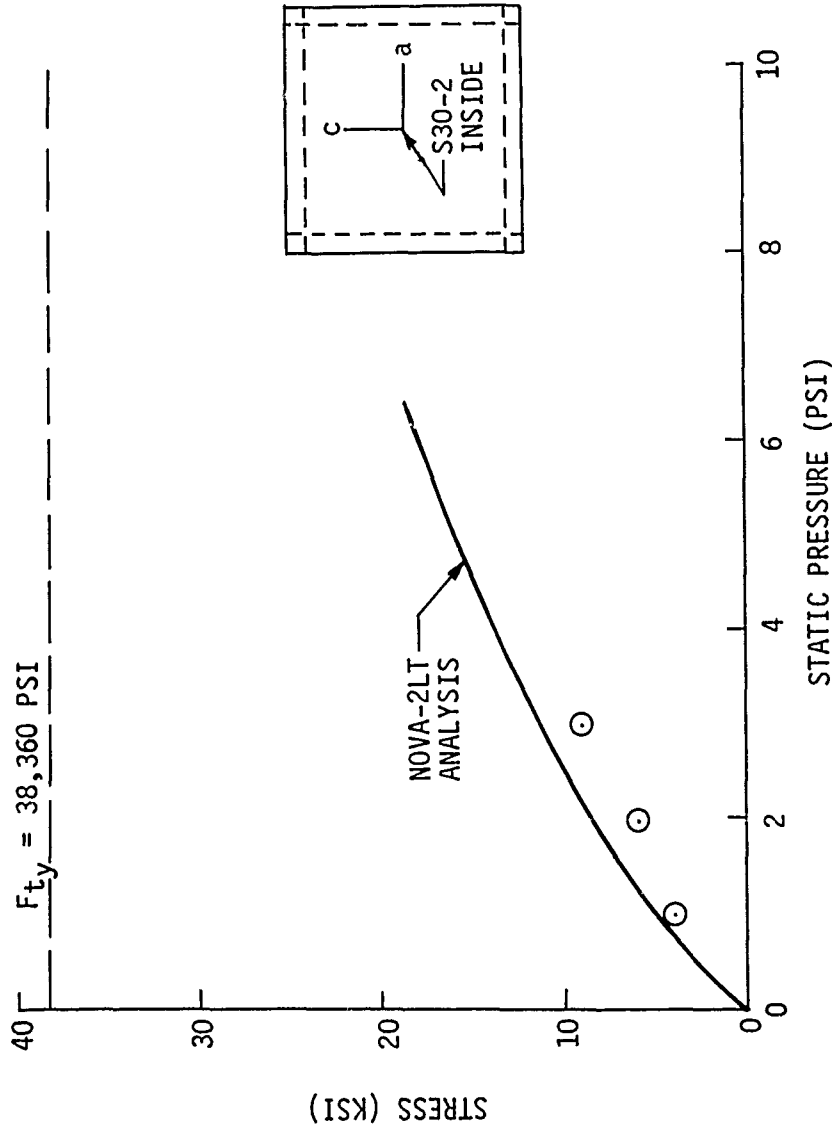


Figure 25. Stress Vs. Static Pressure - Gauge S30-2 - Specimen No. 30

TEST SPECIMEN NO. 31
STRESS AT EDGES OF PANEL

○ AVERAGE OF S31-3 AND S31-5

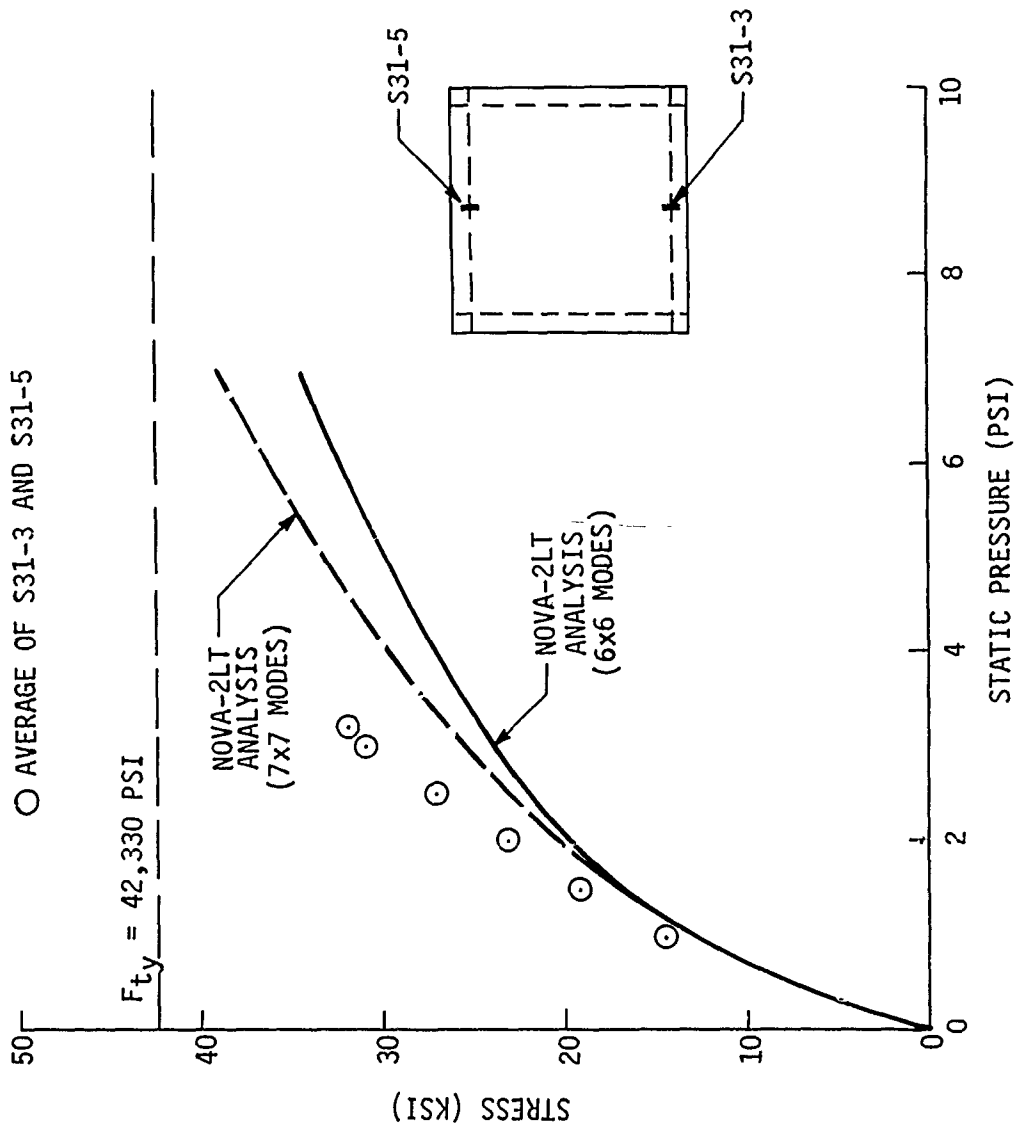


Figure 26. Stress Vs. Static Pressure - Gauges S31-3 and S31-5 - Specimen No. 31

TEST SPECIMEN NO. 31
DEFLECTION AT CENTER OF PANEL

○ GAUGE D31-9

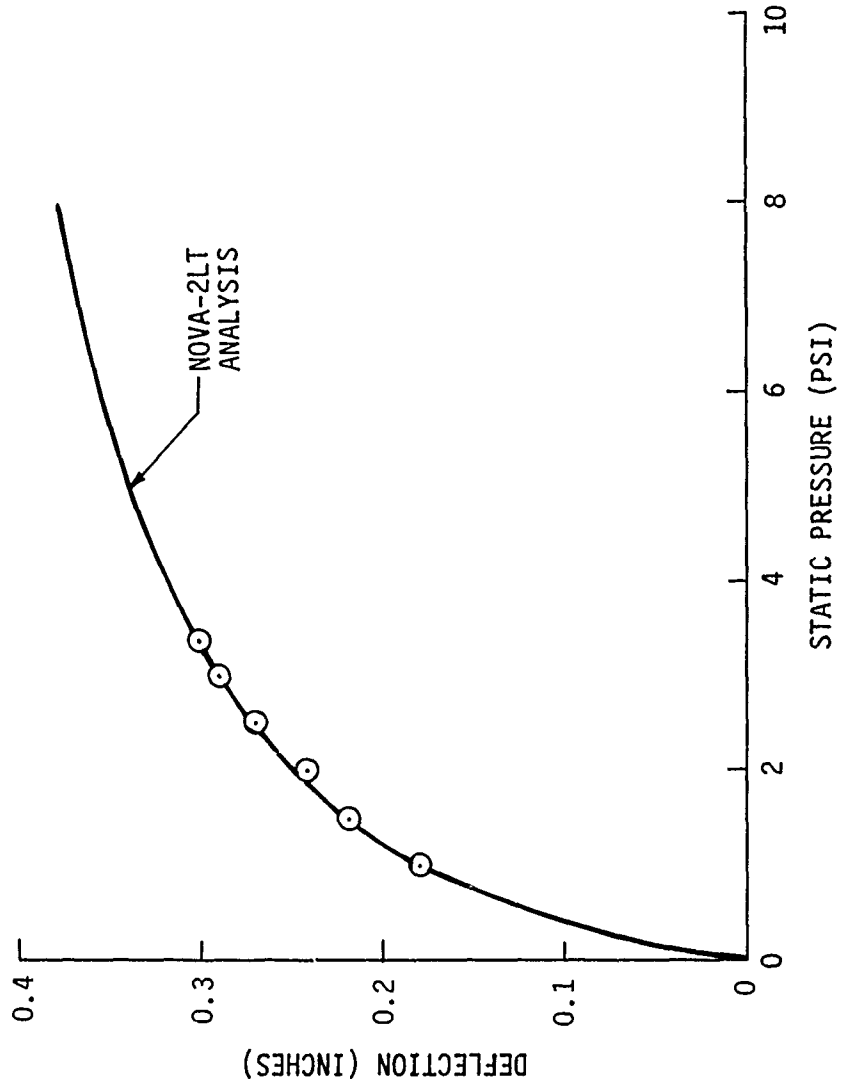


Figure 27. Deflection Vs. Static Pressure - Gauge D31-9 - Specimen No. 31

TEST SPECIMEN NO. 31
STRESS AT CENTER OF PANEL

○ GAUGE S31-2

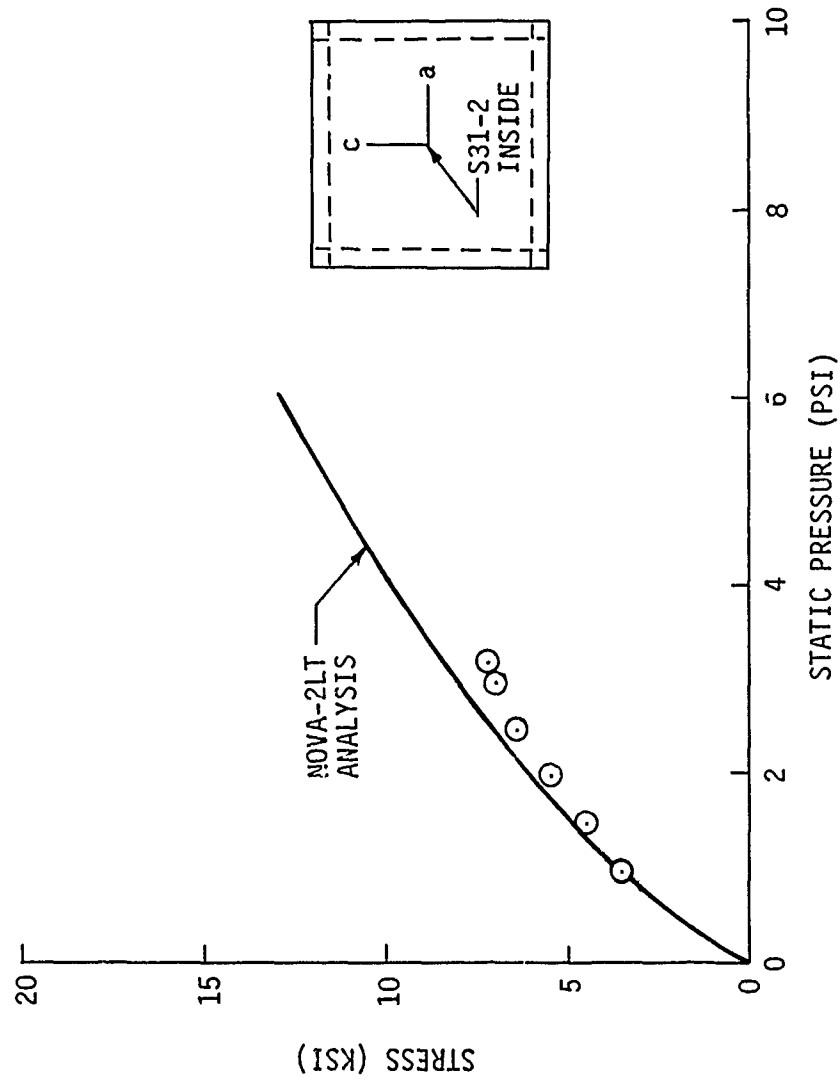


Figure 28. Stress Vs. Static Pressure - Gauge S31-2 - Specimen No. 31

TEST SPECIMEN NO. 32
STRESS AT 5.5° FROM CLAMP POINT

- GAUGE S32-14
- △ GAUGE S32-23

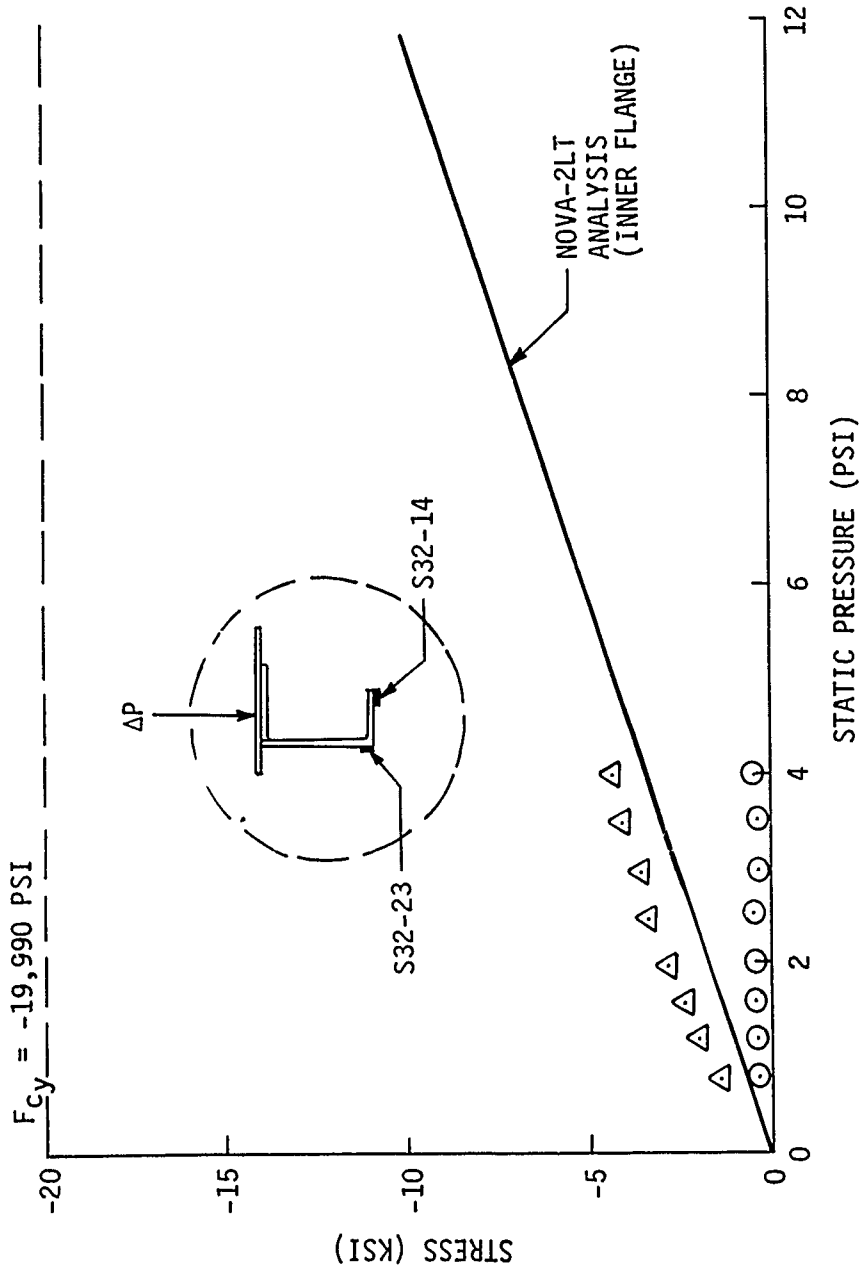


Figure 29. Stress Vs. Static Pressure - Gauges S32-14 and S32-23 - Specimen No. 32

TEST SPECIMEN NO. 32
STRESS AT 90° FROM CLAMP POINT

○ GAUGE S32-2
△ GAUGE S32-18

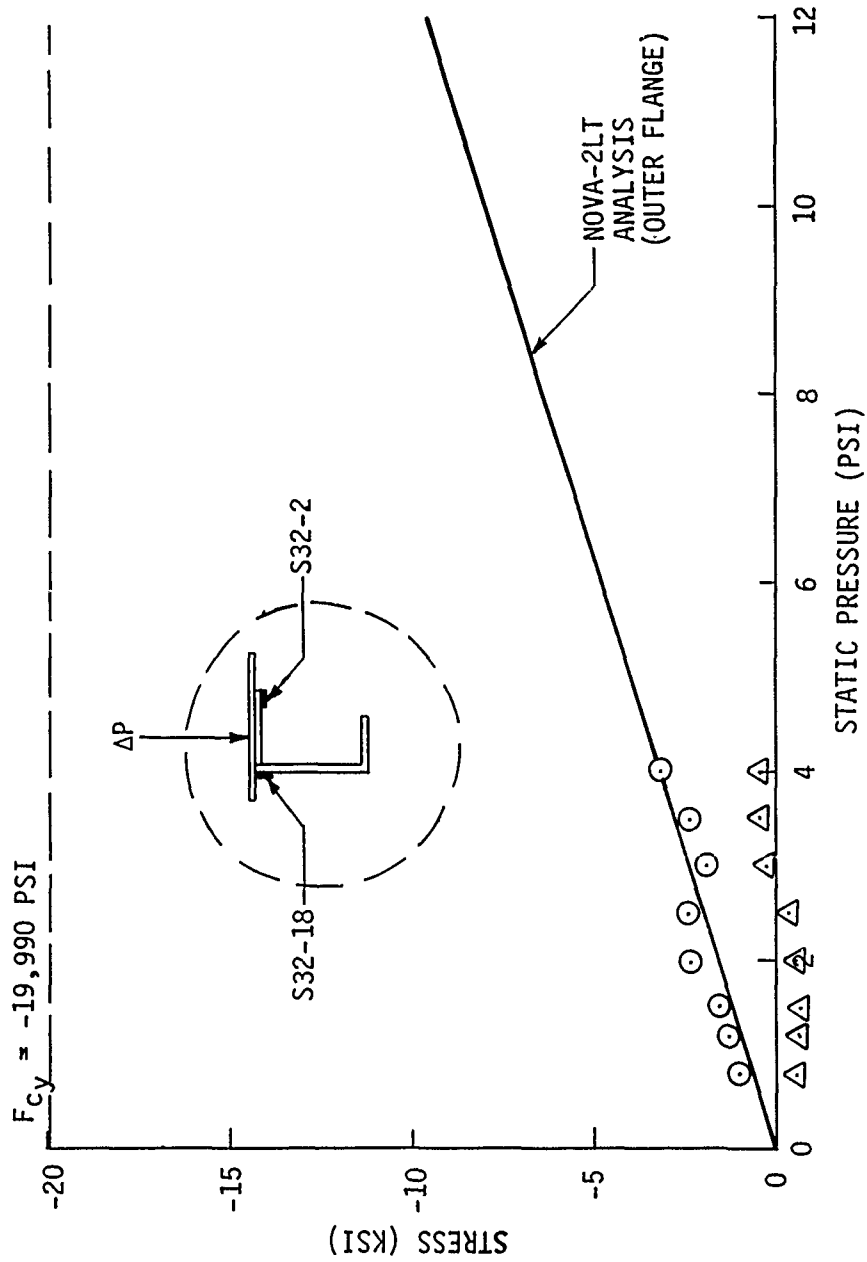


Figure 30. Stress Vs. Static Pressure - Gauges S32-2 and S32-18 - Specimen No. 32

TEST SPECIMEN NO. 32
 STRESS DUE TO 4.0 PSI LOAD
 (INNER FLANGE)

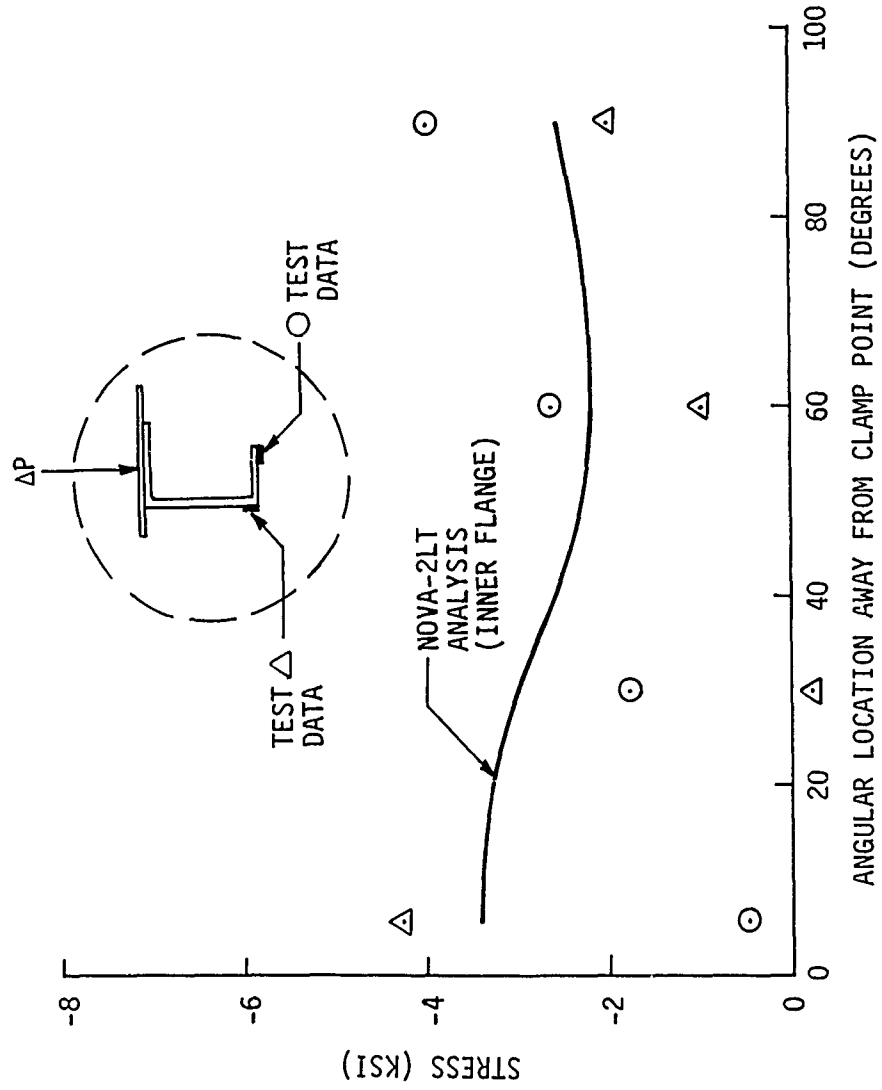


Figure 31. Stress Vs. Angular Location - Specimen No. 32 (Inner Flange)

TEST SPECIMEN NO. 32
 STRESS DUE TO 4.0 PSI LOAD
 (OUTER FLANGE)

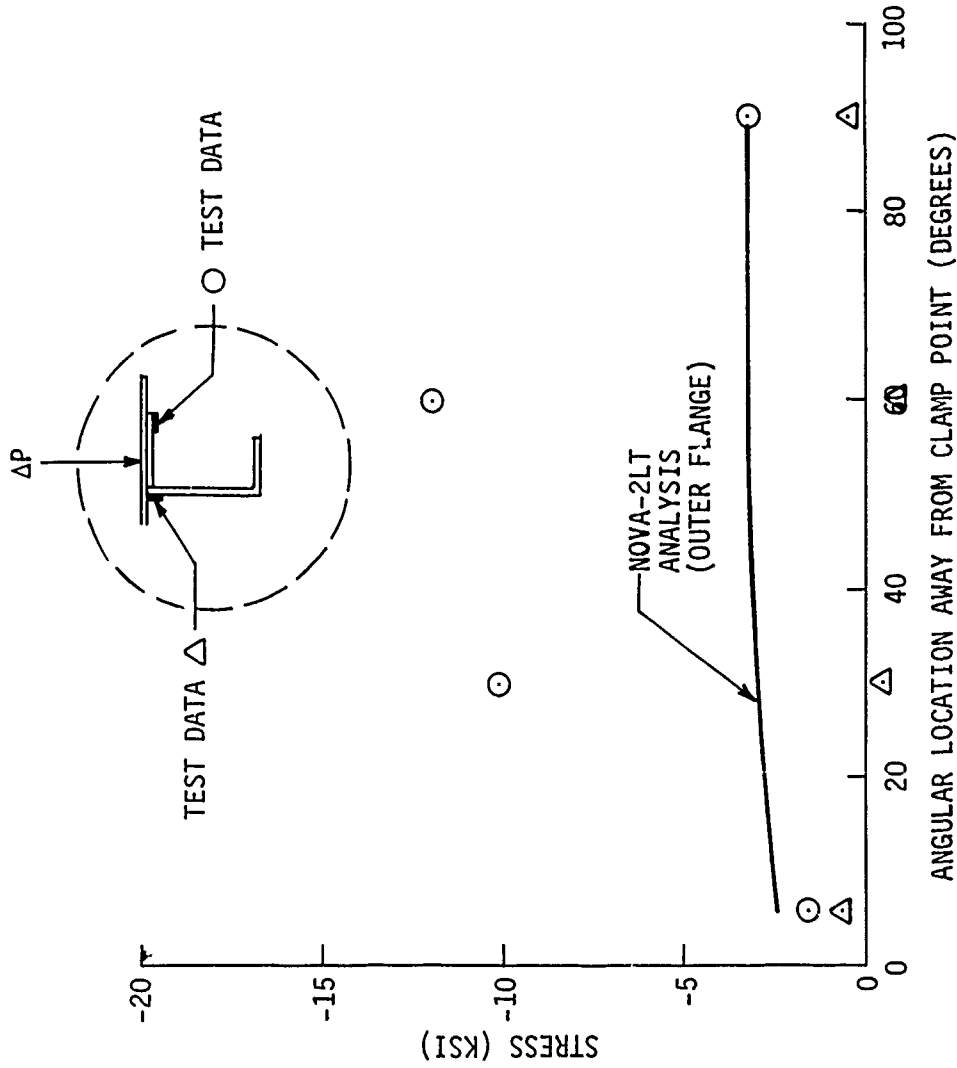


Figure 32. Stress Vs. Angular Location - Specimen No. 32 (Outer Flange)

5.5 degrees away from the clamp point. As shown, gauge S32-14 is located on the inner side of the inner flange, whereas gauge S32-23 is located on the inner portion of the web. The NOVA-2LT computer program forces the analyst to describe the actual cross section by a series of rectangular layers which results in a symmetric cross section. The analysis data shown in Figure 29, therefore, are the strains at the inside of the inner flange. The differences in the strain data for gauges S32-14 and S32-23 are due primarily to frame twist.

Figure 30 illustrates data similar to that shown in Figure 29 except that the location of interest on the frame is the mid-span, i.e., midway between clamp points. Also, this figure shows data for the frame outer flange.

Figures 31 and 32 show data for the frame inner and outer flanges, respectively, as a function of angular position for a 4 psi load.

Referring to the static test data for specimen 12 of Reference 3, it is seen that additional frame strength was obtained by changing from a symmetric cross section to an unsymmetric cross section with almost identical cross-sectional area and bending stiffness about the longitudinal axis of the cylinder. The analysis data for specimens 12 and 32, however, are essentially identical due to the modeling procedures required by NOVA-2LT. This appears to be a potentially serious deficiency of NOVA-2LT.

8.2.9 Test Specimen 33

This specimen is identical to specimen 32 except for frame cross section as described in Section 3.10. In addition, this specimen is similar to specimen 13 of Reference 3 except for the fact that the frame cross section for specimen 33 is unsymmetric. Cross-sectional areas of the frames are similar for specimens 13 and 33. However, bending stiffness of the specimen 33 frames about an axis parallel to the longitudinal axis of the cylinder was 60 percent greater than comparable data for specimen 13. Since the specimen 33 frame is unsymmetric, twisting as well as bending occurred under applied load.

Static test/analysis results for specimen 33 are shown in Figures 33-37. Figure 33 illustrates stress in the inner flange at a location approximately 5.5 degrees away from the clamp point. As shown, gauge S33-14 is located on the inside of the inner leg of the angle. In addition to the NOVA-2LT analysis results, two sets of NASTRAN results are shown. The results labeled "2-D" were obtained from an analysis that did not permit out-of-plane bending, whereas the results labeled "3-D" did permit this type of response. As shown, theoretical buckling analysis results for specimen 33 are strongly a function of out-of-plane motion. Up to 4 psi, test agrees quite well with all three analyses. Beyond 6 psi, NOVA-2LT results differ substantially from NASTRAN results.

Figures 34 and 35 illustrate data similar to that shown in Figure 33 except that the locations of interest on the frame are 30° and 90° away from the clamp point, respectively. The analysis results are for the outside of the outer flange whereas the strain gauge locations are as shown.

Figures 36 and 37 show data for the frame inner and outer flanges, respectively, as a function of angular position for a 4 psi load.

TEST SPECIMEN NO. 33
 STRESS AT 5.5° FROM CLAMP POINT
 ○ GAUGE S33-14

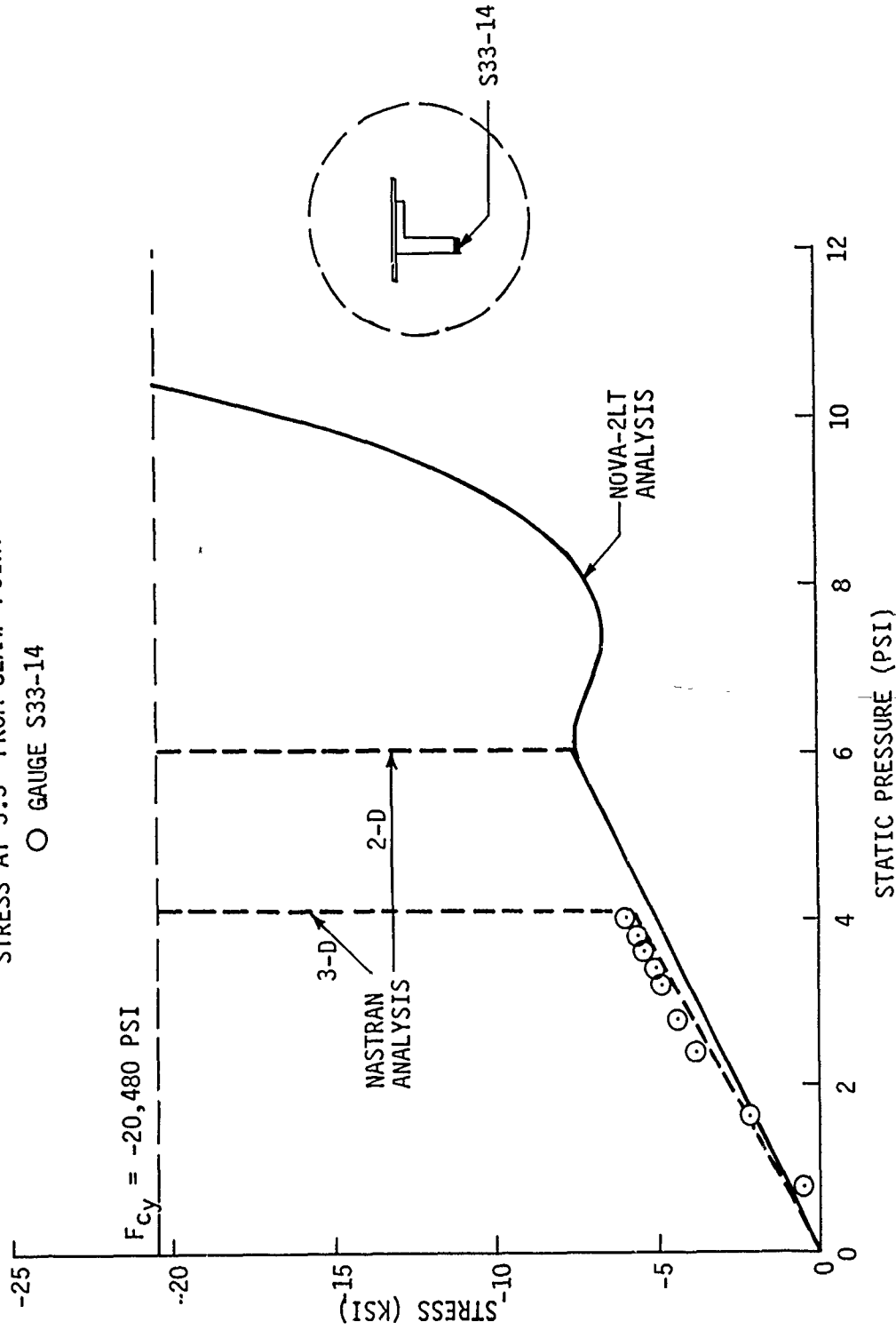


Figure 33. Stress Vs. Static Pressure - Gauge S33-14 - Specimen No. 33

TEST SPECIMEN NO. 33
STRESS AT 30° FROM CLAMP POINT

- GAUGE S33-9
- △ GAUGE S33-17

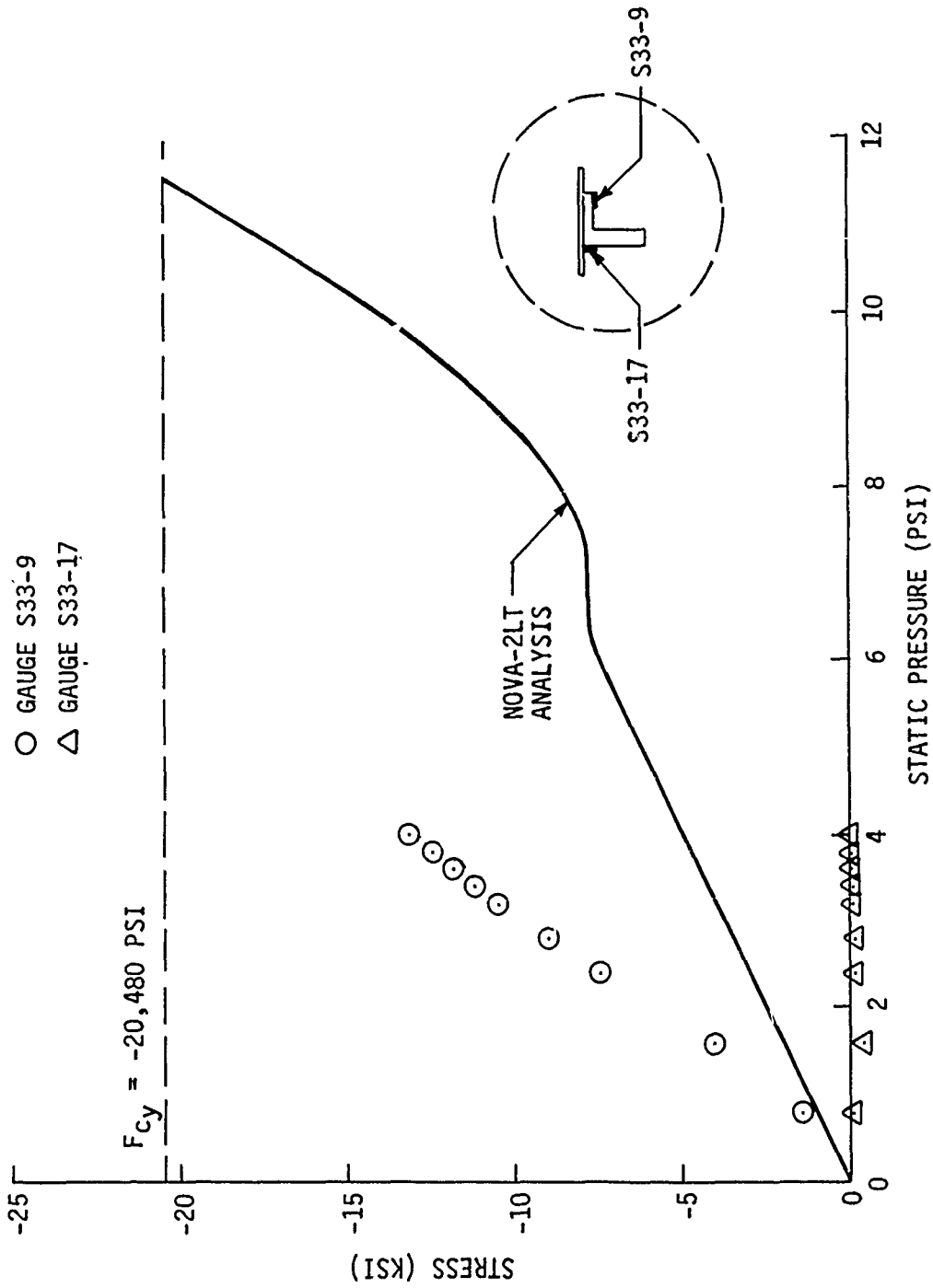


Figure 34. Stress Vs. Static Pressure - Gauges S33-9 and S33-17 - Specimen No. 33

TEST SPECIMEN NO. 33
STRESS AT 90° FROM CLAMP POINT

- GAUGE S33-2
- △ GAUGE S33-18

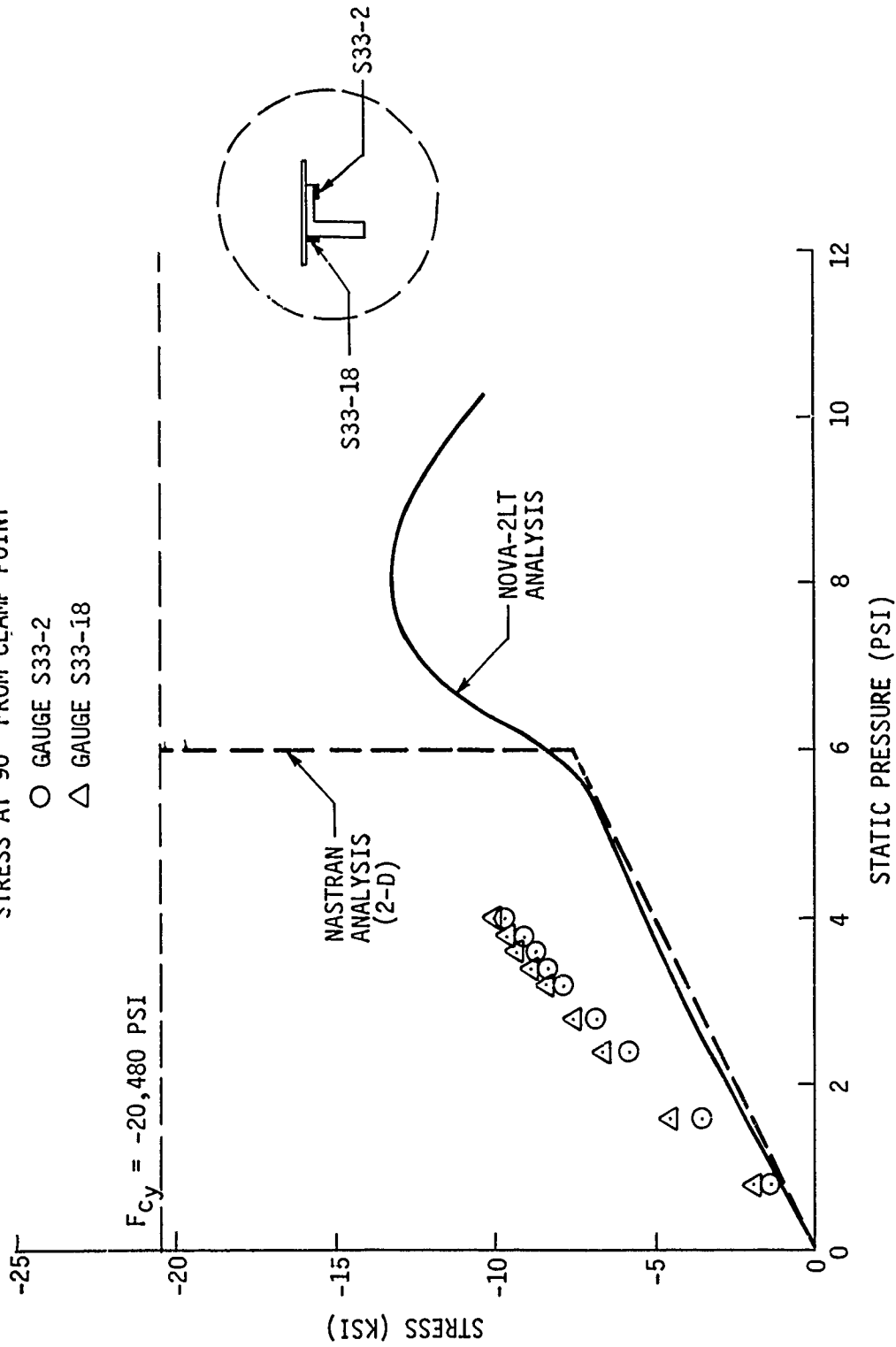


Figure 35. Stress Vs. Static Pressure - Gauges S33-2 and S33-18 - Specimen No. 33

TEST SPECIMEN NO. 33
 STRESS DUE TO 4.0 PSI LOAD
 (INNER FLANGE)

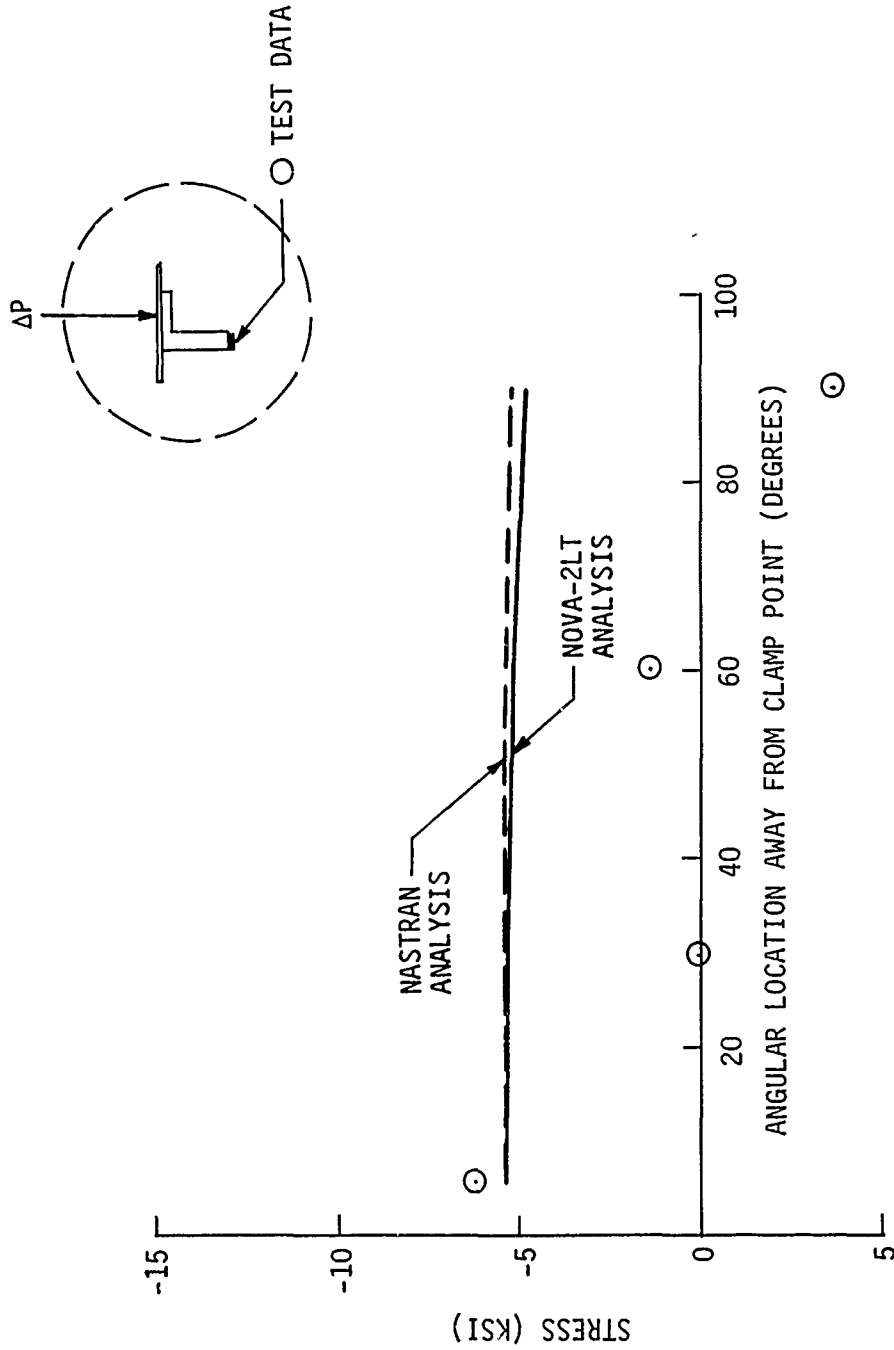


Figure 36. Stress Vs. Angular Location - Specimen No. 33 (Inner Flange)

TEST SPECIMEN NO. 33
 STRESS DUE TO 4.0 PSI LOAD
 (OUTER FLANGE)

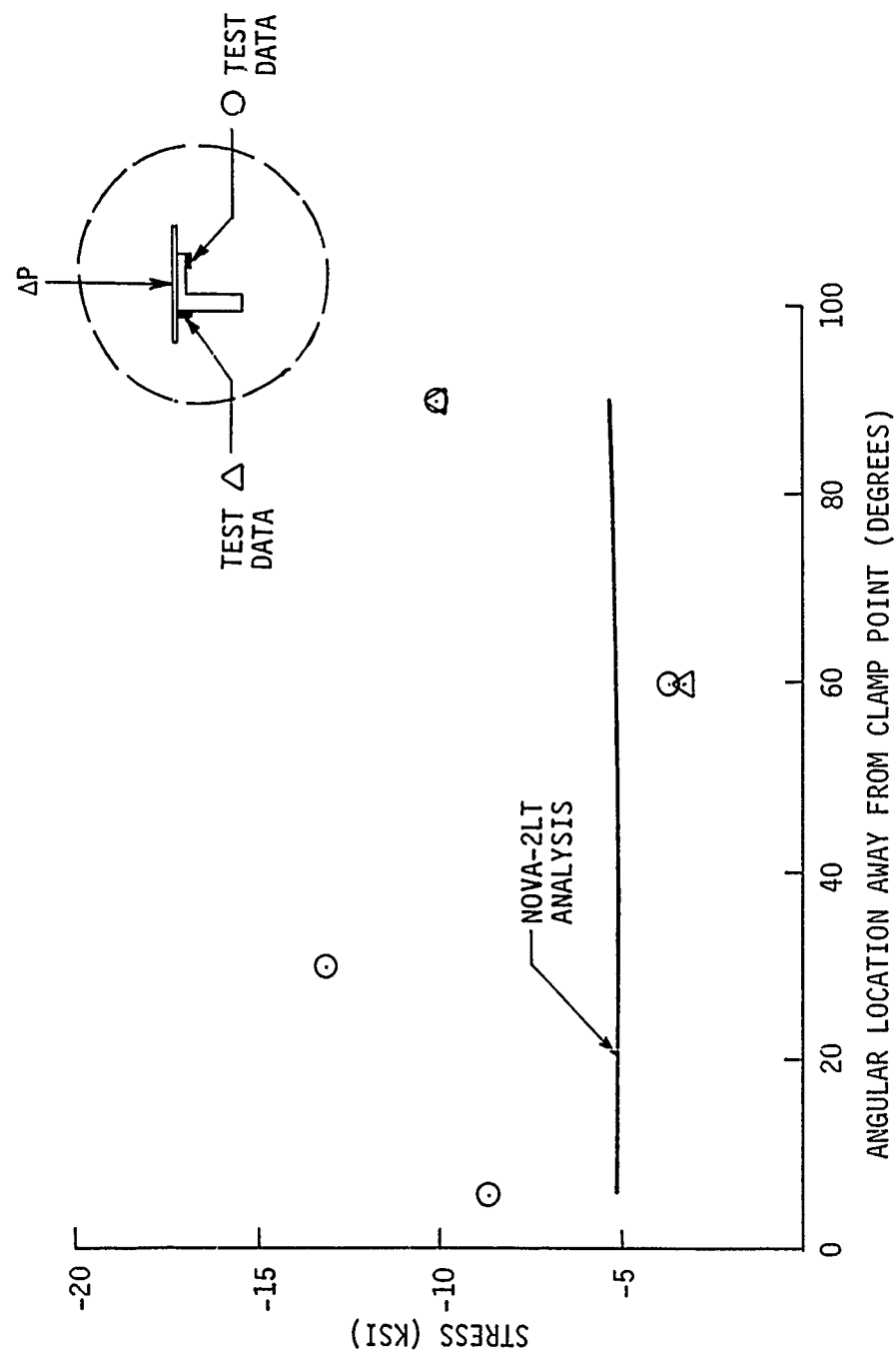


Figure 37. Stress Vs. Angular Location - Specimen No. 33 (Outer Flange)

8.3 Shock Load Test/Analysis

All test specimens were analyzed using the NOVA-2LT computer program with the appropriate measured pressure time histories as the forcing functions. Results of these analyses identified the shock intensity for each specimen that results in the threshold of damage. In addition, elastic-plastic response analyses were accomplished for those test specimens that experienced measurable permanent deformation as a result of their respective final test shots.

All analyses were conducted utilizing modulus of elasticity data and yield strength data established by coupon tests of the material from which the specimen was constructed. The analyses also utilized the actual specimen measured geometry (thickness, area, etc.) to establish the correct section properties.

During the shock load testing of all column specimens, the box holding fixture shown in Figure 38 was utilized. The columns were positioned inside the box holding fixture with one end fixed to prohibit displacement and one end attached to a loading piston permitting axial displacement. Figure 38 shows the position of the four pistons in the box holding fixture. The attachment of the pin-ended columns to their respective pistons is illustrated in more detail in Figure 39, and the clamp-ended columns are shown in Figure 40.

The box holding fixture was oriented such that the shock propagation vector was perpendicular to the piston faces. As the piston faces were loaded by the shock wave, they displaced in the cylinder thereby providing axial load to the columns.

The NOVA-2LT computer program was not designed to analyze the column/loading block/piston structural configuration directly. Therefore, two special versions of NOVA-2LT were obtained from Kaman - Avidyne for analyzing the various columns in this test series. In addition, no provisions were available within NOVA-2LT for including friction forces which may have existed between the pistons and the cylinders. Some sticking of the pistons within the cylinders was observed in the test data. However, test data where sticking was apparent were not included in the results shown in this volume of the report.

The initial imperfections that were measured at the column centers define lateral displacement away from a perfectly straight column. For analysis purposes, the remainder of the column was defined to exhibit initial imperfections described by a sine function for pin-ended columns and a one minus cosine function for clamp-ended columns.

8.3.1 Test Specimens 18-21

Test specimens 18-21 were pin-ended columns which were ten inches long, five inches wide, and 0.033 inches thick as shown in Table 1. Initial lateral imperfections measured at the column centers were 0.015, 0.02, 0.025, and 0.01 inches for specimens 18, 19, 20, and 21, respectively.

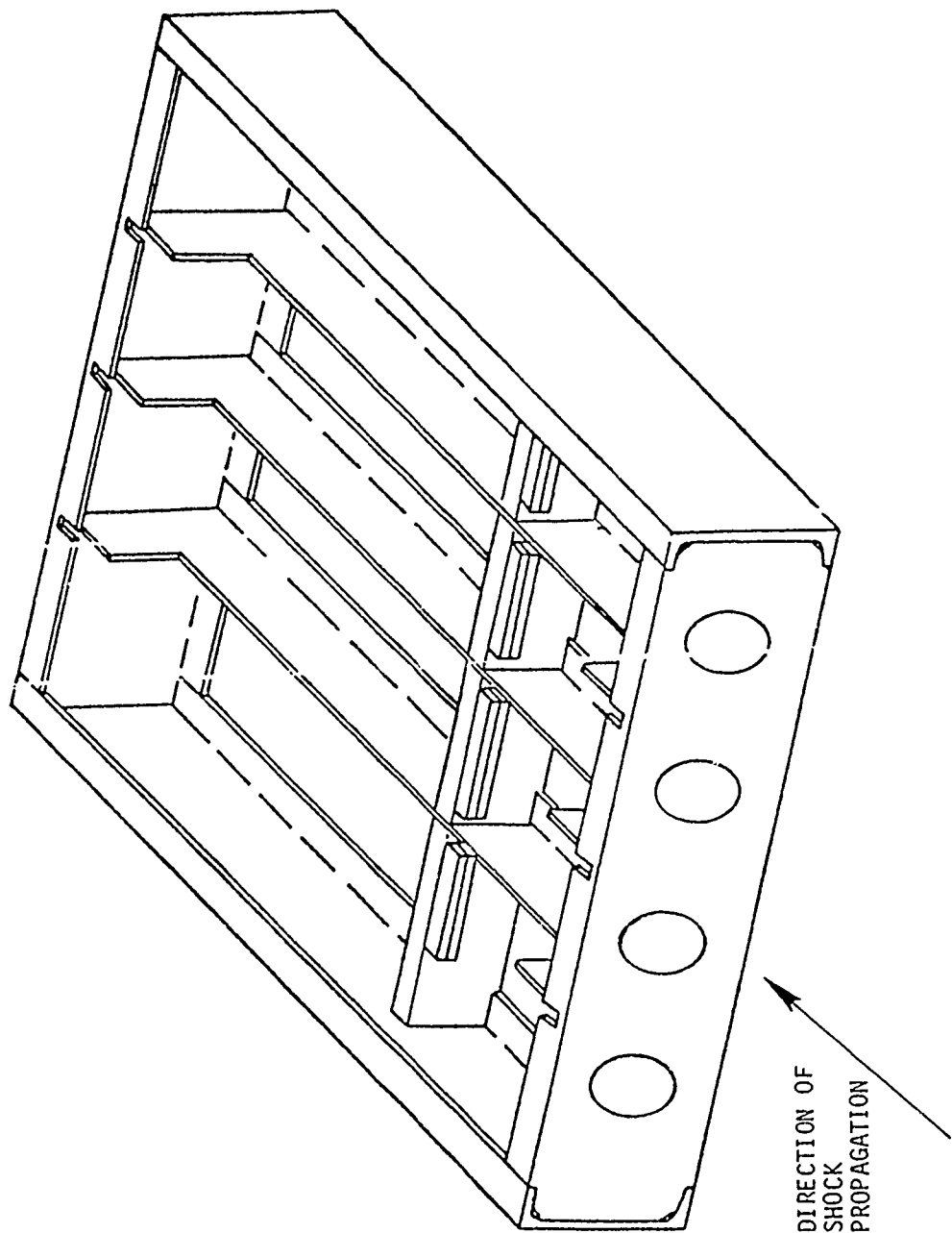


Figure 38. Box Holding Fixture

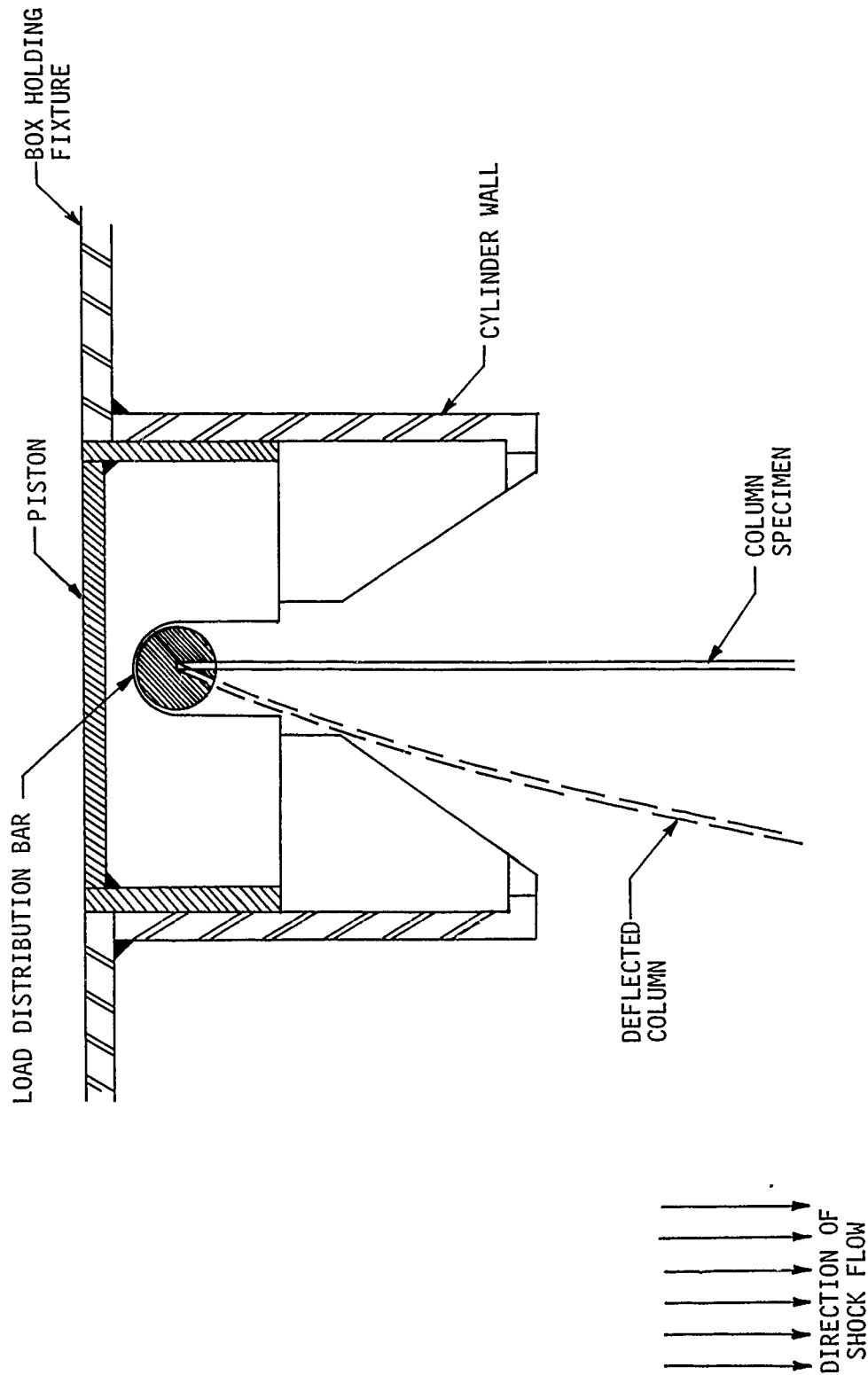


Figure 39. Pin-Ended Column Loading Device

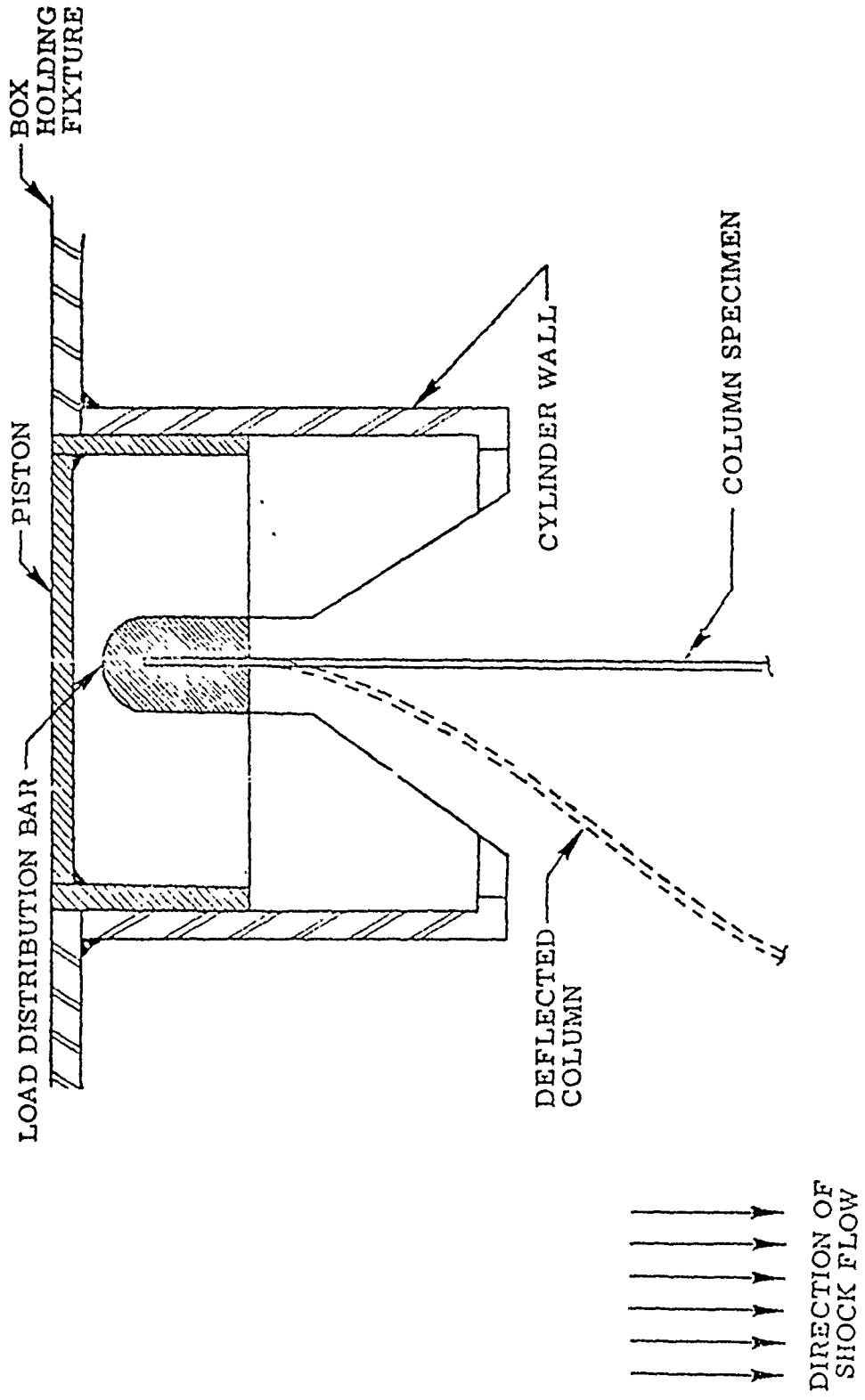


Figure 40. Clamp-Ended Column Loading Device

Due to obvious sticking of various pistons for several test shots, average response data from the shock load tests for the four columns are shown in Figure 41. These data do not include response data where piston sticking was apparent. Peak stress at the column centers is plotted versus peak incident overpressure and indicates that compressive yielding would occur due to a shock intensity of approximately 9 psi. Also shown in Figure 41 are NOVA-2LT analysis results for columns of the same geometry as specimens 18-21 but with initial eccentricities of 0.025, 0.01, and 0.005 inches. Considering that some friction effects are probably influencing the test data shown in Figure 41, the agreement between test and analysis is considered to be very good.

Figure 42 shows test and analysis data for specimen 21 for event 78-298. These data define strain at the column center versus time. Both test and analysis data show a fundamental response frequency of approximately 18 Hz.

8.3.2 Test Specimens 22-23

Test specimens 22-23 were pin-ended columns which were ten inches long, five inches wide, and 0.028 inches thick. Initial lateral eccentricities were determined to be 0.075 and 0.025 inches for specimens 22 and 23, respectively.

Figure 43 shows test and analysis maximum stress data at the center of the columns versus incident overpressure. Test data show that specimen 22 exhibited higher peak strains than specimen 23 for low shock intensities due to the differences in initial eccentricities. However, the test data also indicate that both specimens would yield at approximately 7 psi. Also shown in Figure 43 are NOVA-2LT analysis data for columns of the same geometry as specimens 22-23, but with initial eccentricities of 0.075, 0.025, and 0.010 inches. As shown, the test and analysis agree quite well when initial eccentricities of 0.025 inches or less are assumed. However, the analysis results show considerably more sensitivity to the magnitude of initial eccentricities than was observed in the test.

Figure 44 shows test and analysis strain time histories for the center of the column specimen 23 for event 78-350. As shown, the peak analytical strain was considerably greater than that from the test. However, the test and analysis response frequencies agree quite well (6-7 Hz).

8.3.3 Test Specimens 24-25

Test specimens 24-25 were clamp-ended columns ten inches long, five inches wide, and 0.028 inches thick. Initial lateral eccentricities were 0.57 and 0.05 inches for specimens 24 and 25, respectively. As indicated earlier in this report, specimen 24 was inadvertently yielded during the static test.

Figure 45 shows maximum stress data versus incident overpressure for the center of column specimens 24-25. Similar to the results for other column specimens, test data do not indicate the response of the columns to be as sensitive to initial eccentricities as that predicted by NOVA-2LT analysis. Test results indicate compressive yielding would occur at approximately 13.5 and 16.5 psi for specimens 24 and 25, respectively. These results compare favorably with NOVA-2LT analysis results when initial eccentricities are less than 0.05 inches.

TEST SPECIMENS 18 - 21
 STRESS AT CENTER OF COLUMNS
 ○ AVERAGE OF THE COLUMNS

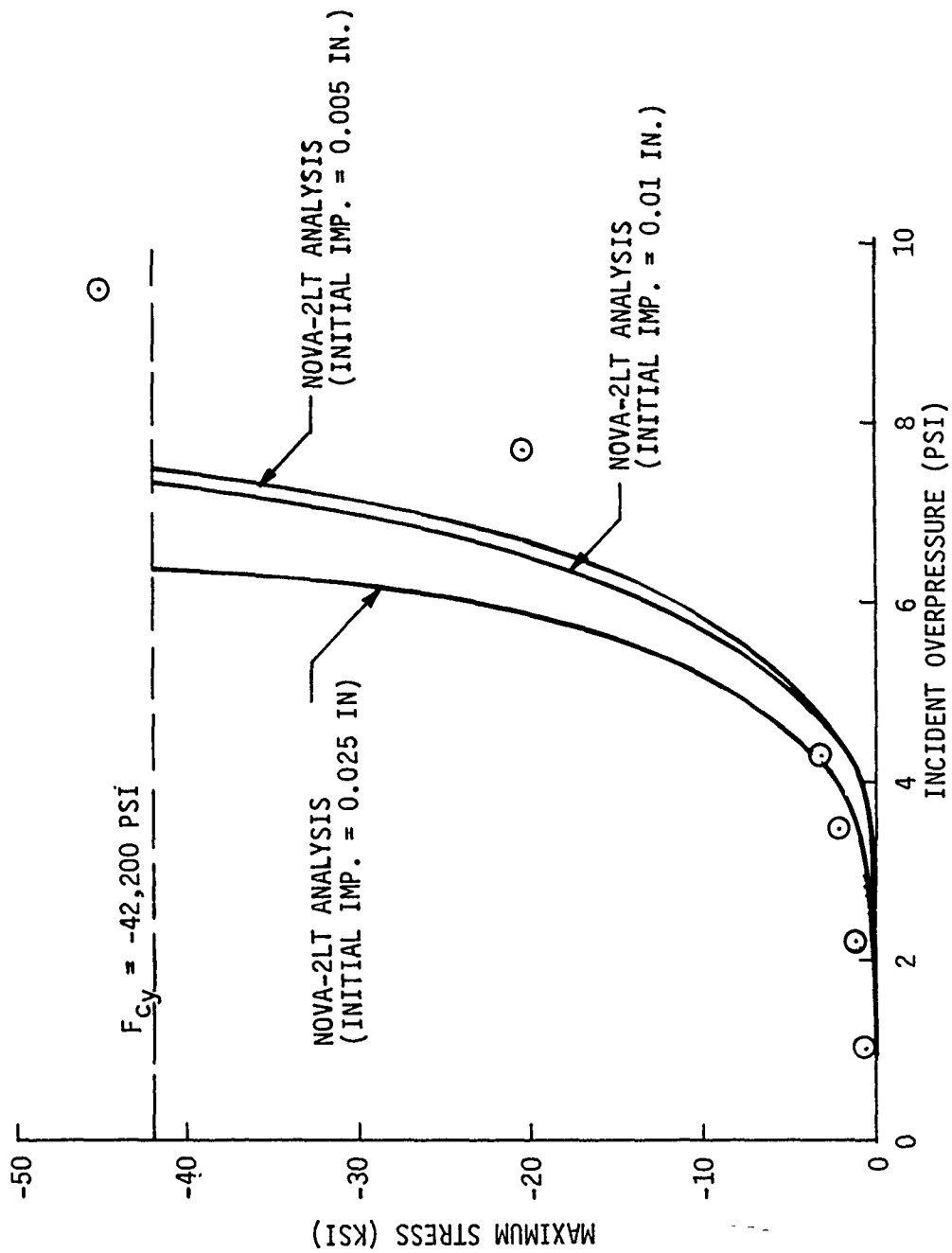


Figure 41. Maximum Stress Vs. Incident Overpressure - Specimens 18-21

TEST SPECIMEN NO. 21
EVENT NO. 78-298
STRAIN AT COLUMN CENTER

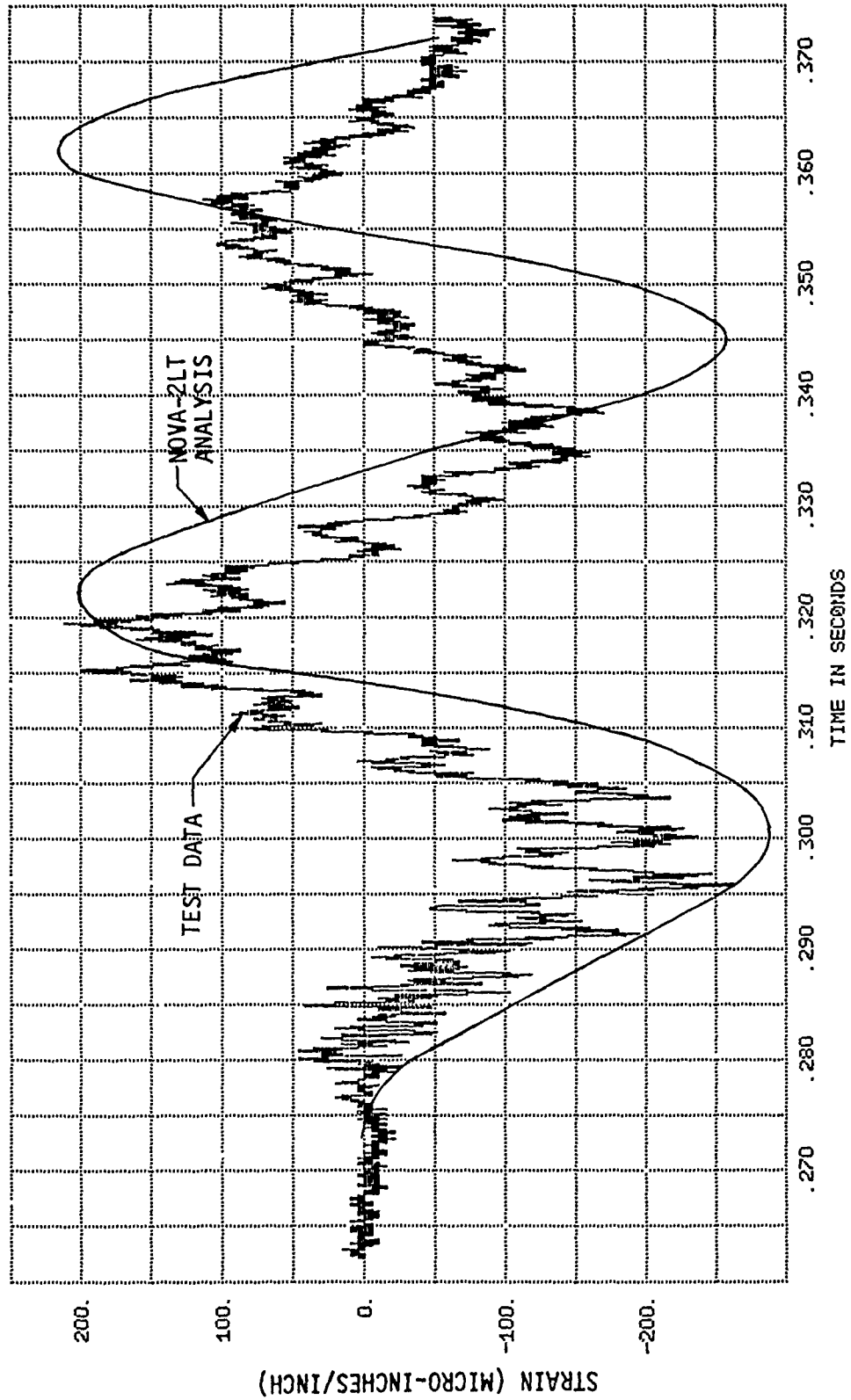


Figure 42. Strain Time History - Specimen 21

TEST SPECIMENS 22-23
 STRESS AT CENTER OF COLUMNS

○ SPECIMEN 22 (INITIAL IMP = 0.075 IN.)
 △ SPECIMEN 23 (INITIAL IMP = 0.025 IN.)

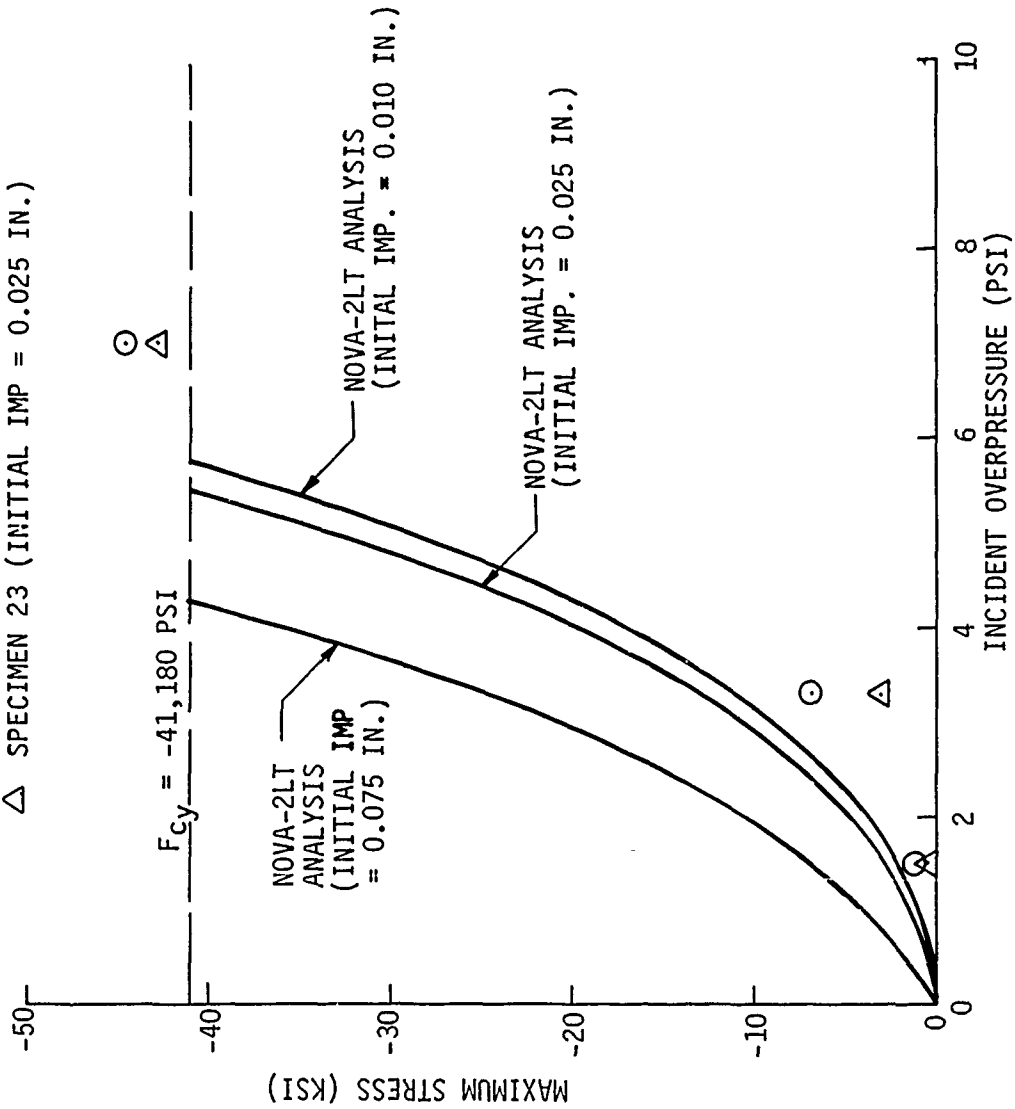


Figure 43. Maximum Stress Vs. Incident Overpressure - Specimens 22-23

TEST SPECIMEN NO. 23
EVENT NO. 78-350
STRAIN AT COLUMN CENTER

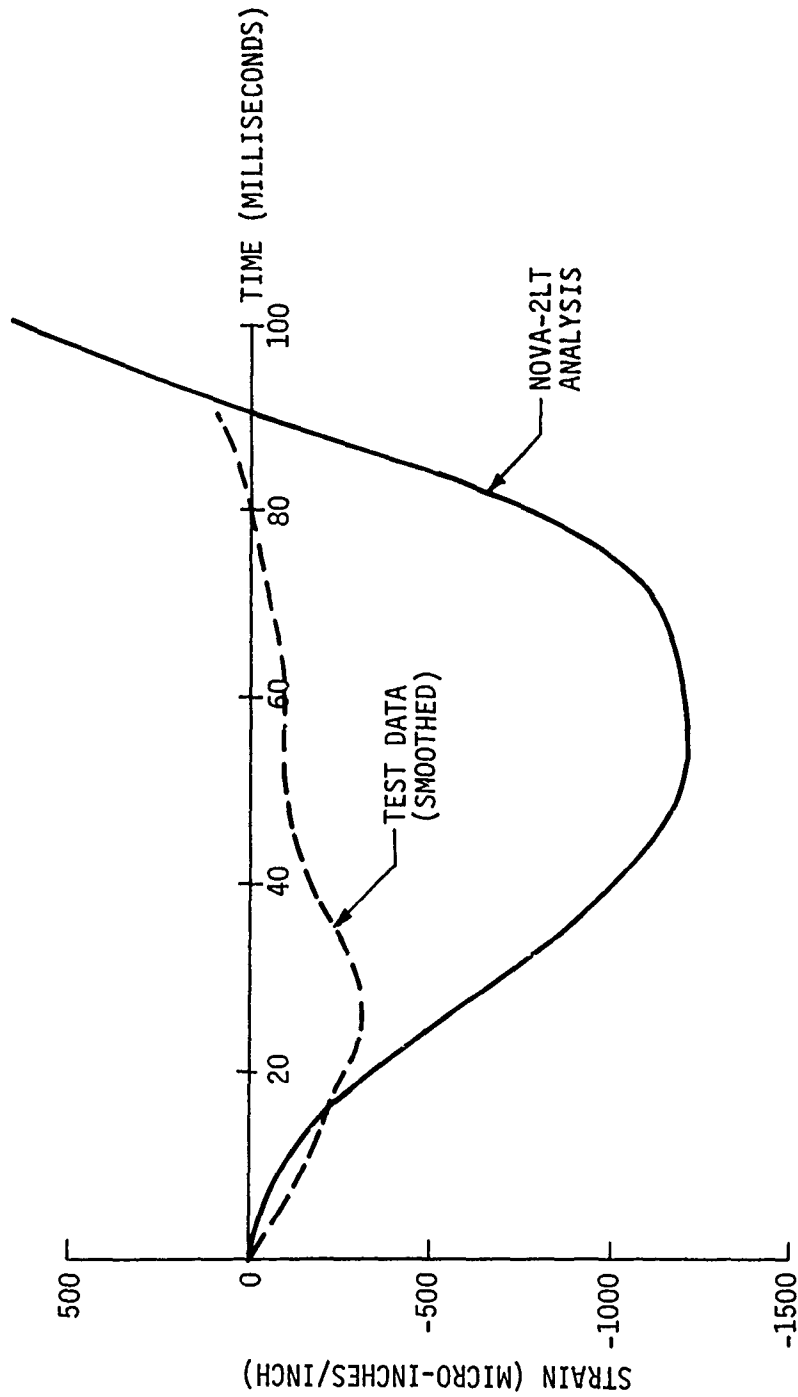


Figure 44. Strain Time History - Specimen 23

TEST SPECIMENS 24-25
 STRESS AT CENTER OF COLUMNS

○ SPECIMEN NO. 24 (INITIAL IMP. = 0.57 IN.)
 △ SPECIMEN NO. 25 (INITIAL IMP. = 0.05 IN.)

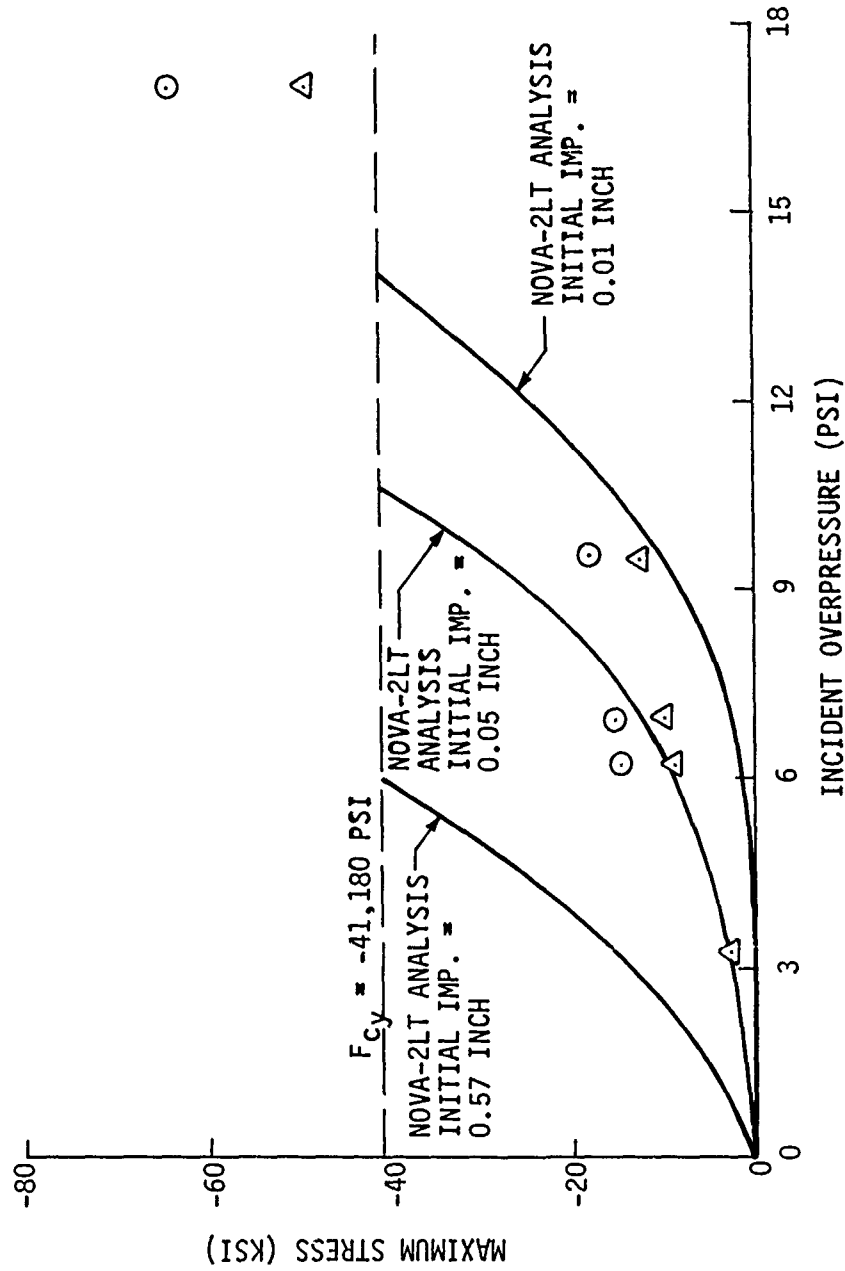


Figure 45. Maximum Stress Vs. Incident Overpressure - Specimens 24-25

Test and analysis strain time history data for specimen 25 and event 78-357 are shown in Figure 46. Analysis results indicate a fundamental response frequency of approximately 17 Hz, whereas test data indicate a frequency of approximately 25 Hz.

8.3.4 Test Specimens 26-27

Test specimens 26-27 were pin-ended columns ten inches long, five inches wide, and 0.025 inches thick. Specimen 26 exhibited an initial eccentricity of 0.13 inches, whereas specimen 27 was essentially free of eccentricities.

Maximum stress versus incident overpressure for specimens 26-27 is shown in Figure 47. Similar to test data for other columns already discussed, the column with the larger initial eccentricity exhibited higher peak stress throughout the test. Test data indicate that compressive yielding of test specimens 26 and 27 would occur at 5 and 6 psi, respectively.

Figure 48 shows test and analysis strain time history data for specimen 26 and event 78-350. Analysis results indicate a fundamental response frequency of 3 Hz, and test data indicate a frequency of approximately 5 Hz.

8.3.5 Test Specimens 28-29

Test specimens 28-29 were clamp-ended columns ten inches long, five inches wide, and 0.025 inches thick. Specimen 28 exhibited an initial eccentricity of 0.01 inches, whereas similar data for specimen 29 was less than 0.005 inches.

The test data shown in Figure 49 are consistent with the other column data already discussed, regarding the effect of initial eccentricity. However, the analysis data indicate essentially the same sensitivity with initial eccentricity as that observed in the test. The agreement between test and analysis is considered excellent. As shown, test data indicate that compressive yielding of specimens 28 and 29 would occur at 9 and 10.5 psi, respectively.

In addition to the excellent agreement between test and analysis regarding peak stress, very good agreement was observed regarding response frequencies as shown in Figure 50. This figure shows data for specimen 28 and event 78-357. As shown, NOVA-2LT analysis predicted a response frequency of approximately 7 Hz compared to test data of 9 Hz.

8.3.6 Test Specimen 30

Test specimen 30 was a 22-inch square homogeneous flat skin panel with a thickness of 0.039 inches. All four sides of the panel were clamped. All tests and analyses for specimen 30 were conducted with the shock propagation vector normal to the plane of the panel. Initially, shock analyses of this specimen were conducted by inputting the measured pressure data to NOVA-2LT via tapes. Results of these analyses indicated extremely high strains for relatively low overpressures. When the same overpressure data was digitized and input on cards, however, the strains were realistic. The strains from

TEST SPECIMEN NO. 25
EVENT NO. 78-357
STRAIN AT COLUMN CENTER

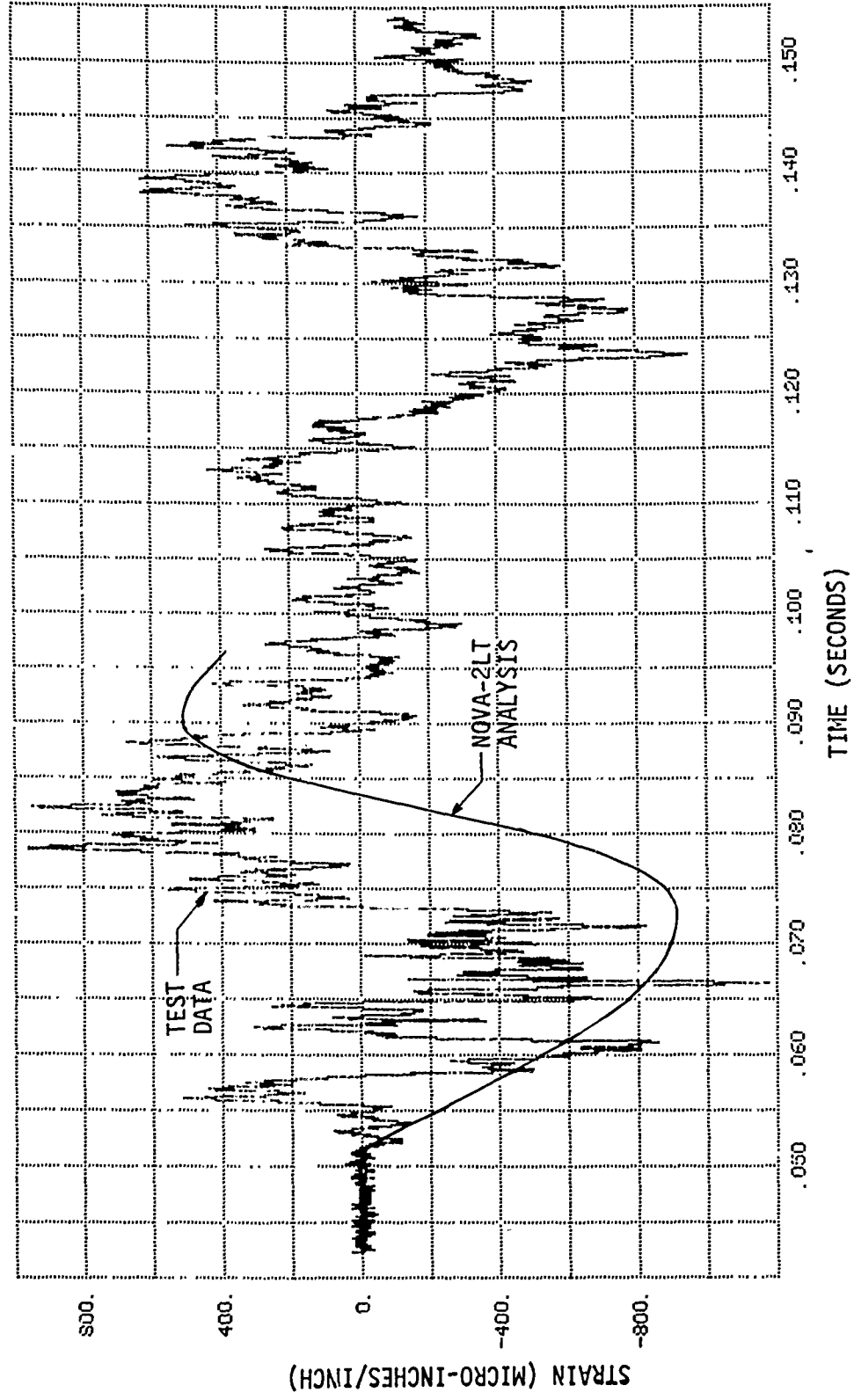


Figure 46. Strain Time History - Specimen 25

TEST SPECIMENS 26-27
 STRESS AT CENTER OF COLUMNS

○ SPECIMEN 26 (INITIAL IMP = 0.13 IN.)
 △ SPECIMEN 27 (INITIAL IMP < 0.01 IN.)

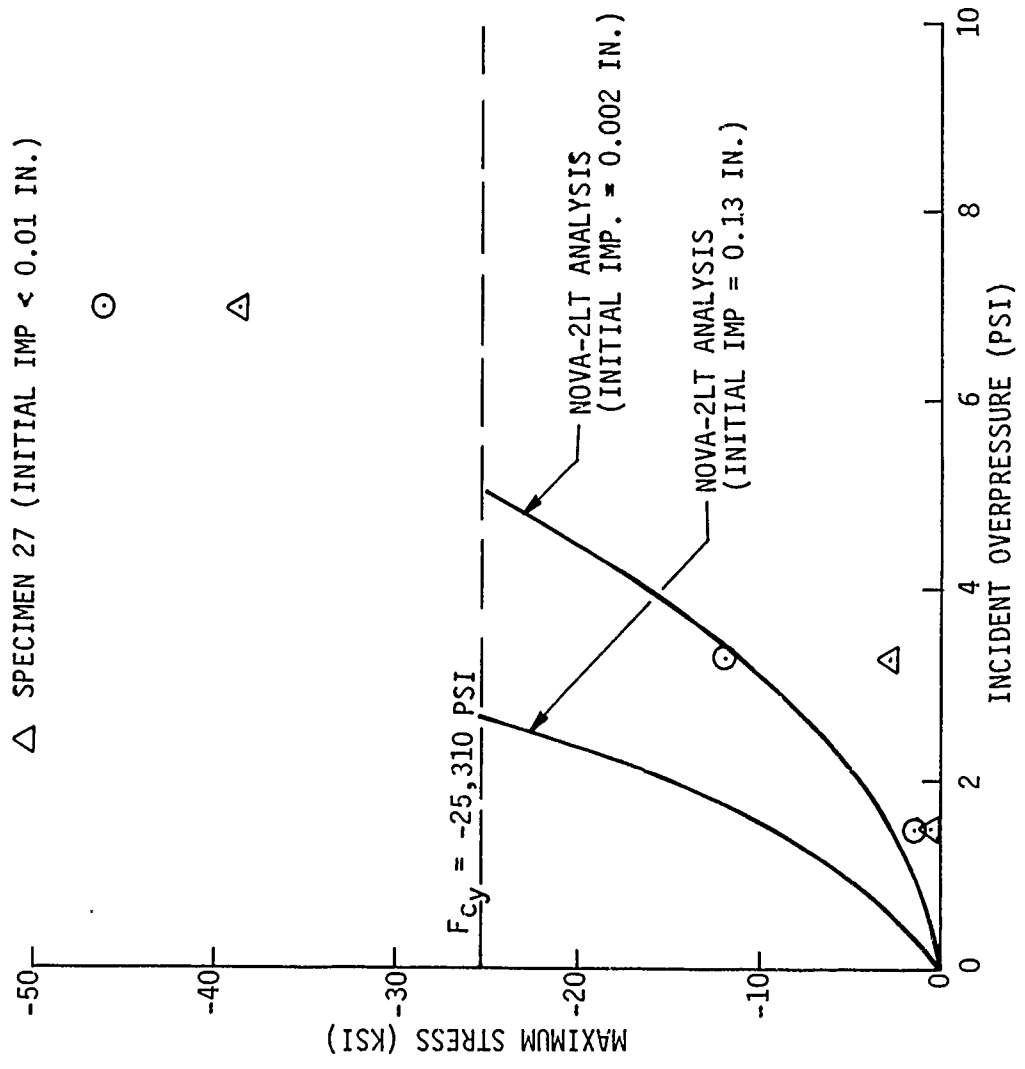


Figure 47. Maximum Stress Vs. Incident Overpressure - Specimens 26-27

TEST SPECIMEN NO. 26
EVENT NO. 78-350
STRAIN AT COLUMN CENTER

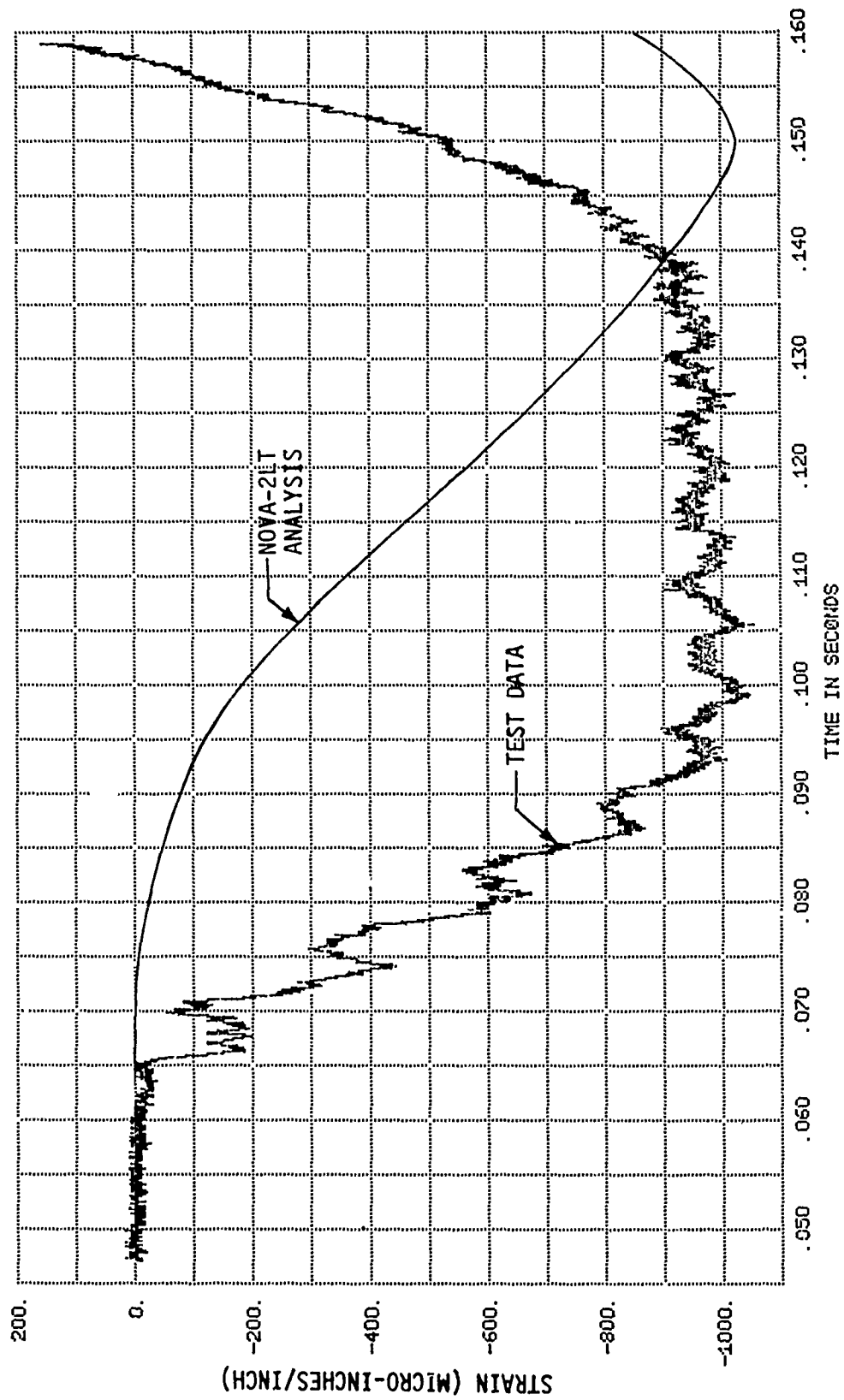


Figure 48. Strain Time History - Specimen 26

TEST SPECIMENS 28-29
STRESS AT CENTER OF COLUMNS

- SPECIMEN NO. 28 (INITIAL IMP. = 0.01 IN.)
- △ SPECIMEN NO. 29 (INITIAL IMP. < 0.005 IN.)

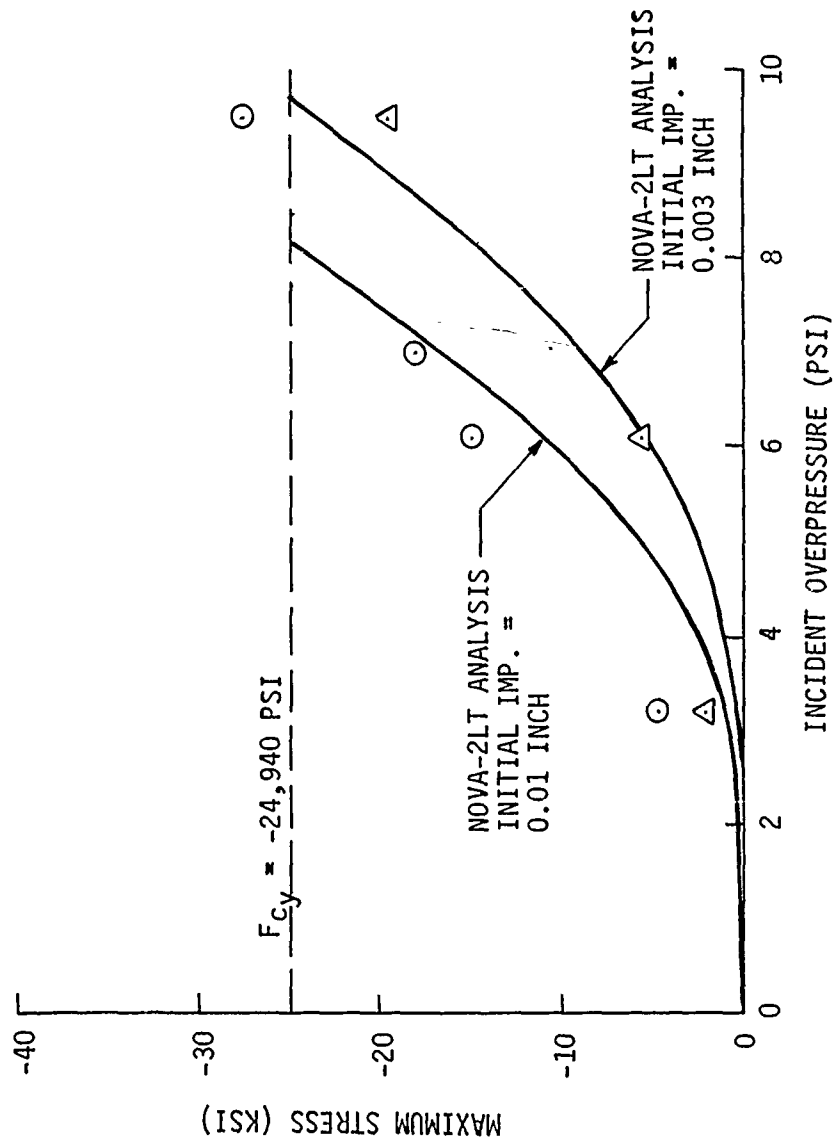


Figure 49. Maximum Stress Vs. Incident Overpressure - Specimens 28-29

TEST SPECIMEN NO. 28
EVENT NO. 78-357
STRAIN AT COLUMN CENTER

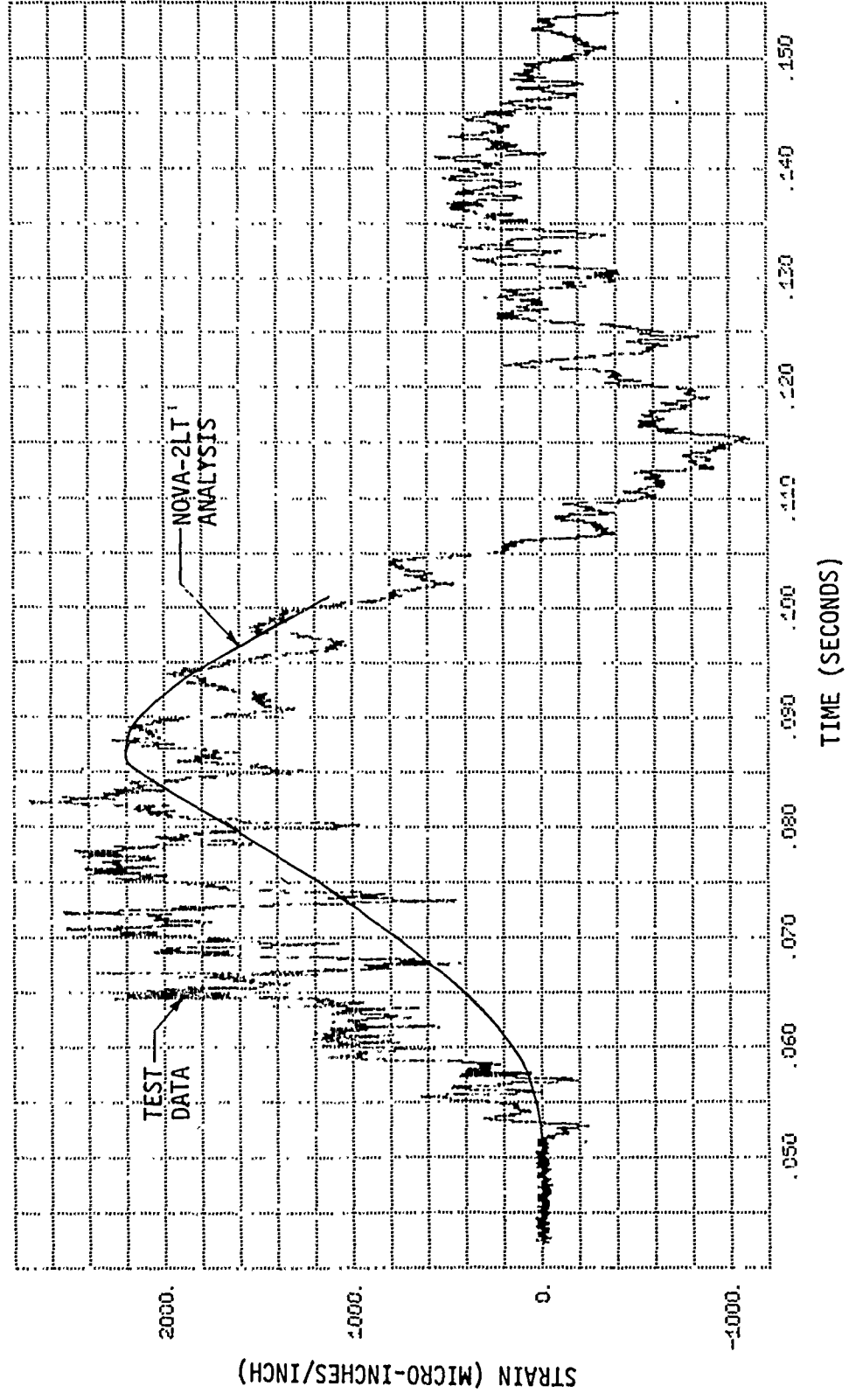


Figure 50. Strain Time History - Specimen 28

the latter analysis approach are documented in this report. The problem with extremely high panel strains was found to occur for all panels analyzed. Therefore, all panels were eventually analyzed by inputting digitized pressure data on cards. This problem has been discussed with Kaman AviDyne personnel on several occasions, but no solution has been discovered.

Analysis results and test results for specimen 30 are shown in Figures 51-54. These data indicate that maximum stress occurred at the center of the edge, and maximum displacement occurred at the panel center as expected. The test data shown in Figure 51 are an average of data for two edges. Similar to the results for the thin panels tested in the Reference 3 study, analysis results at the edge of the panel did not converge to the test data. Some variation in analysis results was apparent when the structural model was expanded from a 6x6 to a 7x7 mode set (see Reference 1). Much better correlation between test and analysis stress occurred at the center of the panel as shown in Figure 52. This was also true of the test and analysis deflection data at the panel center as shown in Figure 53. Excellent agreement between test and analysis response frequencies was also obtained as shown in Figure 54.

In addition, a permanent deformation of 0.24 inches was measured manually at the panel center after the final test shot for this specimen. The NOVA-2LT analysis results for this condition indicated no permanent deformation at the panel center. The maximum recorded strain associated with the final test shot was approximately 19,000 micro-inches per inch (average of two gauges). For this condition, the analysis predicted a maximum strain of approximately 3330 micro-inches per inch.

8.3.7 Test Specimen 31

Test specimen 31 was a 22-inch square homogeneous flat skin panel with a thickness of 0.062 inches. All four sides of the panel were clamped. All tests and analyses for specimen 31 were conducted with the shock propagation vector normal to the plane of the panel. This panel was analyzed by inputting pressure data on cards as discussed in Section 8.3.6 of this report.

Analysis results and test results for specimen 31 are shown in Figures 55-58. These data indicate that maximum stress occurred at the center of the edge, and maximum displacement occurred at the panel center as expected. The test data shown in Figure 55 are an average of data for two edges. Similar to the results for specimen 30, analysis stresses at the center of the edges were essentially the same as test data at relatively low shock intensities. However, at higher shock intensities the NOVA-2LT analysis underpredicted stress levels. Some variation in analysis results was observed when the 6x6 mode structural model was changed to a 7x7 mode model.

Figure 56 shows stress data for the panel center and indicates excellent agreement between test and analysis. Very good agreement between test and analysis deflections at the panel center was also obtained as shown in Figure 57. Figure 58 shows the comparison between test and analysis deflection time histories for event 78-339. Analysis results indicate a fundamental response frequency of approximately 60 Hz and test data indicate approximately 70 Hz.

TEST SPECIMEN NO. 30

STRESS AT CENTER OF EDGE

○ AVERAGE OF GAUGES S30-3 AND S30-5

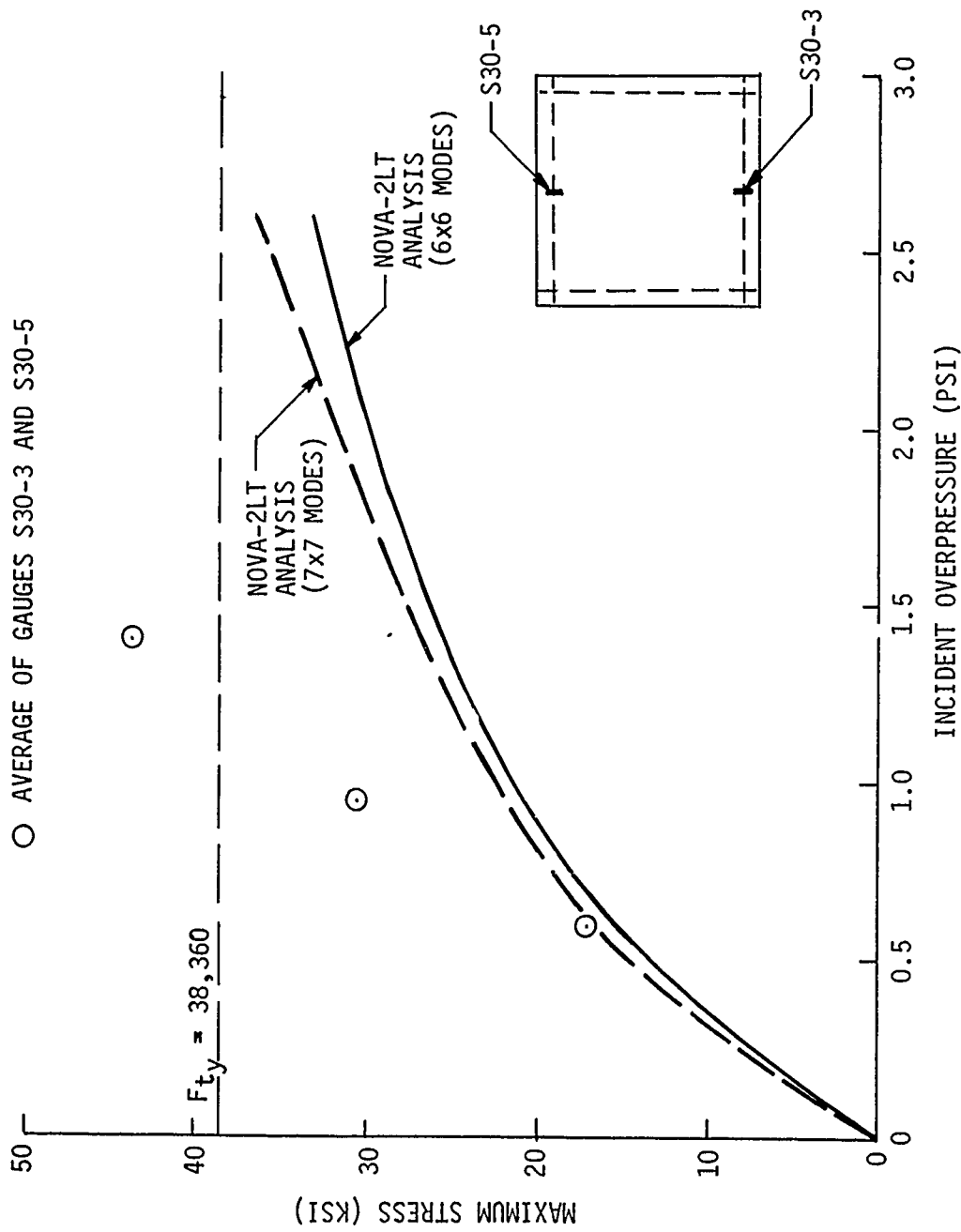


Figure 51. Maximum Stress Vs. Incident Overpressure - Specimen 30 - Gauges S30-3 and S30-5

TEST SPECIMEN NO. 30
STRESS AT CENTER OF PANEL

○ GAUGE S30-2

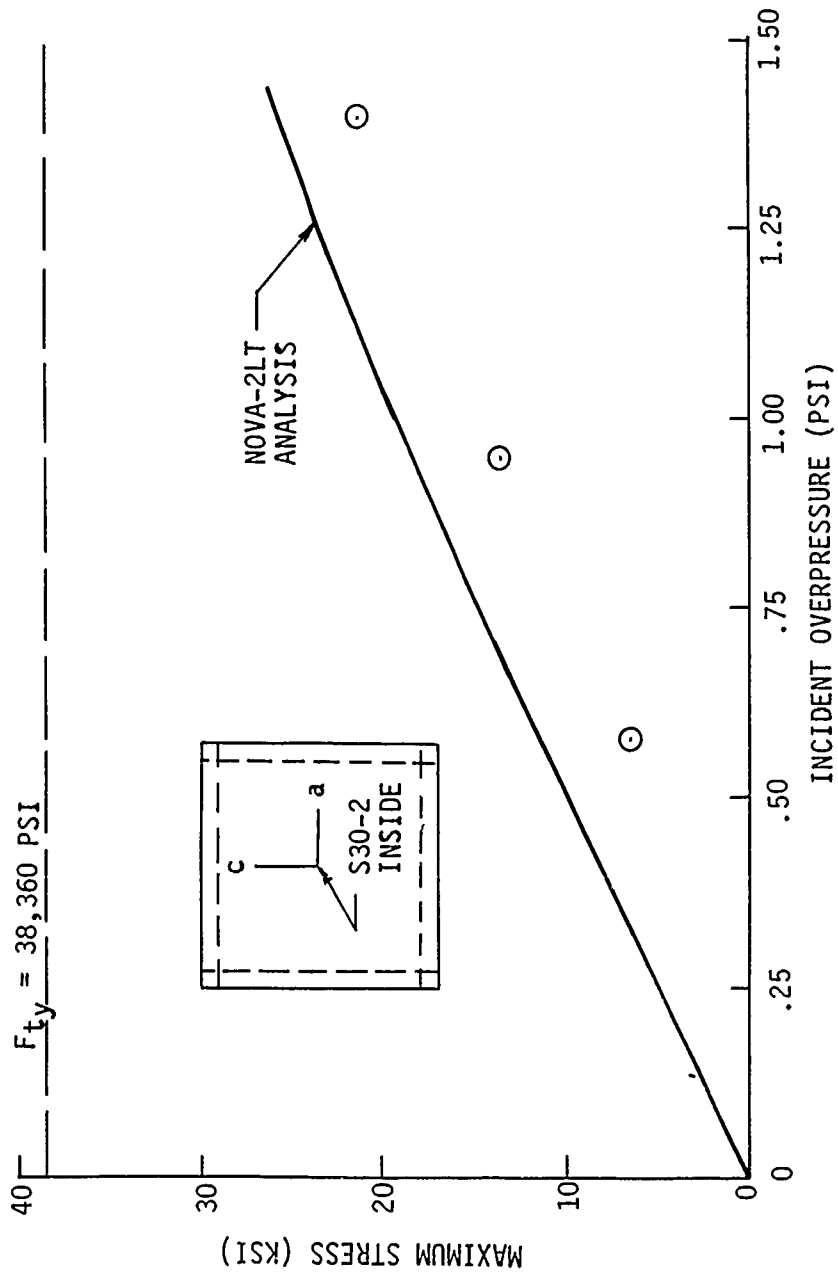


Figure 52. Maximum Stress Vs. Incident Overpressure - Specimen 30 - Gauge S30-2

TEST SPECIMEN NO. 30
DEFLECTION AT CENTER OF PANEL

○ GAUGE D30-9

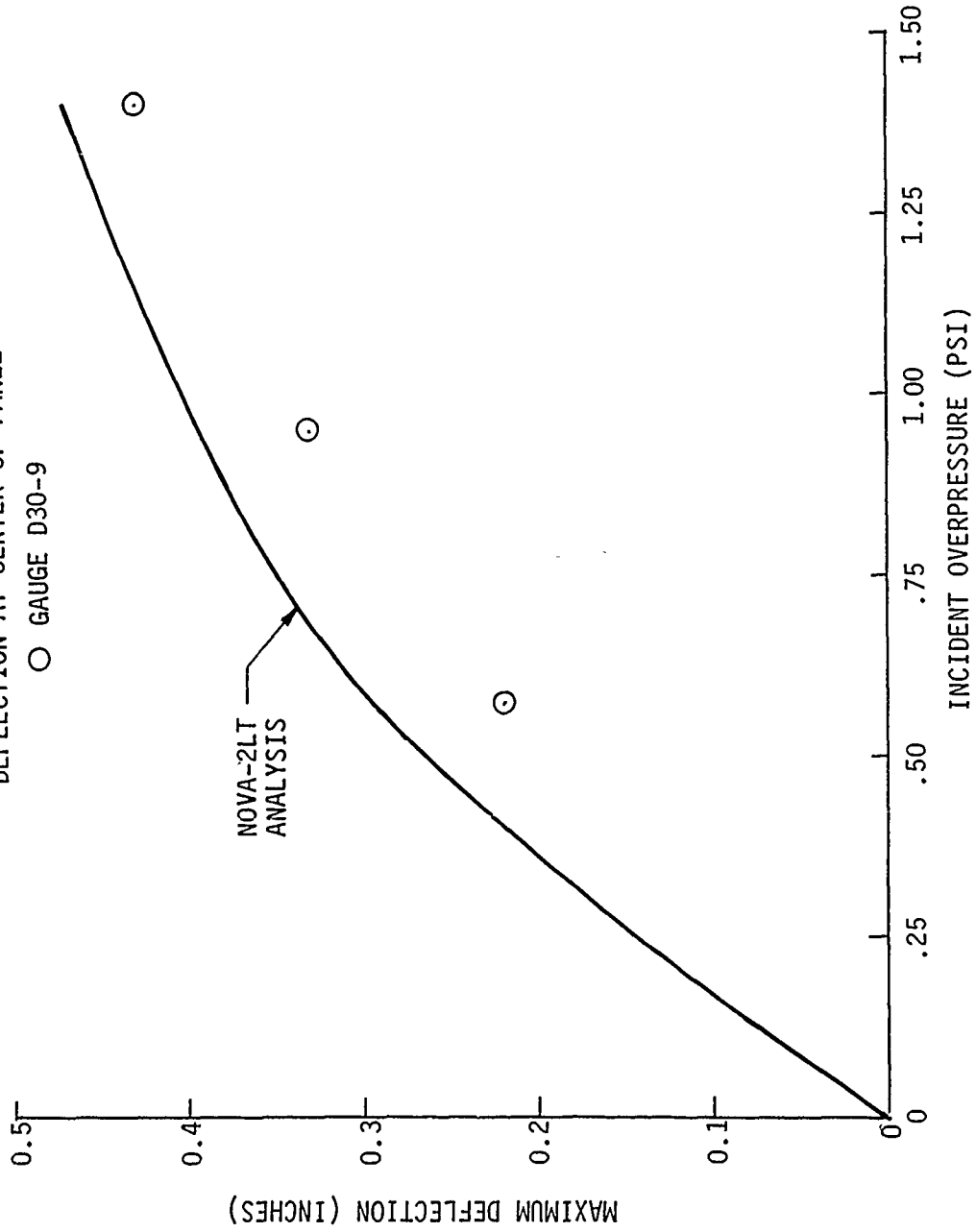


Figure 53. Maximum Deflection Vs. Incident Overpressure - Specimen 30 -
Gauge D30-9

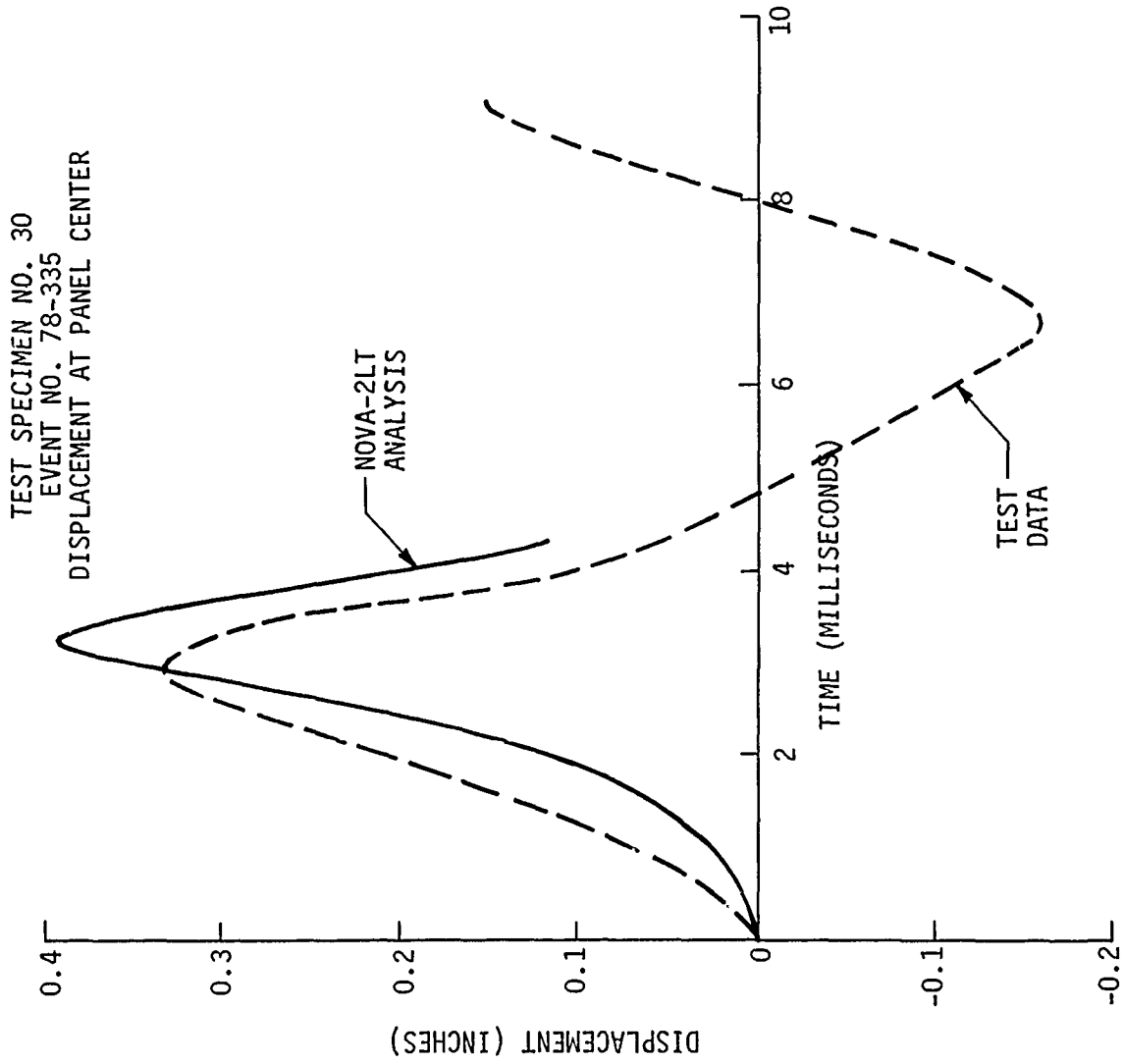


Figure 54. Deflection Time History - Specimen 30

TEST SPECIMEN NO. 31
 STRESS AT CENTER OF EDGE
 ○ AVERAGE OF GAUGES S31-3 AND S31-5

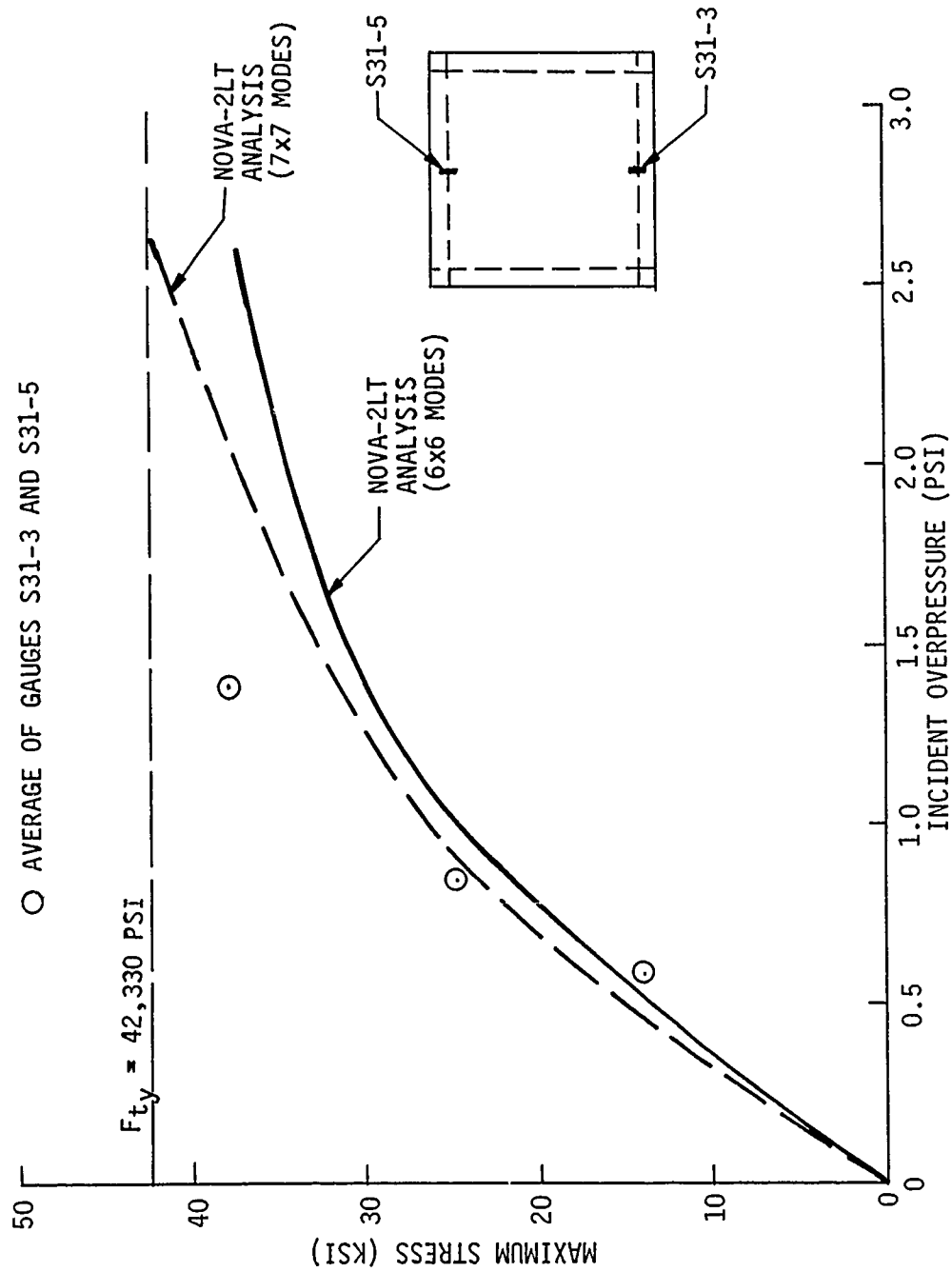


Figure 55. Maximum Stress Vs. Incident Overpressure - Specimen 31 - Gauges S31-3 and S31-5

TEST SPECIMEN NO. 31
STRESS AT CENTER OF PANEL

○ GAUGE S31-2

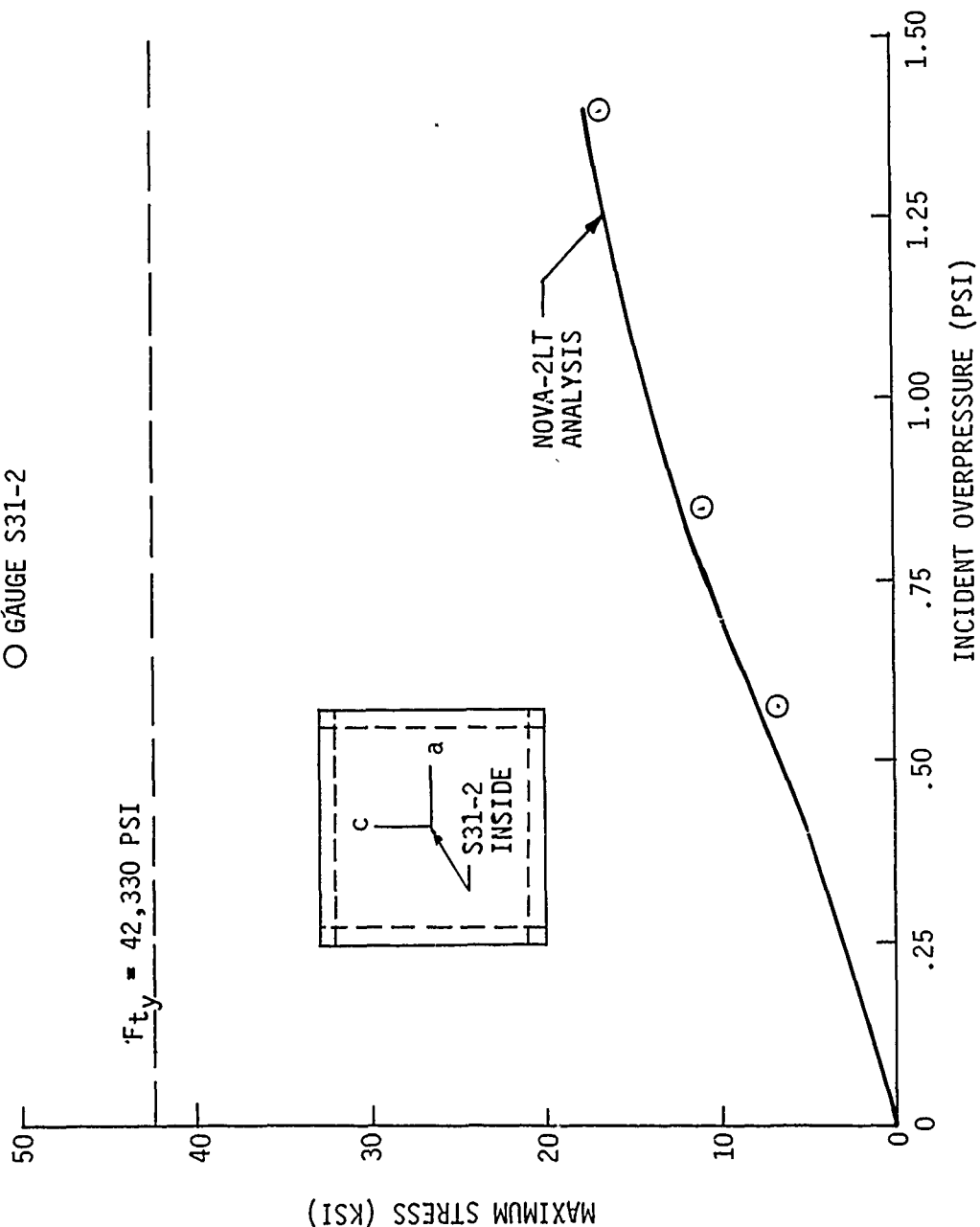


Figure 56. Maximum Stress Vs. Incident Overpressure - Specimen 31 - Gauge S31-2

TEST SPECIMEN NO. 31
 STRESS AT CENTER OF PANEL
 ○ GAUGE S31-2

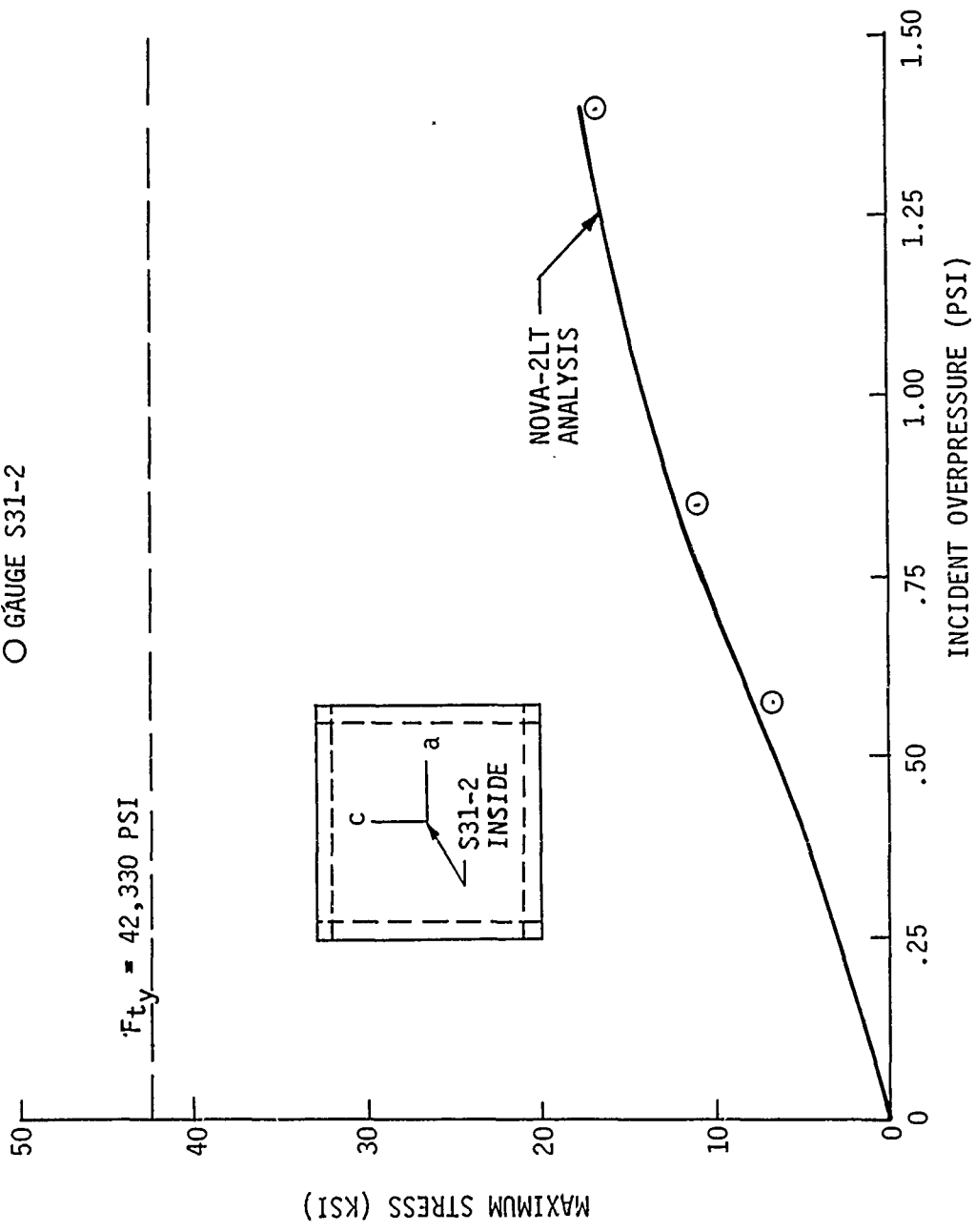


Figure 56. Maximum Stress Vs. Incident Overpressure - Specimen 31 - Gauge S31-2

TEST SPECIMEN NO. 31
DEFLECTION AT CENTER OF PANEL

○ GAUGE D31-9

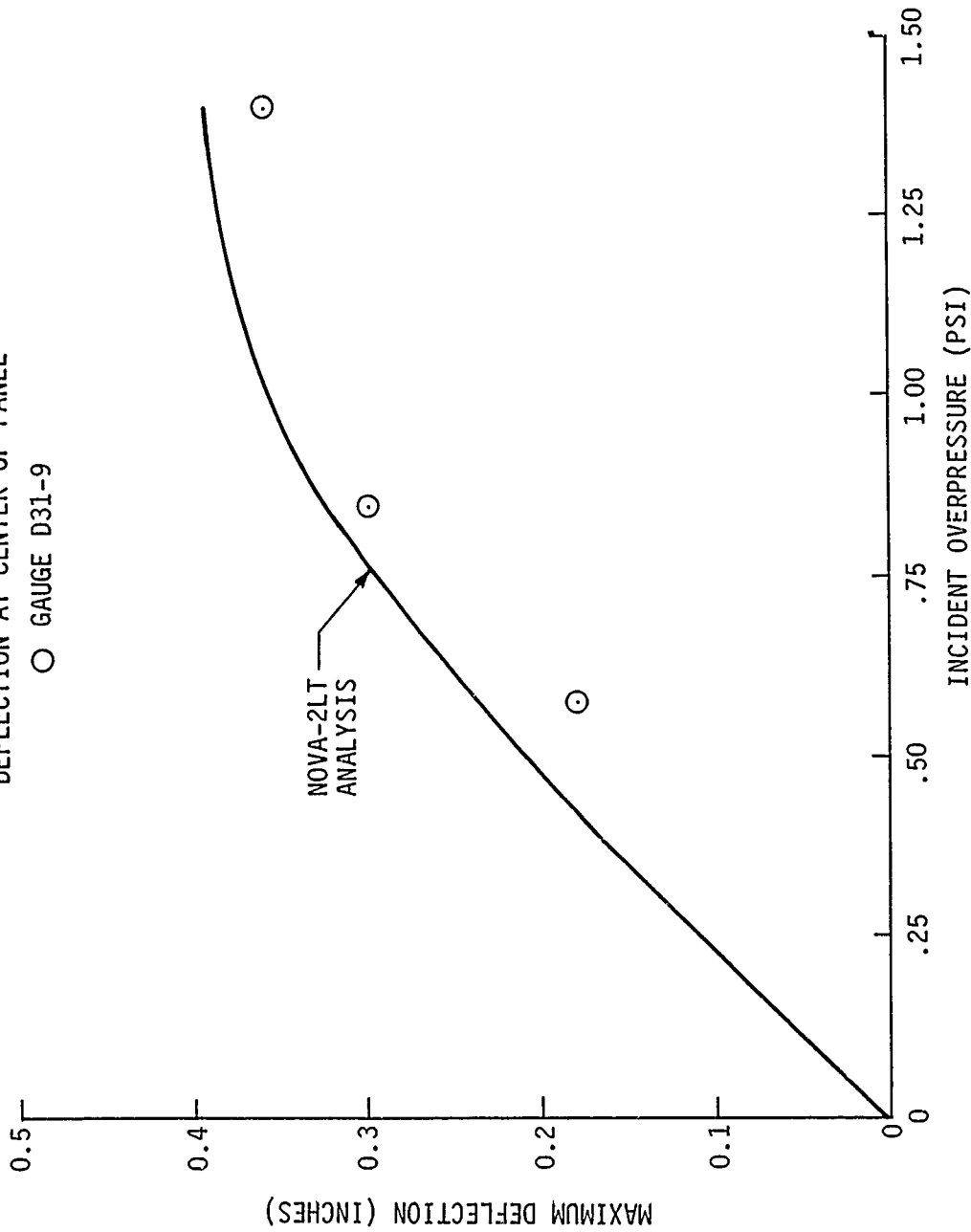


Figure 57. Maximum Deflection Vs. Incident Overpressure - Specimen 31 -
Gauge D31-9

TEST SPECIMEN NO. 31
EVENT NO. 78-339
DISPLACEMENT AT PANEL CENTER

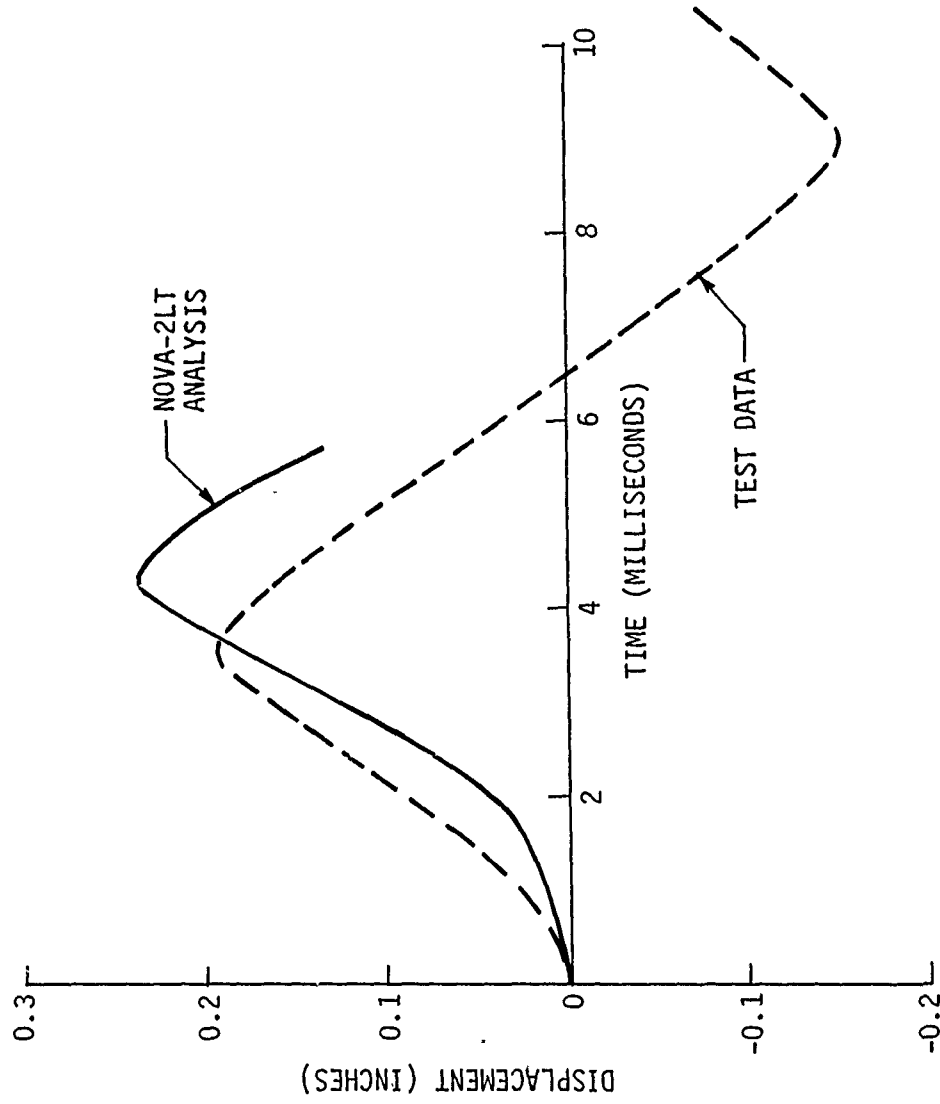


Figure 58. Deflection Time History - Specimen 31

In addition, a permanent deformation of 0.1 inches was measured manually at the panel center after the final test shot for this specimen. The NOVA-2LT analysis results for this condition indicated no permanent deformation at the panel center. The maximum recorded strain associated with the final test shot saturated the strain gauges; however, it was observed that these strains were considerably in excess of 10,000 micro-inches per inch. For this condition, the analysis predicted a maximum strain of approximately 4040 micro-inches per inch.

8.3.8 Test Specimen 32

Test specimen 32 was a skin/frame cylinder as described in Tables 1-3. The element of interest in this specimen was the center frame, which was fixed to a simulated floor beam at $\theta = 0^\circ$ and $\theta = 180^\circ$. All analyses and tests for specimen 32 were conducted for a blast/structure incidence angle of 90° , i.e., the shock propagation vector was perpendicular to the longitudinal axis of the cylinder and also perpendicular to the tangent plane at the midspan of the frame.

Analysis results and test results are shown in Figures 59-63 and illustrate stress response in the inner flange of the center frame at approximately 5.5° from the point of fixity as well as 30° , 60° , and 90° from the point of fixity. No displacements were measured for this test specimen. As shown in Figures 59-62, the agreement between test and analysis is generally somewhat inconsistent. The test data indicate the critical area of the frame to be near the clamp point, whereas the analysis indicates a location 30° away from the clamp to be the critical frame location. Both test and analysis indicate compressive stresses to be more critical than tensile stresses.

The comparison of test and analysis strain time histories for specimen 32 (Gauge S32-14) and event 346 is shown in Figure 63. As shown, the general character of the analysis data is considerably different from the test data.

As discussed earlier, test specimen 32 was essentially identical to specimen 12 of the Reference 3 study except for the shape of the frame cross section. The cross section of specimen 32 was sized to provide essentially the same area and bending stiffness about an axis parallel to the longitudinal axis of the cylinder as specimen 12. Since the specimen 32 frame cross section was unsymmetric (channel section), however, frame twisting as well as bending contributed to overall stress levels. As indicated earlier, the frames of specimen 12 were symmetric I - sections.

Table 10 shows the comparison of test stress data for specimen 12 and 32 due to a simulated nuclear overpressure pulse with a peak intensity of approximately 2.8 psi. The stress data pertain to the frame inner flange and are normalized to unity for specimen 32 at $\theta = 5.5^\circ$.

TEST SPECIMEN NO. 32
STRESS AT 5.5" FROM CLAMP POINT

○ GAUGE S32-14

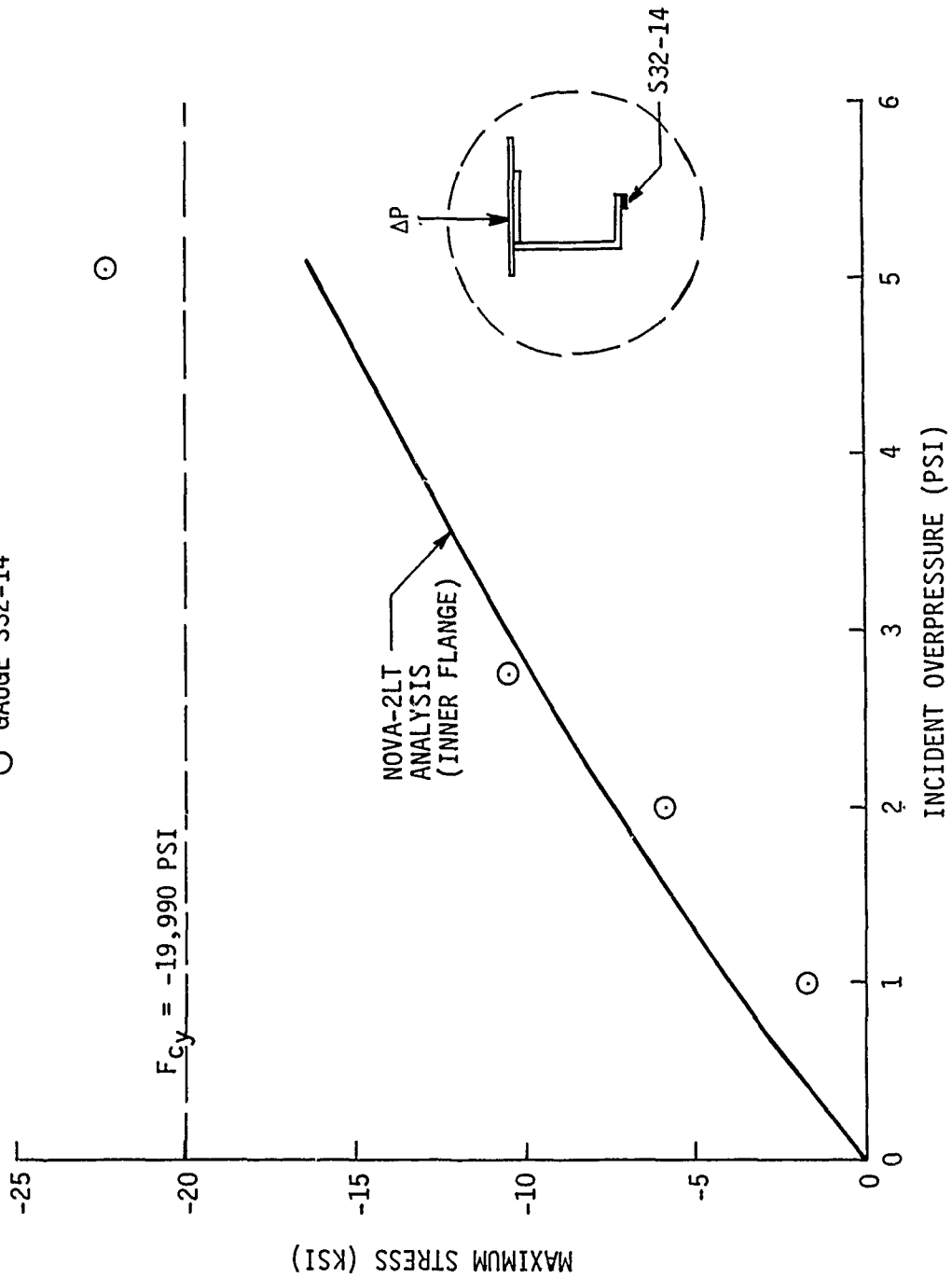


Figure 59. Maximum Stress Vs. Incident Overpressure - Specimen 32 -
Gauge S32-14

TEST SPECIMEN NO. 32
STRESS AT 30° FROM CLAMP POINT

○ GAUGE S32-10
△ GAUGE S32-21

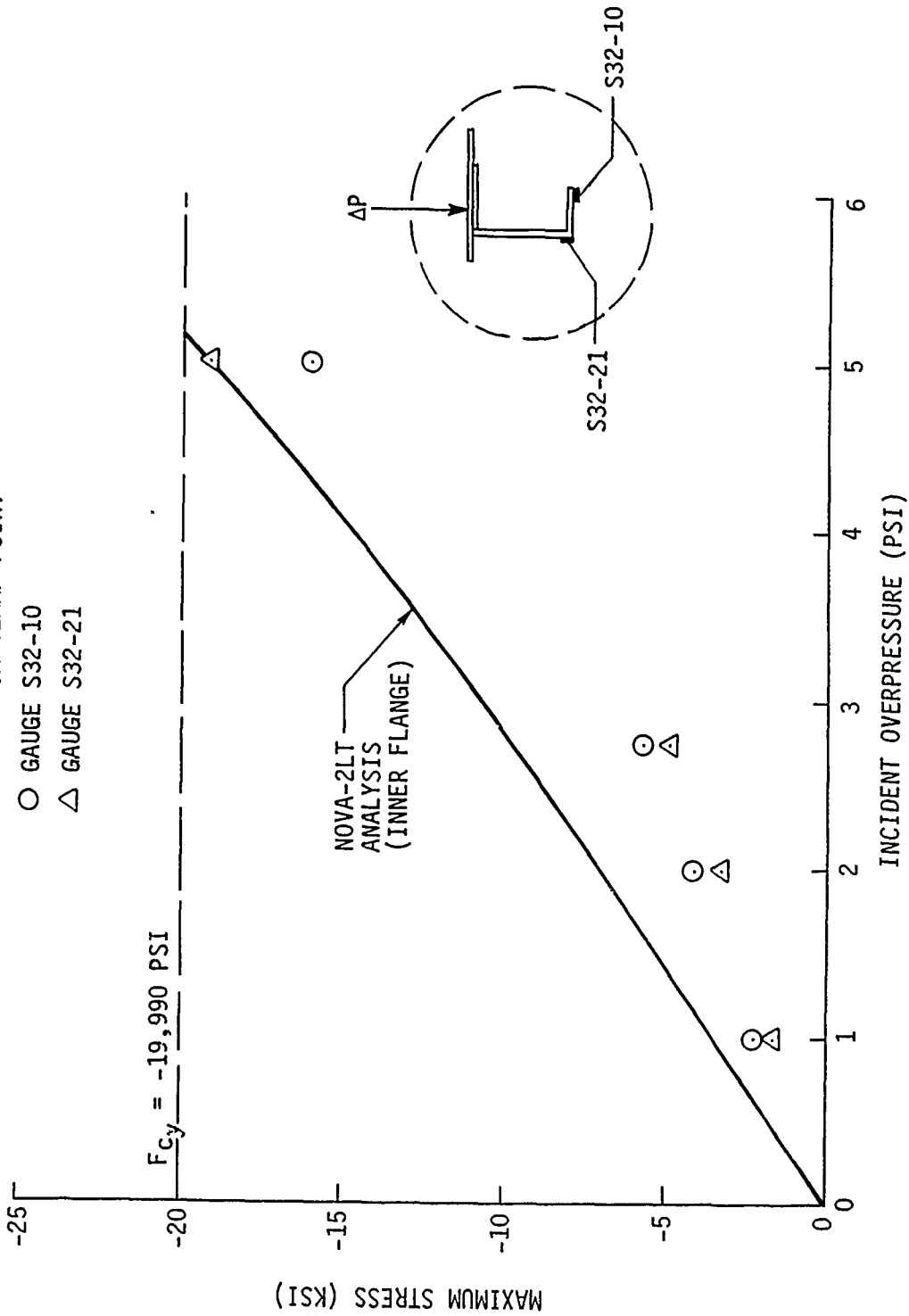


Figure 60. Maximum Stress Vs. Incident Overpressure - Specimen 32 - Gauges S32-10 and S32-21

TEST SPECIMEN NO. 32
STRESS AT 60° FROM CLAMP POINT

○ GAUGE S32-7
△ GAUGE S32-20

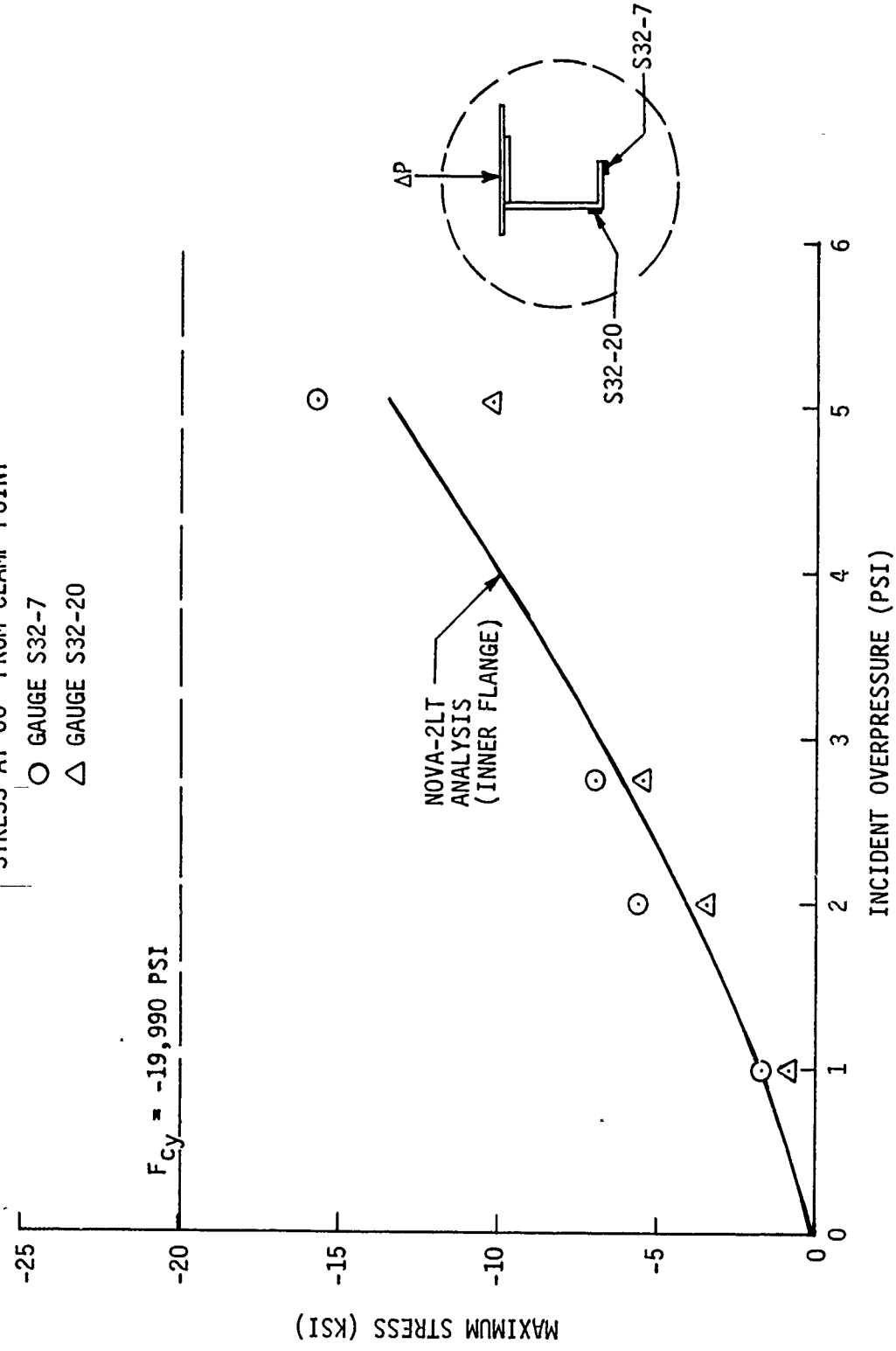


Figure 61. Maximum Stress Vs. Incident Overpressure - Specimen 32 - Gauges S32-7 and S32-20

TEST SPECIMEN NO. 32
STRESS AT 90° FROM CLAMP POINT

○ GAUGE S32-3
△ GAUGE S32-22

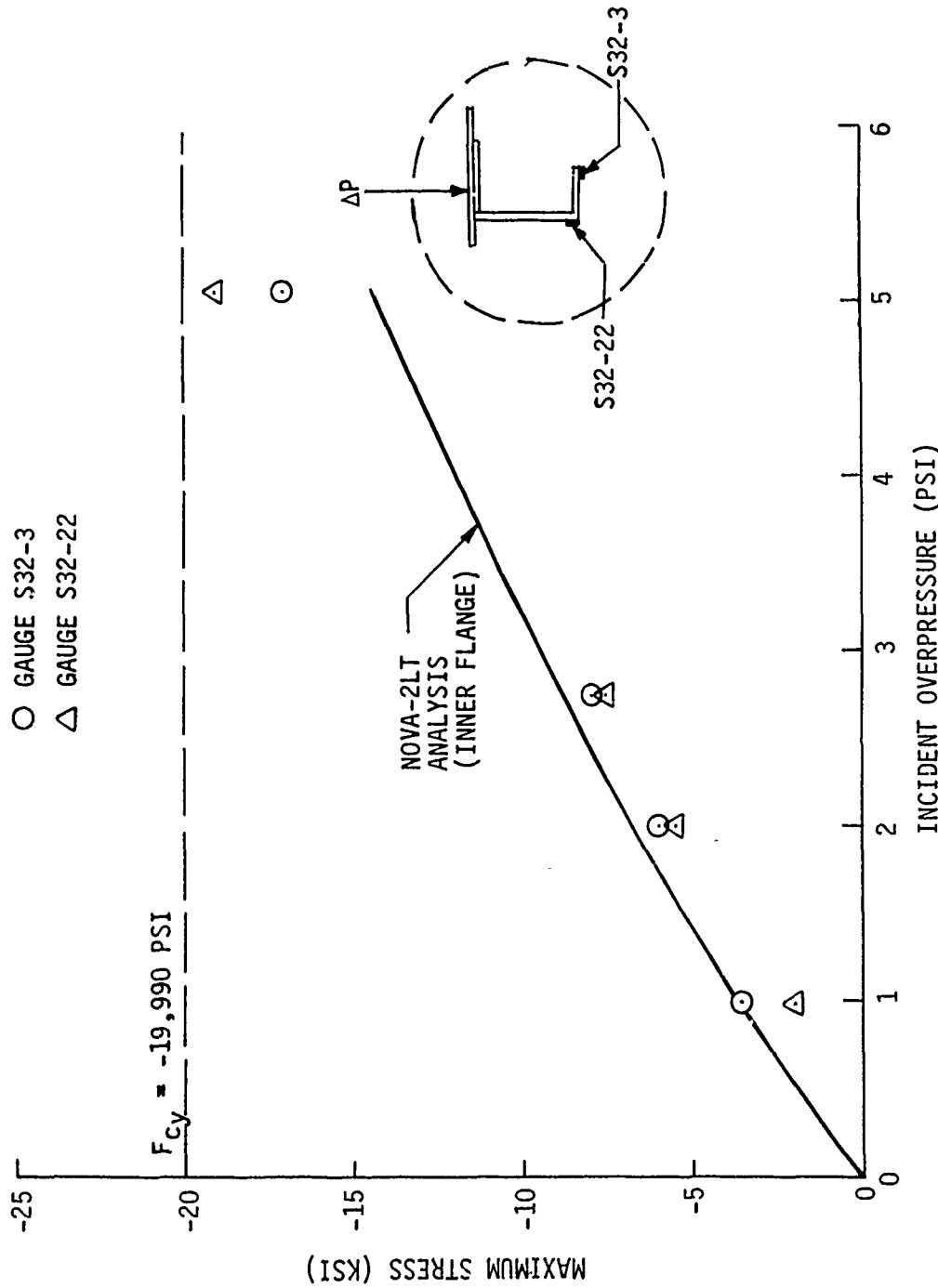


Figure 62. Maximum Stress Vs. Incident Overpressure - Specimen 32 -
Gauges S32-3 and S32-22

TEST SPECIMEN NO. 32
EVENT NO. 78-346
GAUGE S32-14

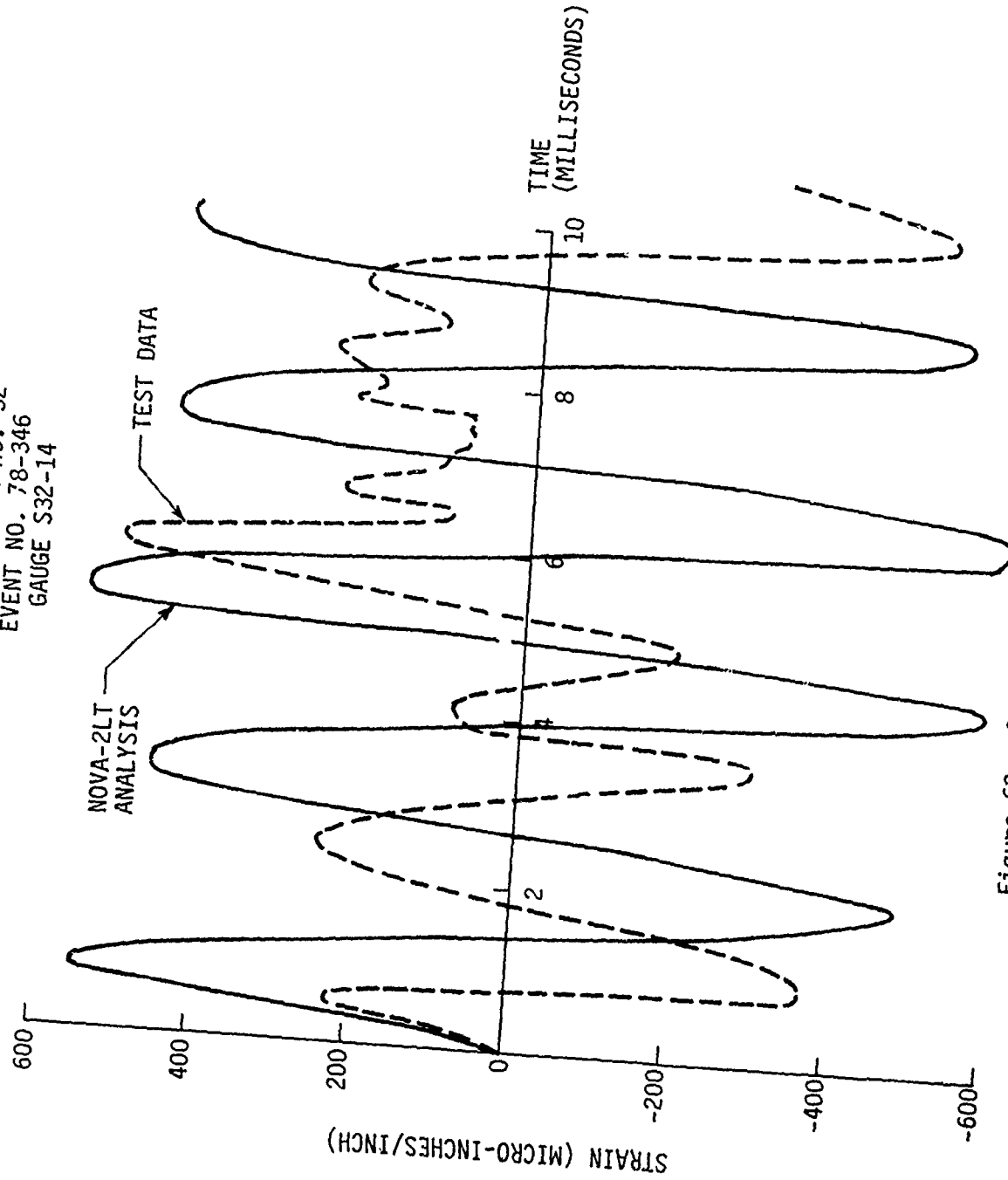


Figure 63. Strain Time History - Specimen 32

TABLE 10

COMPARISON OF SPECIMEN 12 AND 32
STRESS DATA IN FRAME INNER FLANGE

θ (DEGREES)	STRESS IN INNER FLANGE		σ SPEC 32 σ SPEC 12
	SPECIMEN 12	SPECIMEN 32	
5.5	1.67	1.0	0.60
30.0	1.81	0.54	0.30
60.0	0.57	0.66	1.16
90.0	1.02	0.74	0.73

As shown in Table 10, the differences in frame response were dramatic. These differences are due to two primary reasons: (1) the effect of frame twisting due to the unsymmetric cross section of specimen 32, and (2) differences in the overpressure time histories that loaded the two specimens. The loading for the specimen 12 test shot was more intense than that for specimen 32. Due to the limited amount of test data available, it is very difficult to determine which effect was dominant. However, it is anticipated that frame twisting had considerable impact on the differences in specimen 12 and 32 frame stresses. This is further supported by the differences that were observed in specimen 12 and 32 frame stresses due to static load as discussed in Section 8.2.8 of this report.

Based on the manner in which frame cross sections are modeled within NOVA-2LT, the effect of frame twist is not considered. That is, all stiffener cross sections are considered to be symmetric within the DEPROB subroutine of NOVA-2LT. This may be a serious limitation of NOVA-2LT for certain types of beams for which twisting is significant.

In addition, a permanent deformation of 0.06 inches in a radial sense at $\theta = 90^\circ$ was measured manually after the final test shot for this specimen. The NOVA-2LT analysis results for this condition indicated no permanent deformation. The maximum recorded compressive strain in the inner flange at 5.5° from the clamp point was 1950 micro-inches per inch, whereas NOVA-2LT analysis indicated 1450 micro-inches per inch for the condition and frame location.

8.3.9 Test Specimen 33

Test specimen 33 was a skin/frame cylinder as described in Tables 1-3. The element of interest in this specimen was the center frame, which was fixed to a simulated floor beam at $\theta = 0^\circ$ and $\theta = 180^\circ$. All analyses and tests for specimen 33 were conducted for a blast/structure incidence angle of 90° , i.e., the shock propagation vector was perpendicular to the longitudinal axis of the cylinder and also perpendicular to the tangent plane at the midspan of the frame.

Analysis results and test results are shown in Figures 64-69 and illustrate stress response in the inner flange of the center frame at approximately 5.5° and 60° from the point of fixity as well as in the outer flange of the center frame at approximately 30° and 90° from the point of fixity. No displacements were measured for this test specimen. As shown in Figures 64-67, the analysis predicted substantially higher stresses than those observed in the test. Furthermore, the test data indicate the maximum strain occurs in Gauge S33-18 at $\theta = 90^\circ$, whereas the NOVA-2LT analysis results indicate the maximum strain occurs in gauge S33-14 at $\theta = 5.5^\circ$. Both test and analysis indicate compressive stresses to be dominant.

The comparison of test and analysis strain time histories for specimen 33 (Gauge S33-14) and event 327 is shown in Figures 68 and 69. As shown, the general character of the analysis data is considerably different from the test data.

8.4 Summary of Static Load Test/Analysis Results

As indicated earlier in this report, all test specimens were static tested, but not to failure. Since the test specimens were purposely not tested up to their respective yield points, it is not possible to compare static test and analysis loads resulting in yield stress without significantly extrapolating test results. As an alternative, Table 11 shows a comparison of measured stress and predicted stress for the maximum static load that was imposed on each test specimen. Data for the columns (specimens 18-29) are not included in Table 11, since they were not analyzed using NOVA-2LT. In general, the maximum static load for each specimen produced a stress equal to 60-80 percent of the yield stress. Table 11 does provide valuable trend information; however, the results would change for some of the specimens if the static test had resulted in yielding of the specimens, and if the comparison had been made regarding the respective static pressure levels required to cause this yielding.

TEST SPECIMEN NO. 33
STRESS AT 5.5° FROM CLAMP POINT

○ GAUGE S33-14

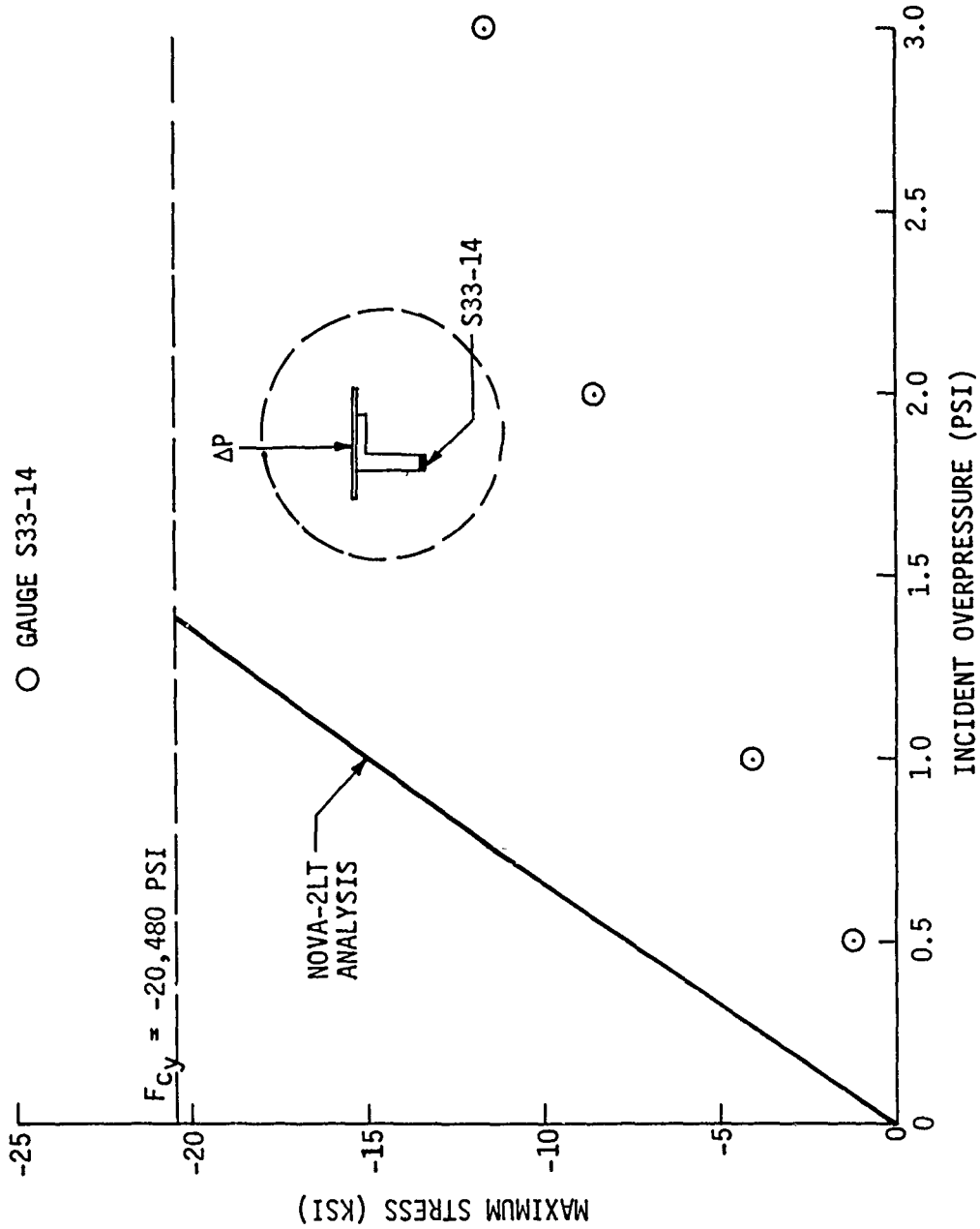


Figure 64. Maximum Stress Vs. Incident Overpressure - Specimen 33 - Gauge S33-14

TEST SPECIMEN NO. 33
STRESS AT 30° FROM CLAMP POINT

○ GAUGE S33-9

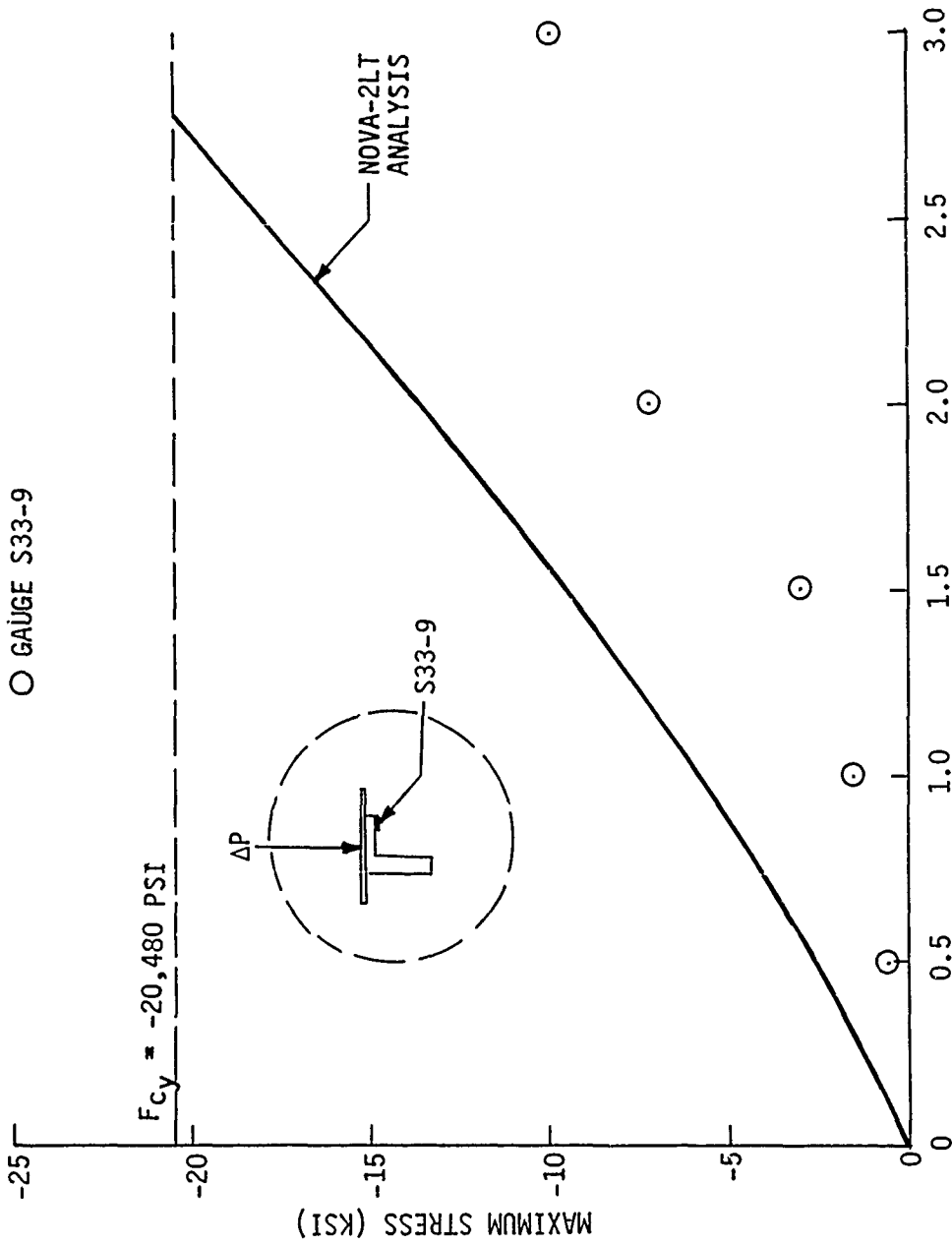


Figure 65. Maximum Stress Vs. Incident Overpressure - Specimen 33 -
Gauge S33-9

TEST SPECIMEN NO. 33
STRESS AT 60° FROM CLAMP POINT

○ GAUGE S33-7

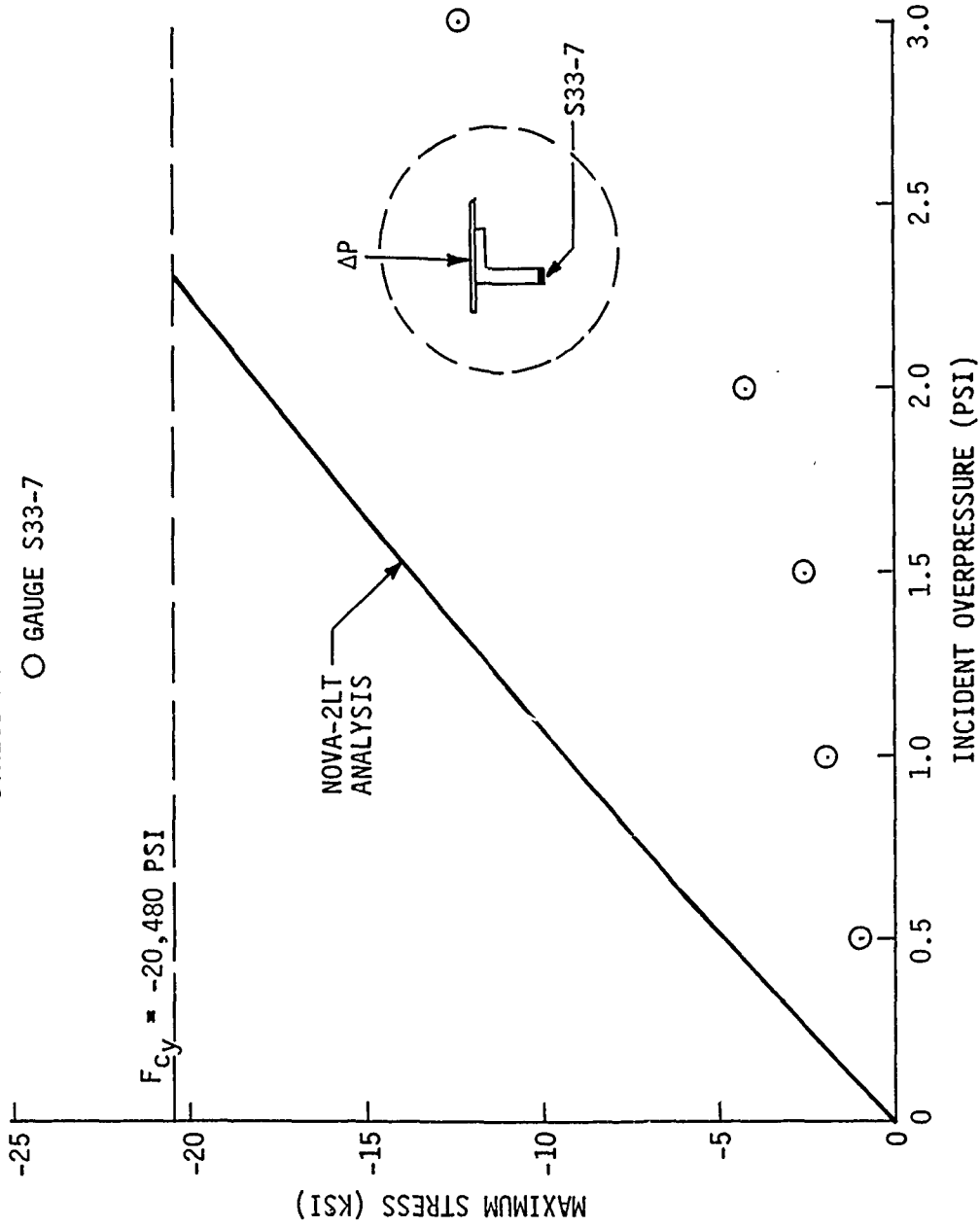


Figure 66. Maximum Stress Vs. Incident Overpressure - Specimen 33 -
Gauge S33-7

TEST SPECIMEN NO. 33
STRESS AT 90° FROM CLAMP POINT

○ GAUGE S33-18

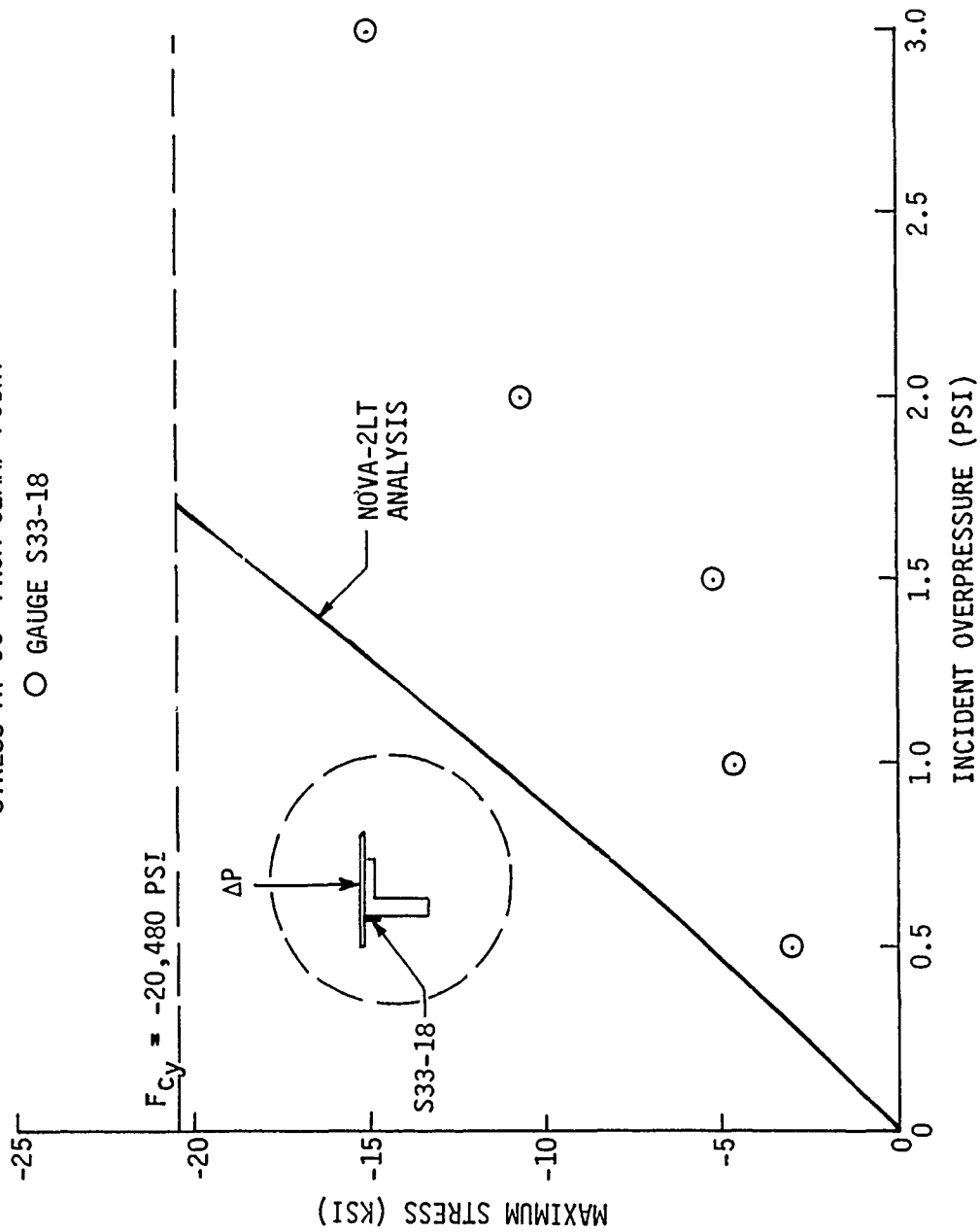


Figure 67. Maximum Stress Vs. Incident Overpressure - Specimen 33 -
Gauge S33-18

TEST SPECIMEN NO. 33
EVENT NO. 78-327
GAUGE S33-14

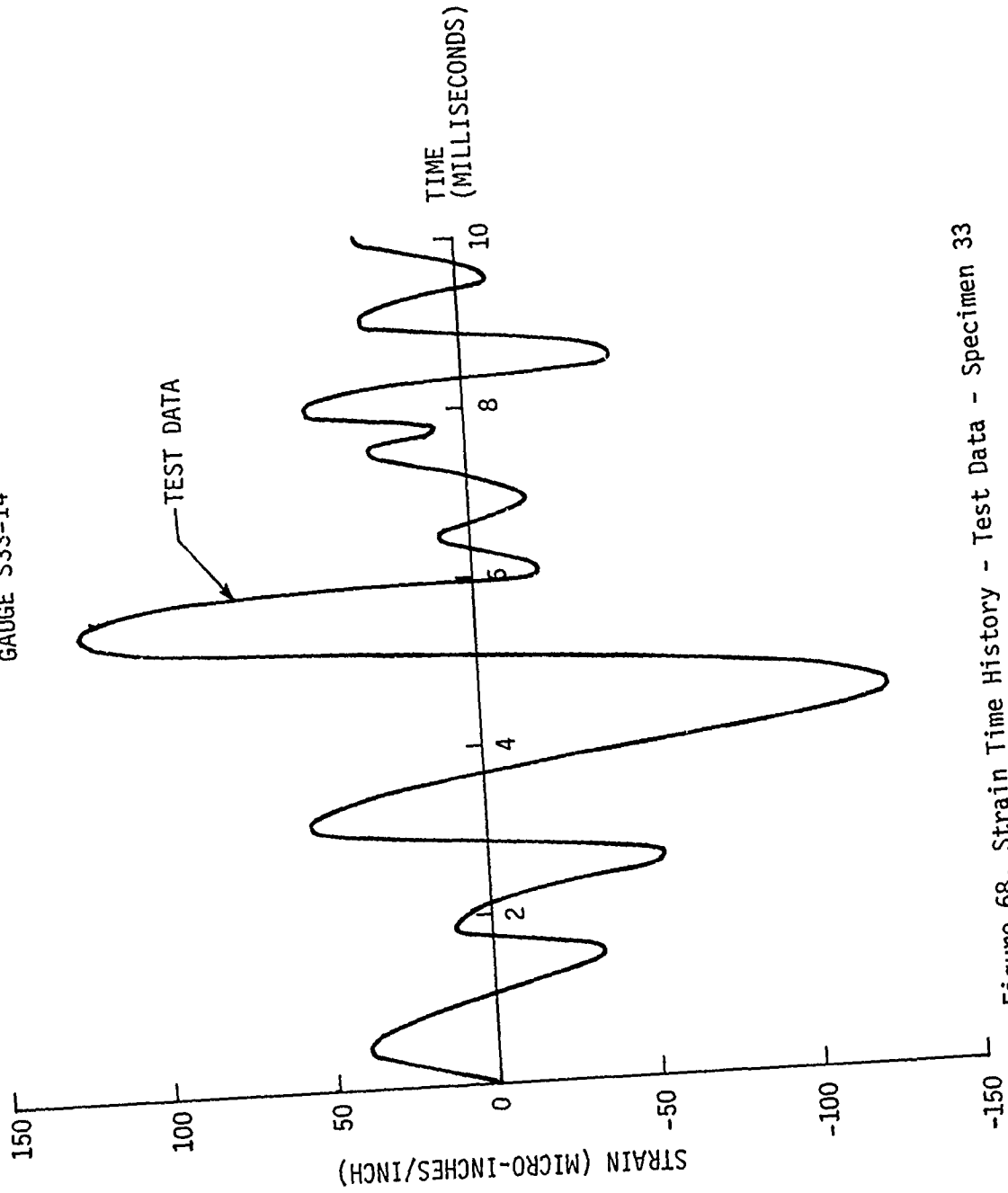


Figure 68. Strain Time History - Test Data - Specimen 33

TEST SPECIMEN NO. 33
EVENT NO. 78-327
GAUGE S33-14

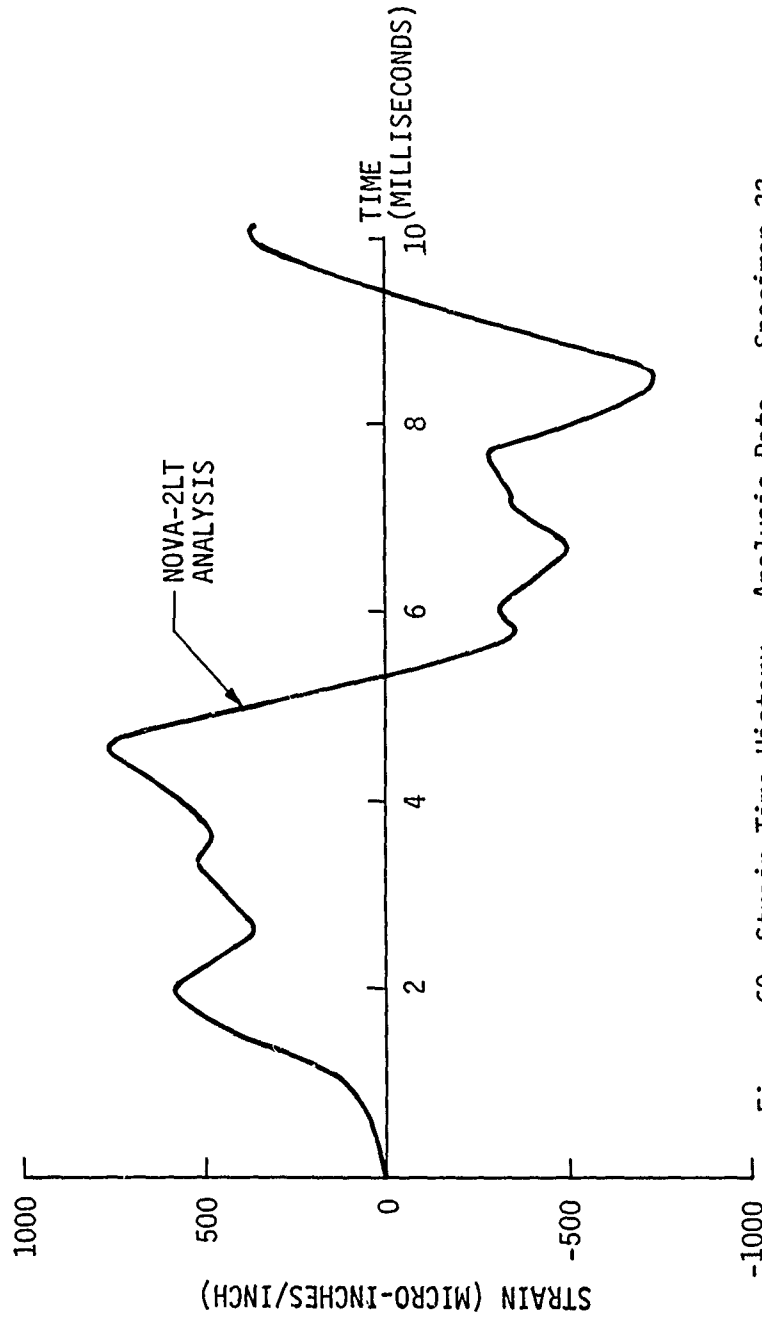


Figure 69. Strain Time History - Analysis Data - Specimen 33

TABLE 11
 STATIC LOAD TEST/ANALYSIS RESULTS - SPECIMENS 30-33

SPECIMEN NO.	MAXIMUM STRESS DUE TO MAXIMUM STATIC LOAD		$\frac{\sigma_{TEST}}{\sigma_{ANALYSIS}}$
	TEST	ANALYSIS	
30	31500	20000	1.58
31	31800	26200	1.21
32 (INNER FLANGE)	-4300	-3450	1.25
32 (OUTER FLANGE)	-12000	-3200	3.75
33 (INNER FLANGE)	-6200	-5400	1.15
33 (OUTER FLANGE)	-13200	-5100	2.59

Similar to the data presented in the Reference 3 study, NOVA-2LT under-predicted the strains at the clamped boundaries of thin skin panels. This is shown by the Table 11 data for test specimens 30 and 31. Based on these data and similar data in Reference 3, it is apparent that the larger the ratio of panel length to panel thickness, the poorer the correlation between test and analysis. Combining data for specimens 1, 4, and 5 from the Reference 3 study with data for specimens 30 and 31 from this study, the effect of panel geometry on the accuracy of analysis results at the center of the clamped edges of the panel was obtained as shown in Figure 70. The analysis models all retained 25 modal combinations from a 7 X 7 mode set.

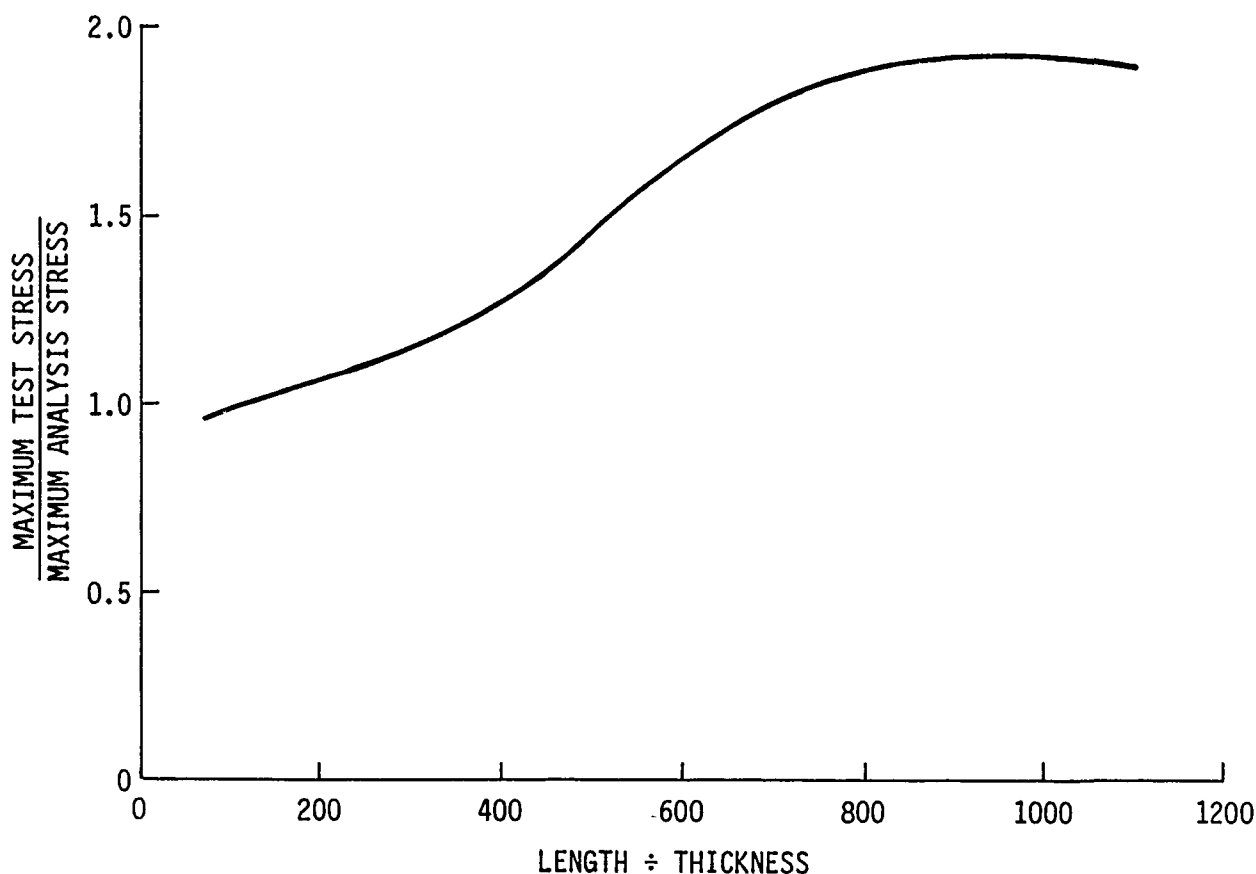


Figure 70. Effect of Panel Geometry on Accuracy of Static Load Stress Predictions at Center of Clamped Edge

Table 11 also indicates that NOVA-2LT more accurately predicted maximum strains in the inner flange of specimens 32 and 33 than in the outer flange. However, the strain gauges were not located exactly on the outside of the outer flange of specimens 32 and 33 as shown in Figures 5 and 6, whereas the analysis results do pertain to the outside of the outer flange. Similar results were observed in the Reference 3 study of skin/frame cylinder specimens 12 and 13.

8.5 Summary of Shock Load Test/Analysis Results

As discussed earlier, all test specimens were exposed to a series of simulated nuclear overpressure environments resulting in stresses up to yield and beyond. The test specimens were analyzed by using the measured reflected overpressure time histories as input to the NOVA-2LT computer program. The test/analysis results are summarized in Table 12. This table indicates that the NOVA-2LT consistently predicted the column specimens (18-29) to be weaker than that observed in the shock load test. One possible explanation for this

is that friction forces between the piston and the cylinder may have retarded piston movement to a certain degree. In addition, the initial lateral eccentricities in the columns may not have exhibited a 1-cosine variation along the span of the column as assumed in the NOVA-2LT mathematical models. The sensitivity of the analysis results to the initial eccentricity data was pronounced as discussed earlier in this report.

As discussed in Section 8.4, the NOVA-2LT analysis results indicated substantially lower strains at the center of the clamped edges of the skin panels (specimens 30-31) than that observed in the static test. This was also true regarding shock load test/analysis results as shown in Table 12. The trend of the test/analysis results as a function of panel thickness was similar to that exhibited in the static test/analysis. That is, as the ratio of panel length to panel thickness increased, the differences between shock load test and analysis results increased. Combining the results for specimens 30 and 31 with those for specimens 1, 4, and 5 of the Reference 3 study, the effect of panel geometry on the accuracy of analysis results at the center of the clamped edges was obtained as shown in Figure 71. The trend of these data is similar to that for the static load test/analysis data shown in Figure 70. An exception to this are the results for the membrane panel (length ÷ thickness = 1100). A rational explanation for the membrane panel results is not available.

TABLE 12

SHOCK LOAD TEST/ANALYSIS RESULTS - SPECIMENS 18-33

SPECIMEN NO.	SHOCK STRENGTH (PSI) 		ANALYSIS
	ANALYSIS	TEST	TEST
18-21	7.4	9.0	0.82
22	4.2	6.6	0.64
23	5.4	6.9	0.78
24	6.0	13.5	0.44
25	10.7	16.5	0.65
26	2.7	5.0	0.54
27	5.1	6.1	0.84
28	8.2	9.0	0.91
29	9.7	10.5	0.92
30	2.8	1.3	2.15
31	2.6	1.7	1.53
32	5.2	4.7	1.11
33	1.4	3.5	0.40

 INCIDENT SHOCK INTENSITY RESULTING IN YIELDING

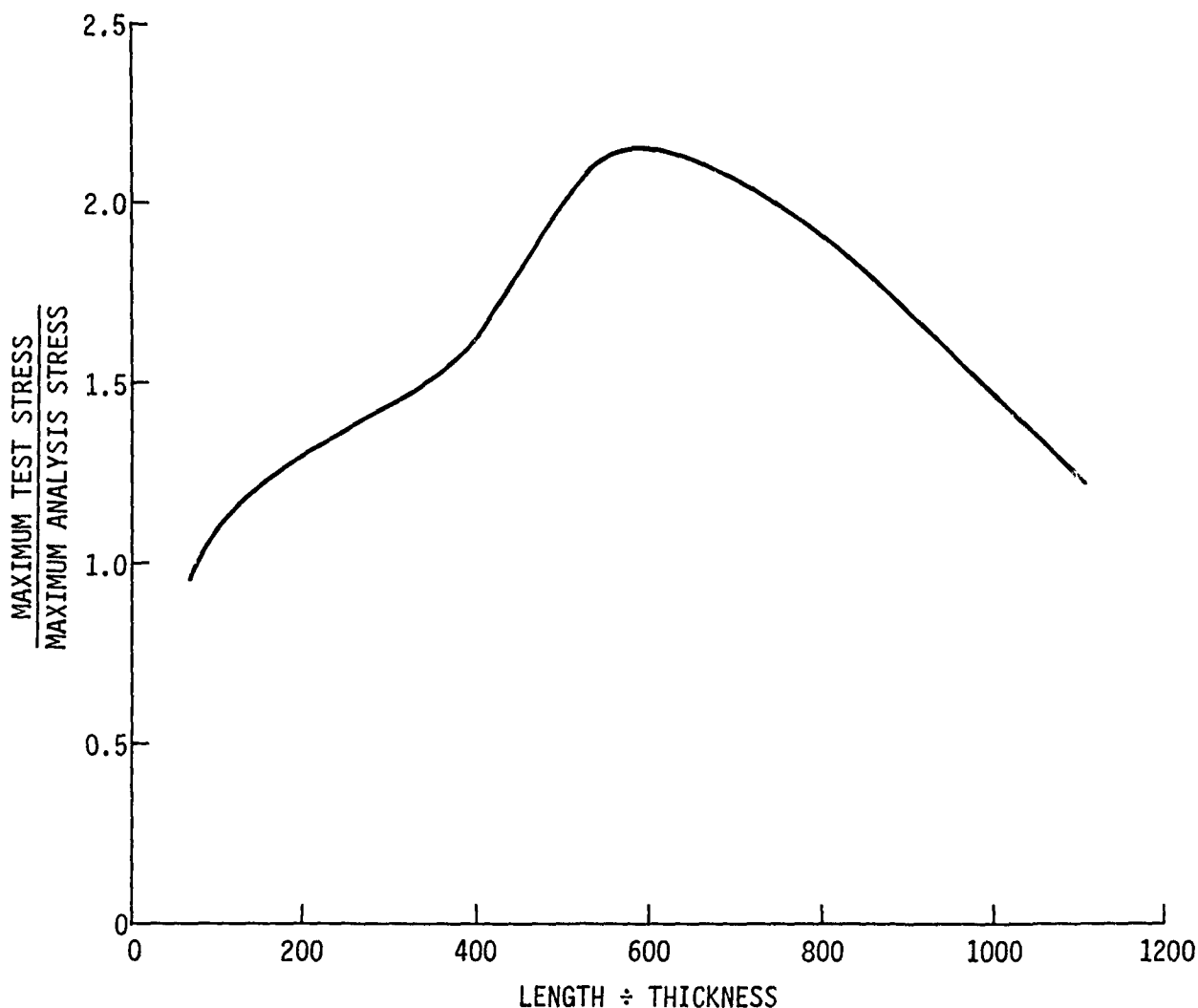


Figure 71. Effect of Panel Geometry on Accuracy of Shock Load Stress Predictions at Center of Clamped Edge.

Table 12 also shows that the NOVA-2LT analysis results predicted the shock strength of the specimen 32 skin/frame cylinder within 11 percent. Figures 59 and 60, however, indicate that analysis predicted the critical area of the frame to be the inside of the inner flange at a location 30° away from the clamp point. Test data indicated that the inside of the inner flange was slightly more critical at 5.5° from the clamp point than at 30° from the clamp point. Both test and analysis data indicated that compressive stresses were dominant.

Analysis results for the specimen 33 skin/frame cylinder were significantly different from test results as shown in Table 12. The analysis results indicated that the inside of the unsupported leg of the angle near the clamp point was critical in compression. Test data, however, indicated that the center frame was critical in compression $60-90^\circ$ away from the clamp point.

In addition to the shock load testing discussed above, the test specimens were each exposed to one test shot of sufficient intensity to cause measurable permanent deformation. One exception to this was specimen 33. Also, since the NOVA-2LT computer program solution terminates when buckling of a column has occurred, the comparison of test and analysis data in the plastic region was limited to specimens 30-32. These data are presented in Table 13. ϵ_{MAX} refers to the maximum strain and δ refers to the permanent deformation resulting from the final test shot.

TABLE 13
TEST AND ANALYSIS RESULTS IN THE PLASTIC REGION

SPECIMEN NO.	INCIDENT SHOCK INTENSITY (PSI)	TEST		ANALYSIS	
		ϵ_{MAX} (IN/IN)	δ (IN)	ϵ_{MAX} (IN/IN)	δ (IN)
30	4.80	.019	0.24	.0033	0.0
31	4.80	> .010	0.10	.0040	0.0
32	5.05	.00195	0.06	.0015	0.0

Table 14 shows the comparison of shock load test and analysis fundamental response frequencies of test specimens 18-33. In general, the test and analysis response frequencies compare very well.

TABLE 14
TEST AND ANALYSIS STRUCTURAL RESPONSE FREQUENCIES

SPECIMEN NO.	FUNDAMENTAL RESPONSE FREQUENCY (Hz)	
	TEST	ANALYSIS
18-21	19.	17.
22-23	6.3	5.6
24-25	25.	17.
26-27	5.2	2.9
28-29	8.9	6.8
30	125.	100.
31	70.	60.
32	570.	430.
33	600.	100/500 

 Secondary Response Frequency

8.6 Static Test Results Vs. Shock Test Results

Structural response due to a shock load environment can be significantly greater than that resulting from exposure to a static overpressure environment even though the peak pressure intensities of the two environments are identical. This phenomenon occurs because: (1) the free field (incident) overpressure is enhanced due to reflection and (2) magnification of the response results from the dynamic nature of the loading. In other words, a specific structural response in a particular test specimen will be caused by exposure to a simulated nuclear overpressure pulse whose peak incident intensity is, in general, considerably less than the magnitude of static overpressure which causes the same structural response. This amplification of the response is shown for specimens 30-33 in Table 15. This table does not include data for specimens 18-29 (columns) because inertia effects of the piston would be present in the shock load response data and not present in the static load response data. Specifically, Table 15 compares the peak shock load response to the static load response for the maximum pressure load that was applied during the static test.

TABLE 15
COMPARISON OF STATIC TEST DATA AND SHOCK
LOAD TEST DATA - SPECIMENS 30-33

SPECIMEN NO.	ΔP (PSI)	STATIC STRESS (PSI)	MAXIMUM DYNAMIC STRESS (PSI)	σ DYNAMIC
				σ STATIC
30	1.25	22000.	38400.	1.75
31	1.25	17000.	42300.	2.49
32 (Inner Flange)	4.0	-4300.	-16200.	3.77
32 (Outer Flange)	4.0	-12000.	-20100.	1.68
33 (Inner Flange)	3.0	-4700.	-12200.	2.60
33 (Outer Flange)	3.0	-9800.	-15000.	1.53

9.0 OBSERVATIONS AND CONCLUSIONS

Results from the static load test, shock load test, and associated analyses led to the following observations and conclusions:

(a) The THUNDERPIPE shock tube is a useful blast simulation facility for shock load tests of the nature described in this report. For the lower intensity test shots (5 psi and less), composition -4 explosive was detonated in the 2-foot diameter driver to generate the overpressure pulse. For these test shots, the shock tube was approximately 643 feet long. For the higher intensity test shots, the 2-foot diameter driver section of the pipe was removed and primacord was detonated in the 6-foot diameter driver to generate the overpressure pulse. As a result, the modified shock tube was approximately 400 feet long. This was done because of strength limitations of the 2-foot diameter driver section. Overpressure time histories shown in Volume II of this report indicate that use of composition -4 in the 2-foot diameter driver section resulted in overpressure pulses that were considerably smoother than those obtained from the use of primacord. However, positive phase durations of the overpressure pulses were essentially the same for both tunnel configurations and explosive sources.

(b) Significant enhancement of the incident overpressure pulse due to interaction with the test specimens was observed throughout the test as expected. This shock enhancement, coupled with dynamic application of the pressure load, caused significantly greater stress in the test specimens than was observed for corresponding static loads. For a number of test shots, the reflected overpressure measured on the test specimen experienced an instantaneous rise to a peak value followed by a rapid decay for approximately 1.5 milliseconds followed by an instantaneous rise to a second peak value. For several test shots, this second peak was observed to be 50 percent greater than the initial reflected peak. These observations were also made in the Reference 3 study. A possible explanation of this phenomenon was obtained from personnel at R&D Associates, Marina del Rey, California, and was included in Reference 3. It is repeated here for completeness: The large secondary peak loadings measured on the structures may have been due to geometric focusing of waves reflected off the shock tube walls (particularly the diverging section). In the acoustic approximation, the amplitudes of such waves vary as $r^{-1/2}$, where r is the radius from the tube centerline, and show no variation with distance down the centerline. The repetitive nature of the pressure fluctuations was probably caused by radial reverberations in the driver section of the shock tube.

(c) In general, the level of agreement between static test results and static analysis results was fairly good. As stated earlier in this report, the NOVA-2LT computer program that was available for use in this program was not designed to perform a static analysis of buckling sensitive columns. Therefore, the static analysis results shown in this report for test specimens 18-29 were obtained by use of classical Euler buckling techniques. However, Kaman Aviodyne personnel have modified a

special version of NOVA-2 that is suited for analysis of static buckling of columns. Limited analysis results that were made available to the authors of this report indicate good agreement with test results. With regard to the flat panel specimens 30-31, it has already been discussed that NOVA-2LT stresses at the center of the clamped edges were significantly less than those observed during the static test. However, very good agreement between test and analysis stress and displacement was observed at the center of specimens 30 and 31. For test specimens 32 and 33 (skin/frame cylinders), the agreement between test and analysis stress in the frame inner flange was good. In the outer flange, however, measured stresses were substantially higher than predicted. It is possible that the complex wrinkling pattern experienced by the skin caused the frame to experience bending in a higher order mode than was anticipated, thereby resulting in higher stresses in the outer flange than anticipated. As mentioned earlier in this report, beam cross sections were considered to be symmetric by NOVA-2LT regardless of the actual cross section. Comparing the static test results of specimens 32 and 33 (non-symmetric frame cross sections) with similar data for Reference 3 specimens 12 and 13 (symmetric frame cross sections), it was observed that the effect of symmetry on structural response can be significant. For certain types of structure, this could be a serious limitation of NOVA-2LT.

(d) Many of the comments in the previous paragraph also apply to the comparison of shock load test/analysis results. However, the shock analysis stresses for specimen 33 were substantially larger than those observed in the test. This was opposite to the trend of the static load test/analysis stress results. In addition, the agreement between test and analysis stresses for the column specimens 18-29 was considered to be generally very good. If friction forces were known and were incorporated into the analysis, it is anticipated that the test/analysis stresses would exhibit even better agreement. Also, the predicted response frequencies were very similar to the measured values. With regard to structural response in the plastic region, the analysis significantly underpredicted peak strain and permanent deformation for panel specimens 30-31. Better agreement between test and analysis results in the plastic region was seen for test specimen 32. Similar to the findings in the Reference 3 report, shock intensity required to cause measurable permanent deformation was substantially larger than the shock intensity associated with the threshold of permanent damage for the same specimen. This implies that even though a structural component may begin to yield at a relatively low overpressure intensity, a relatively high intensity shock load may be required to cause enough of the structure to exhibit plastic behavior that measurable permanent deformation results. The implications of this regarding "sure-safe" nuclear hardness and "mission-completion" nuclear hardness are obvious.

REFERENCES

1. NOVA-2 - A Digital Computer Program for Analyzing Nuclear Overpressure Effects on Aircraft. AFWL-TR-75-262, Air Force Weapons Laboratory, Kirtland AFB, New Mexico, August 1976.
2. Nuclear Blast and Shock Simulators. Panel N-2 Report N2: TR-72, Washington, D. C., 28 December 1972.
3. Structural Response to Simulated Nuclear Overpressure: A Test Program Establishing a Data Base for Evaluating Present and Future Analytical Techniques, DNA 4278 F-1 and F-2, Defense Nuclear Agency, Washington, D. C., October 1977.
4. Structural Response to Simulated Nuclear Overpressure: Follow-on Program Task I Static and Shock Loads Test Procedures, D3-11108-5, Boeing Wichita Company, Wichita, Kansas, August 1977.
5. Formulas for Stress and Strain, R. J. Roark, McGraw-Hill Book Company, Inc., New York, 1954.
6. Airplane Structural Analysis and Design, E. E. Sechler and L. G. Dunn, Dover Publications, Inc., New York, 1963.
7. The NASTRAN Theoretical Manual, NASA SP221, National Aeronautics and Space Administration, Washington, D. C., June 1973.
8. The NASTRAN User's Manual, NASA SP222, National Aeronautics and Space Administration, Washington, D. C., June 1973.
9. The NASTRAN Programmer's Manual, NASA SP223, National Aeronautics and Space Administration, Washington, D. C., June 1973.
10. The NASTRAN Demonstration Problem Manual, NASA SP224, National Aeronautics and Space Administration, Washington, D. C., June 1973.

DISTRIBUTION LIST

DEPARTMENT OF DEFENSE

Assistant to the Secretary of Defense
Atomic Energy
ATTN: Executive Assistant

Defense Intelligence Agency
ATTN: DB-4C, V. Fratzke

Defense Nuclear Agency
ATTN: SPAS
4 cy ATTN: TITL

Defense Technical Information Center
2 cy ATTN: DD

Field Command
Defense Nuclear Agency
ATTN: FCT, W. Tyler

Field Command
Defense Nuclear Agency
Livermore Branch
ATTN: FCPRL

Undersecretary of Def for Rsch & Engrg
ATTN: Strategic & Space Sys (OS)

DEPARTMENT OF THE ARMY

Harry Diamond Laboratories
Department of the Army
ATTN: DELHD-N-P, J. Gwaltney

U.S. Army Ballistic Research Labs
ATTN: DRDAR-BLT, J. Keefer
ATTN: DRDAR-BLT, W. Taylor

U.S. Army Materiel Dev & Readiness Cmd
ATTN: DRCDE-D, L. Flynn

U.S. Army Nuclear & Chemical Agency
ATTN: Library

DEPARTMENT OF THE NAVY

Naval Material Command
ATTN: MAT 08T-22

Naval Research Laboratory
ATTN: Code 1221 for Code 2627

Naval Surface Weapons Center
ATTN: Code F31, K. Caudle

Naval Weapons Evaluation Facility
ATTN: L. Oliver

Office of Naval Research
ATTN: Code 465

Strategic Systems Project Office
Department of the Navy
ATTN: NSP-272

DEPARTMENT OF THE AIR FORCE

Aeronautical Systems Division
Air Force Systems Command
ATTN: ASD/YYEF
ATTN: ASD/ENFT, R. Bachman
4 cy ATTN: ASD/ENFTV, D. Ward

Air Force Systems Command
ATTN: SDNI
ATTN: DLWB

Air Force Weapons Laboratory
Air Force Systems Command
ATTN: SUL
ATTN: NTYV, A. Sharp
ATTN: NT, D. Payton
ATTN: NTYV, G. Campbell
ATTN: NTYC (S/V Data Base)

Air Force Wright Aeronautical Laboratories
ATTN: MBL, G. Schmitt
ATTN: POTX, M. Stibich

Assistant Chief of Staff
Studies & Analyses
Department of the Air Force
ATTN: AF/SASB, R. Mathis
ATTN: AF/SASC, B. Adams

Deputy Chief of Staff
Research, Development, & Acq
Department of the Air Force
ATTN: AFRDQI, N. Alexandrow

Foreign Technology Division
Air Force Systems Command
ATTN: SDBF, S. Spring

Strategic Air Command
Department of the Air Force
ATTN: XPS
2 cy ATTN: XPFS, F. Tedesco

OTHER GOVERNMENT AGENCY

Central Intelligence Agency
ATTN: OSWR/NED

DEPARTMENT OF ENERGY CONTRACTOR

Sandia National Lab
ATTN: A. Lieber

DEPARTMENT OF DEFENSE CONTRACTORS

Boeing Co
ATTN: M/S 85/20, E. York
ATTN: M/S 40-19, R. Dahl

Boeing Wichita Co
ATTN: R. Syring

Calspan Corp
ATTN: M. Dunn

DEPARTMENT OF DEFENSE CONTRACTORS (Continued)

University of Dayton
ATTN: B. Wilt

Effects Technology, Inc
ATTN: R. Globus
ATTN: R. Parisse
ATTN: E. Bick

General Research Corp
ATTN: T. Stathacopoulos
ATTN: J. Cunningham

Kaman—TEMPO
ATTN: DASIAC

Kaman—TEMPO
ATTN: J. Moulton

Kaman Avidyne
ATTN: B. Lee
ATTN: E. Criscione
ATTN: N. Hobbs
ATTN: R. Ruetenik

DEPARTMENT OF DEFENSE CONTRACTORS (Continued)

Kaman Sciences Corp
ATTN: D. Sachs

Los Alamos Technical Associates, Inc
ATTN: P. Hughes

Pacific-Sierra Research Corp
ATTN: H. Brode

PDA Engineering
ATTN: J. McDonald
ATTN: H. Moody
ATTN: C. Thacker

R & D Associates
ATTN: F. Field
ATTN: J. Carpenter
ATTN: A. Kuhl
ATTN: P. Rausch
ATTN: P. Haas

Science Applications, Inc
ATTN: J. Cockayne